A computational approach to identify biomarkers for lack of response to immunotherapies.

Master Student
Reinier K. Groeneveld
Computational Biology Track
Molecular and Cellular Life Sciences - Utrecht University

Supervisor
Dr. Can Keşmir
Immunological Bioinformatics Group
Theoretical Biology and Bioinformatics - Utrecht University

External examiner
Dr. Patrick Kemmeren
Genetic Interactions
Pediatric Oncology - Princess Maxima Center

Abstract

Melanoma is one of the most immunogenic tumours and has the greatest potential to be treated by immune checkpoint blockade (immunotherapy). Tumour mutational burden (TMB, expressed as somatic mutations per MB coding DNA) is suggested as a good marker for prognosis of immunotheraphy. Still, it is not enough to explain why less than half of all patients respond to immunotherapy. To get better insight into other factors that shape the outcome of an immunotherapy, we focused on the data provided by Riaz et al., 2017. Interestingly, in this data set TMB and neoantigen counts are not significantly different between responders and non-responders, giving us more room to search for additional factors. Still, we found that the average number of mutations in mutated genes were significantly higher in responding patients than non-responding ones. We identified 458 mutated genes unique to a positive or partial response, and 1106 mutated genes unique for stable or progressive disease, which in Gene Ontology (GO) analysis and heatmaps reveal similarity in molecular functions, biological processes, cellular components, protein classes, and pathways. Next, we found highly expressed Human leukocyte and cluster of differentiation antigens (HLA and CD antigens) in these patients, and a possible role for immune evasion and immune response likely through antigen presentation to T and NK cells. However, the expression of HLA-A, HLA-B, and HLA-C were not significant between response groups, but HLA class II molecules were, suggesting an important role for CD4 T cell responses in immunotheraphy outcome. Moreover, the expression of possible T cell targets (i.e., mutated genes) in the response group was higher than in the non-response group, suggesting that the success of the immunotherapy is not only depending on the number of mutations but also how well the mutated genes are expressed. Finally, we identified a "response-signature" consisting of six genes: COL3A1, HLA-DRA, TMSB4X, RPSA, A2M, LDHA, that are the most differentially expressed genes in responding patients and are all related to melanoma. This study exposes that the average expression of neo-antigens (possible T cell targets) should be considered for therapy prediction, and that only a part of the underlying gene expression from non-synonymous mutations of a patient should appeal to personalized vaccines.

Keywords: mutational, response, immunotherapy, antigens, melanoma, tumour, TMB, load, somatic, SNVs.

Table Of Contents

Table of figures

List of Tables

Introduction

Melanoma is the rarest and the most aggressive type of skin cancer that develops from pigment-producing cells known as melanocytes (Linares et al., 2015). Other types of cancers that occur in the skin, non-melanomas, are also malignant. However, they are far less likely to spread to other parts of the body and are therefore more easily treatable. Favourably, melanoma has been identified as one of the most immunogenic tumours, which means that it has the greatest potential to be treated by immunotherapy (Marzagalli et al., 2019) as the formation of T lymphocyte (T cell) reactivity against neo-antigens is more common in melanoma (Schumacher and Schreiber, 2015). This has stimulated the use of immunotherapy, and in particularly, immune checkpoint blockade (ICB) therapies such as programmed cell death protein 1 (PD-1), PD-1 ligand (PD-L1), and cytotoxic T lymphocyte antigen 4 (CTLA4) (Eggermont et al., 2018) in melanoma patients.

These ICBs have managed to improve the overall survival outcomes of patients i.e., mortality rates dropped: the median survival time for metastatic melanoma patients was 9 months until 2011, and in 2017 it was reported to exceed 2 years (Schreuer et al., 2017). More recently, clinical trials reported the same in advanced stages of melanoma: a 5-year survival rate of 34% for patients treated with pembrolizumab, and 52% for patients treated with combination of nivolumab and ipilimumab (Hamid et al., 2019, Larkin et al., 2019).

Aside from overall survival, analytical improvements have been achieved as well. Next-generation sequencing (NGS) helped in estimating tumour mutational burden (TMB), identifying (expressed) neoantigens, developing new therapies to boost the immune response, and understanding how genomic and transcriptomic variation can influence efficacy. More advances include gene databases such as the Cancer Genome Atlas (TCGA) (Blum et al., 2018), bioinformatics tools like gene set enrichment analysis (GSEA) (Subramanian et al., 2007), and RNA sequencing data (Riaz et al., 2017) or single cell approaches (Sade-Feldman et al., 2018) that investigated the dynamics between cancer and immune cells during ICB in melanoma.

Importantly, there are biomarkers envisioned within the cancer-immunity cycle that can contribute to the ICB response prediction (Chen and Mellman, 2013; Schumacher and Kesmir, 2015). The TMB, which is the somatic mutations per mega base (Mb) of coding DNA (Schumacher and Schreiber, 2015; Sha et al., 2020; Heydt et al., 2020; Jardim et al., 2021) is one of these. It is frequently reported on as a biomarker for assessing tumour immunogenicity (Morrison et al., 2018; Van Allen et al., 2015) and for the efficacy of ICBs in many cancer types including melanoma (Rizvi et al., 2015; Wang et al., 2019; Forschner et al., 2019). Furthermore, in several clinical trials TMB has been shown to be a good predictor of immunotherapeutic efficacy (Ajona et al., 2017; Razzak, 2013; Hugo et al., 2016; Cristescu et al., 2018).

Recent examples of studies with TMB in melanoma involved (1) the correlation between TMB and immune infiltration by Wang et al. (2021), (2) the correlation between TMB and differentially expressed genes (DEGs) by Kang et al. (2020), (3) the integrative modelling of multi-omics sequence data that incorporated genomic, transcriptomic and T cell repertoire characteristics by Anagnostou et al. (2020), (4) the systematic pan-tumour analyses that collated whole-exome and transcriptomic data by Litchfield et al. (2021), (5) the sequencing of whole-exome, transcriptome, and/or T cell receptor (TCR) by Riaz et al. (2017), and (6) the identification of TMB-related hub genes and their competing endogenous RNA networks by Zhang et al. (2021).

These studies concluded that (1) in cutaneous melanoma, elevated TMB levels were associated with better survival outcomes, (2) in cutaneous melanoma, TMB was positively correlated with prognosis, (3) TMB is associated with improved treatment response, and that the mutation frequency in expressed genes is superior in predicting outcome, (4) clonal TMB was the strongest predictor of ICBs response, followed by total TMB (and CXCL9 expression), (5) total and clonal TMB are associated with overall survival and response in nivolumab-treated whilst ipilimumab-naïve patients, and (6) elevated TMB levels were significantly correlated with improved survival outcomes and had a substantial effect on melanoma, respectively.

However, despite these promising results, additional biomarkers are necessary because the TMB as a marker by itself is insufficient. Namely, less than half of all patients respond to these immunotherapies (Schumacher and Kesmir, 2015). There are patients that attain high TMB and yet still do not produce an (effective) anti-tumour immune response. Similarly, there are also ICB responders with low TMB as well. Thus, only a part of the variation in the quality of the anti-tumour immune response in the setting of immunotherapy (Chen et al., 2016) can be explained by TMB. More novel predictive biomarkers for melanoma treatment are needed to instruct clinical decision-making, and subsequently to predict the response to immunotherapy.

In this study, we aim to identify such predictive biomarkers that can explain the failure in immunotherapy in almost half of the patients that get the chance to use this new treatment. Our analysis focusses on somatic, exomic, neo-antigenic and transcriptomic data by integrating somatic mutations with gene expression data. We show that aside from the number of possible T cell targets (neo-antigens), also the underlying tumour expression pattern can dictate the outcome of the immunotherapies.

Methods

Data acquisition and experimental details

To investigate the mutational landscape of cancer patients with a known response to immunotherapy we analysed genomic data identified by Riaz et. al (2017). This dataset consists of 68 patients with advanced melanoma, who ranged from 22 till 89 years old (median age was 55 years) and had sufficient material for genomic analysis. There were 15 patients with a response (partial or complete response: PRCR) and 53 patients with no response (stable or progressive disease: SDPD).

Moreover, 33 patients were naïve to the treatment whilst the 35 others had already progressed on Nivolumab. These patients received Nivolumab in doses of 3mg/kg every 2 weeks until progression, or for maximum 2 years, with a (radiography) response assessment every 8 weeks. Upon progression, a CT scan was performed 4 weeks later for confirmation. Biopsies were collected from the same site and were performed before therapy (1-7 days before first dose) and on cycle 1 (day 23-29) (Riaz et. al, 2017).

Here we describe briefly how this data was generated. We examined the whole-exome sequencing (WES), neoantigen typing, and the RNA Sequencing (RNA-seq) datasets provided by Riaz et al. In brief, after DNA was extracted from samples, exonic sequences were enriched, sequenced, and used to identify single nucleotide variations (SNVs). These SNVs were additionally filtered based on read count (less than 5 or with corresponding normal coverage of less than 7 reads) and followed by a determination of insertions and deletions (indels), of which only high- or moderate-impact indels determined by callers were selected. We used the sum of these remaining SNVs (non-synonymous mutations) provided by Riaz et al. to calculate the TMB (from WES).

Second, neo-antigen analysis was performed from exome-sequencing data, with each non-synonymous SNV translated into a 17-mer peptide sequence, which were used to create 9-mers for determination of MHC class I binding. Next, the binding strength of mutated peptides to patient-specific Human leukocyte antigen (HLA) alleles were calculated and those with a rank < 2% were considered for further analysis. If a mutation generated multiple 9-mer

peptides that bound to patient-specific HLA alleles, it was only counted as one neoantigen, whilst neo-peptides were calculated as the total number of predicted 9-mers that bound to patient-specific HLA alleles. Thus, one mutation can generate multiple neo-peptides, however, only the best binder is considered as a predicted neoantigen. This part was completely provided by Riaz et. al.

Third, RNA-seq data for transcriptome analysis was produced from raw FASTQ files that were aligned on the hg19 genome. These aligned fragments were counted with Rsamtools v3.2 and we used these fragments provided by Riaz et al., annotated it with the TxDb.Hsapiens.UCSC.hg19.knownGene transcript database and normalized it per kilobase per million mapped reads (FPKM) by using the robust FPKM estimate function of DESeq2 v1.26. Before normalization, genes were filtered as a measure of quality control: we removed genes with low read counts (minimum 4 samples and minimum 2 read count, and variances and standard deviations >1).

All subsequent differential gene analysis was conducted using the DESeq2 package, which use a generalized linear model, where counts are modelled using a negative binomial distribution with fitted mean and a gene-specific dispersion parameter. The differentially expressed genes (DEGs) for the pre-therapy samples were modelled according to response variables (influencing factor) i.e., we stratified two cohorts for analysis: SDPD (stable and progressive disease) and PRCR (partial and complete response).

Finally, for a GO enrichment analysis we conducted the panther DB Gene Ontology knowledgebase v16.0. with homo sapiens as only organism (Ashburner et al.,2000; The Gene Ontology resource, 2021) and Human CD antigens were taken from abcam's human CD markers chart (Updated August 5, 2021).

For more specificalities regarding corrections, alignments, method names in the WES, neoantigen analysis, RNA-seq and other methods, or experimental details such as antibodies, biological samples, critical commercial assays, tumour tissue storage and division, or resource sharing, please refer to the original methodology by Riaz et al. (2017).

Statistical analysis

Statistical analyses in this study were performed with R software environment v3.6.1. For measuring the statistical significance of continuous variables between groups, the data (two vectors) were compared by the paired two-sample Wilcoxon tests ('Mann-Whitney' test). Alternative hypotheses testing were used for further specification of significant results (direction testing). Before applying all these comparisons, the Shapiro-Wilk normality checks were performed to test for skewed distributions (if a score is significant, the data is not normally distributed, and we thus apply Wilcoxon test because normality is not needed). All figures shown passed this test. Next, all heatmaps were scaled and centred in the column direction.

For an overview of package versions and miniconda environment installations please refer to the supplementary materials.

Results

Dataset synopsis

The number of patients (sample size) differed between results. A summary of this is shown in figure 1, which shows the amount of patients for each analysis throughout this report. As stated in the previous section, patients in this study were either naïve or progressive to immunotherapy treatments, which means that we have included patients who also potentially built-up resistance to immunotherapy. Since limited effective treatment options are available as soon as a patient develops resistance (Weiss et al., 2019) it is interesting to include these progressive patients to see if their response will also be differentiable. Therefore, we decided not to separate patients based on previous treatments; we only differentiate between PRCR (responders) and SDPD (non-responders). In the next paragraph we pick up from here and start our analysis by exploring the neo-antigenic and the exomic measurements.

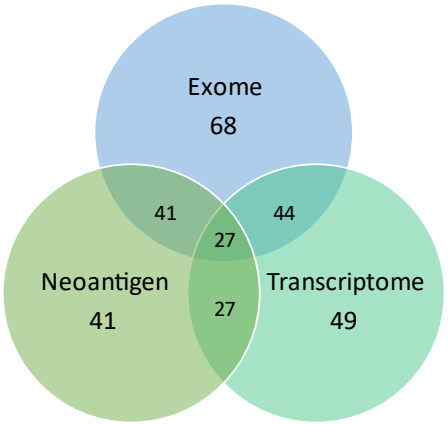

Figure 1: Summary of the amount of patients per analysis. The distribution of each number is as follows: Exomic data **(68)** is shown for 15 responders and 53 non-responders. Neo-antigenic data itself, and the overlap of neo-antigenic with exomic data **(41)** is shown for 9 responders and 32 non-responders. Transcriptomic data **(49)** is shown for 10 responders and 39 non-responders. Transcriptomic overlap with exomic data **(44)** is shown for 10 responders and 34 non-responders. Transcriptomic overlap with both neo-antigenic and exomic data, as well as the transcriptomic overlap with only neo-antigenic data **(27)**, is shown for 7 responders and 20 non-responders.

Tumour neoantigen landscape of patients

An important aspect in the cancer-immunity cycle is whether the tumour is likely to contain T cell recognizable antigens (Schumacher and Kesmir, 2015). As TMB increases, the probability increases that neo-antigens (expressed by tumour cells) produce higher neo-antigenic load (Chan et al., 2019), and tumours with a high number of clonal neo-antigens might be more likely to bring forth an effective immune response (McGranahan et al., 2015). To analyse this foreign antigen space (neo-antigen landscape), generated by mutations of the cancer patients, we related the non-synonymous mutations (from SNVs) with the neo-antigens (figure 2).

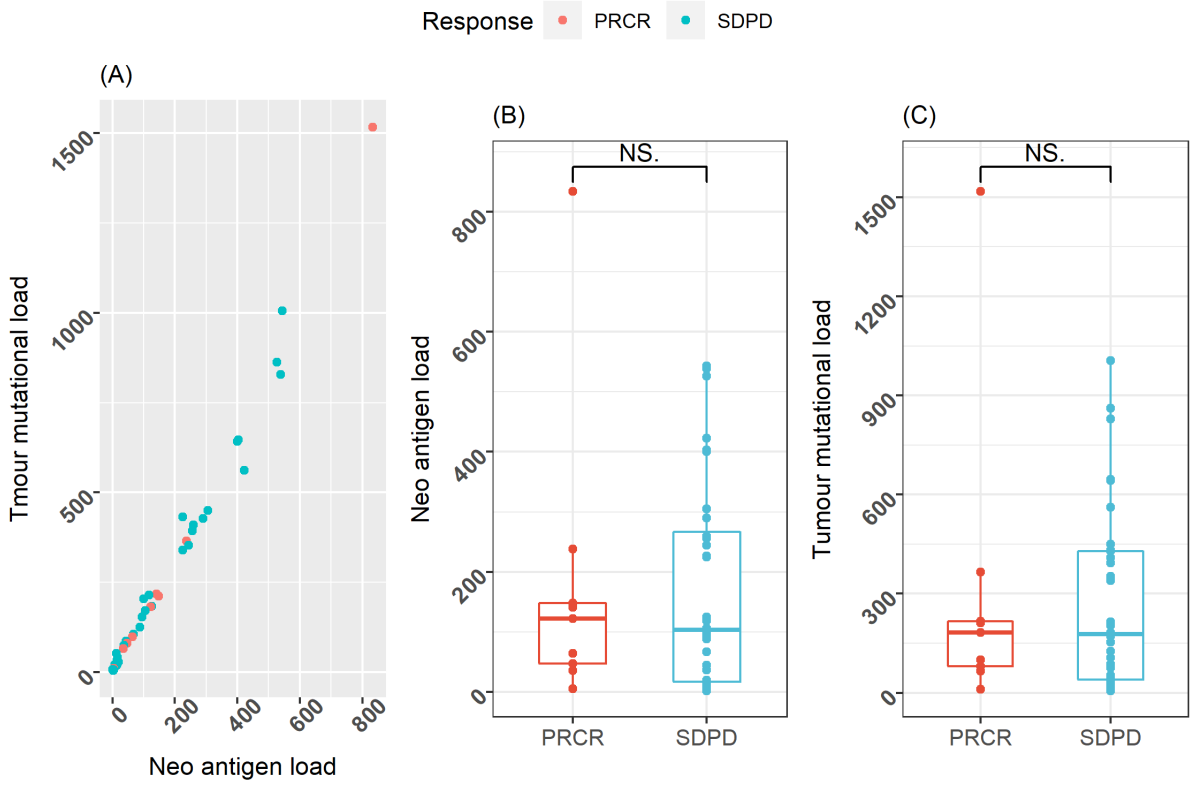

Figure 2: Comparison of neo antigenic and mutational load (TMB) of the patients (n=41). **(A)** Neo antigenic load is plotted as a function of TMB. Mutational load correlates with neoantigen load by a (Pearson's) correlation coefficient of almost 1 (r=0.99, p-value < 0.001). **(B)** Comparison of two response groups using neoantigens (not significant). **(C)** Comparison of two response groups using TMB (not significant). Comparisons were both computed with non-paired two-sample test (Wilcoxon). NS: p>0.05.

When plotted as a function of one another, the tumour neo-antigen load and tumour mutation load were nearly linearly correlated (figure 2a: r=0.99, p-value < 0.001). However, when statistically tested for differences, antigenicity did not differ between responders and non-responders (figure 2b). The same was true for the mutational load (figure 2c). Together,

this indicates that a higher mutational or neo-antigenic load did not necessarily translate into more sensitivity to ICB. An explanation for this is that besides antigenicity, an anti-tumour immune response is also affected by the infiltrative features such as the activation and recruitment of T cells to the tumour microenvironment, the composition of the tumour microenvironment, as well as the resistance to immune checkpoint blockade (Tumeh et al., 2014). Nevertheless, it can still be argued that a higher mutational load generates more T cell targets, which contribute to the success of the immunotherapies in PRCR patients because anti-tumour T cell responses were stimulated.

Tumour mutational landscape of genes

Identifying mutations in all patients might indicate which genes affect response to immunotherapy. Therefore, we characterized the exomic landscape of the mutations in each patient by performing data analysis on the SNVs. We first counted genes that were affected by non-synonymous mutations (NSMs): a total of 10939 mutated genes were found across all patients. Afterwards, to decrease stochastic effects in our analysis, we only considered genes that were mutated in at least 2 patients. This filtering reduced the profile of genes to a total

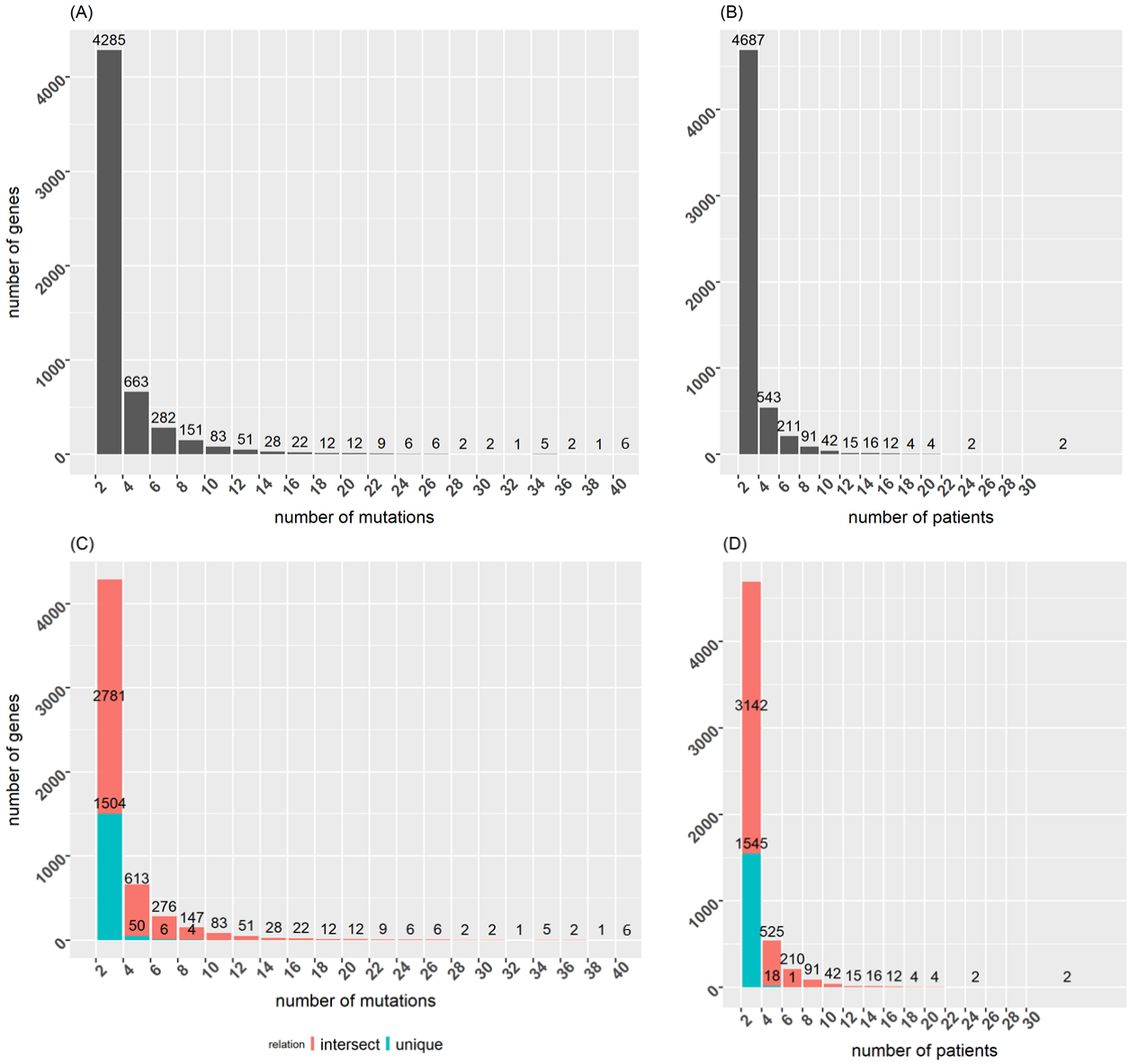

Figure 3: Histograms of the non-synonymous mutations identified across all patients. **(A,B)** Summary of the distribution of mutations. **(C,D)** The distribution of mutations separated by its relation to either one, or two, therapy outcomes. Results are shown for 5629 genes which remain after filtering for stochasticity: genes shown have mutated in at least 2 patients. Turquoise indicates that a gene is related to one therapy outcome (unique). Red indicates that a gene is related to both therapy outcomes (intersect).

of 5629 in which 6 genes had at least 30 mutations in the entire dataset (figure 3a) and two genes which had mutated in at least 30 patients (figure 3b). These most frequently mutating genes are listed below in Table 1.

Table 1: Overview of top mutated genes that had a minimum of 30 SNVs (left side of table) throughout the entire dataset or mutated in minimum 20 patients (right side). All genes in this table were involved in both therapy outcomes (intersect). Top mutated genes also found in top 10 of Kang et. al (2020) and Zhang et. al (2021) include TTN, MUC16, DNAH5, PCLO, LRP1B, ANK3, ADGRV1, BRAF.

Have 30 or more mutations SNVs			*Occur in 20 or more patients*		
Gene	Total mutations	Total patients	Gene	Total mutations	Total patients
TTN	196	38	TTN	196	38
MUC16	164	37	MUC16	164	37
DNAH5	58	21	PCLO	55	25
PCLO	55	25	MUC4	52	25
MUC4	52	25	LRP1B	37	22
OBSCN	41	20	CSMD1	35	22
MGAM	40	20	DNAH5	58	21
LRP1B	37	22	BRAF	21	21
NEB	37	14	OBSCN	41	20
PKHD1L1	36	20	MGAM	40	20
ANK3	36	16	PKHD1L1	36	20
CSMD1	35	22			
FAT3	35	18			
ZFHX4	35	17			
HYDIN	33	16			
ADGRV1	31	18			
MUC17	31	18			
APOB	30	15			

Previously, several studies have identified genes that are frequently mutated in cancer patients. For example, Kandoth et. al. (2013) looked into 3,281 tumours across 12 cancer types (excluding melanoma) from The Cancer Genome Atlas (TCGA) database. Using these data sets, they identified 127 genes that were significantly more mutated than the others across cancer types. Interestingly, the genes we identified in Table 1 have hardly any overlap with these more pan-cancer mutated genes. In the same way, we also performed our response-unique data transformation on SNVs identified by Mariathasan et al. (2018). However, the study focussed on urothelial tumours and compared much less mutated genes than Riaz et al. (100s rather than 1000s), thus were not included for this analysis.

On the other hand, more recently, Kang et. al (2020) and Zhang et. al (2021) also computed mutated genes in melanoma-patients from the TCGA database. Though their data sets

contained less patients (467 and 472 patients, respectively) the two studies both analysed melanoma patients only, in contrast to the pan-cancer study from above. Notably, our genes from Table 1 contained 8 of the top 10 identified genes from both Kang et. al (2020) and Zhang et. al (2021) (RP1 and DNAH7 not ranked high enough in our case). Together, these results suggest that the genes identified in Table 1 are specific for melanoma patients. Additionally, we performed a GO analysis for these melanoma-genes (n=19) listed in Table 1, however, this did not help us to describe this gene set further (results not shown).

Tumour mutational landscape of response unique genes

It is unclear whether a gene is important for either PRCR or SDPD response. It is very interesting to see if mutated genes are exclusive to responders i.e., are not found in the patients with no response to the therapy. To further identify 'responder-genes' which might facilitate response to therapy, we classified a gene as 'unique' when it mutated only in patients of one response group (either PRCR or SDPD) and as an 'intersect' gene if it mutated in patients of both.

This separation by therapy outcome identified a total of 1564 genes found to be unique to a response (PRCR or SDPD) and 4065 genes which mutated for both response groups. Moreover, the response-intersecting-genes accumulated relatively more mutations and occurred in more patients than response-unique-genes (figure 4). For example, the melanoma-related genes from the previous section in Table 1 had most mutations and were all response-intersecting genes. Since our interest lies in differentiating between the PRCR and SDDP response groups, we decided to provide a second classification to improve the separation of genes by therapy outcome: SDPD and PRCR response-unique genes (figure 4).

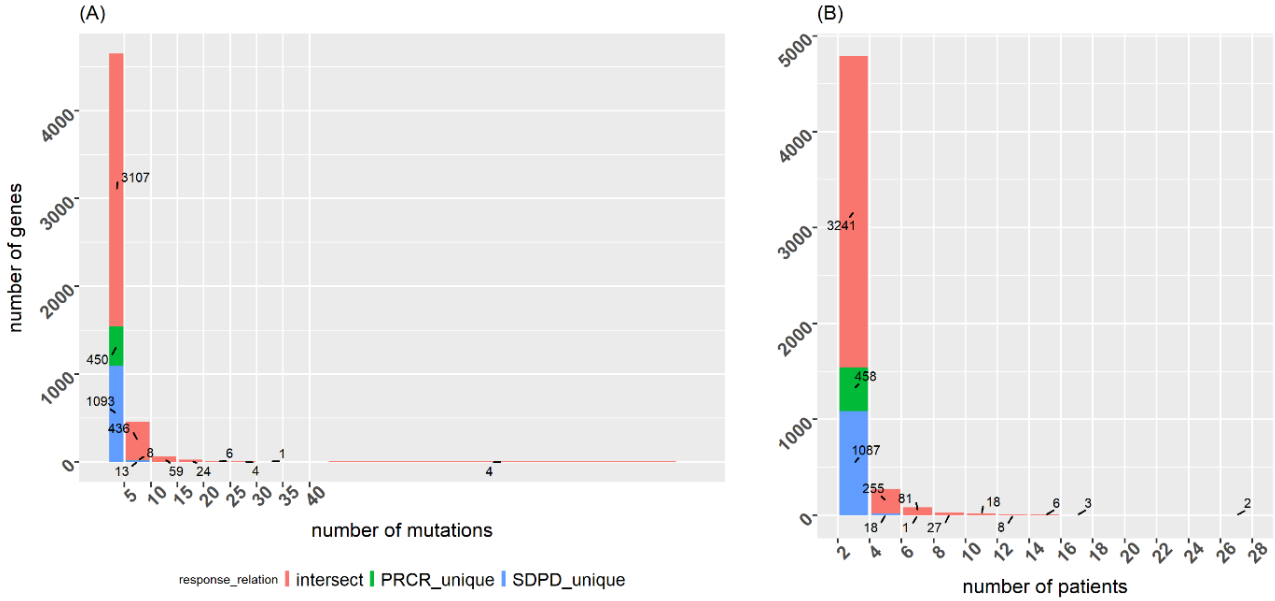

Figure 4: Histograms of the non-synonymous mutations with response-indication. Distributions of mutations separated by (1) indication of overlap with response groups (unique or intersect), and (2) by response itself (only for unique-related genes). Results are shown for 5629 genes. Genes have mutated in at least 2 patients. Red indicates that a gene is related to both therapy outcomes (intersect). Blue indicates that a response-unique-gene is related to the SDPD therapy outcome (SDPD-unique). Green indicates that a response-unique gene is related to the PRCR therapy outcome (PRCR-unique).

This additional characteristic divided the total of 1564 response-unique-genes from above even further and resulted in 458 mutated genes unique to the PRCR response group whilst 1106 genes unique to SDPD (figure 4a, 4b). The same could be done for the 4065 response-intersecting-genes and resulted in 1503 PRCR- and 2138 SDPD-response-intersecting-genes, respectively (suppl. figure 1).

An important notice is that none of the genes had mutated across all patients. Still, there were response-unique-genes that mutated for more than 2 PRCR or SDPD patients. The top of these genes are shown in Table 2 for both response groups. Similar to the top mutated genes from Table 1, we performed a GO analysis for these SDPD-unique (n=19) and for the PRCR-unique genes (n=8) from Table 2. However, this did not provide a better data description. Furthermore, an interesting result from Table 2 was the class II major histocompatibility complex protein HLA-DQB1 which was found to be SDPD-response-unique, which indicates that HLA immunity genes are prone to non-synonymous mutations as well.

Table 2: Overview of genes that mutated only for patients in the SDPD (SDPD-unique) or in the PRCR response group (PRCR-unique). Note that the SDPD group (n=53) is larger than the PRCR response group (n=15).

Gene	Total mutations	Total patients	Response indication	Gene	Total mutations	Total patients	Response indication
RNF213	9	7	SDPD unique	ZDBF2	9	4	PRCR unique
ARMCX4	7	6	SDPD unique	A1CF	9	4	PRCR unique
GHR	7	6	SDPD unique	PCDHB6	7	4	PRCR unique
ZNF727	6	6	SDPD unique	UROC1	6	4	PRCR unique
HLA-DQB1	9	5	SDPD unique	KAT6A	5	4	PRCR unique
CATSPERB	8	5	SDPD unique	PRDM10	4	4	PRCR unique
ITGAX	6	5	SDPD unique	DLG1	4	4	PRCR unique
NAV2	6	5	SDPD unique	PRR23B	4	4	PRCR unique
ZNF626	5	5	SDPD unique				
MUC5AC	5	5	SDPD unique				
PTPN13	5	5	SDPD unique				
RHAG	5	5	SDPD unique				
UBXN11	5	5	SDPD unique				
PTPRR	5	5	SDPD unique				
OR4B1	5	5	SDPD unique				
OR10H5	5	5	SDPD unique				
ZNF257	5	5	SDPD unique				
DCX	5	5	SDPD unique				
PTCHD4	5	5	SDPD unique				

Tumour mutational landscape of SNVs

Aside from the gene-specific annotation, mutations could also be characterized by nucleotide change, chromosome, or variant classification instead (see supplementary materials). We found that the G>A and C>T nucleotide changes had occurred far more than others in this data set (n=5629 genes, suppl. table 1), as was found earlier for the non-synonymous mutations (see e.g., Iengar, et al. 2012; Kang, et. al 2020; Zhang, et. al 2021). When further characterized by response (suppl. table 2) these nucleotide changes were also found to occur more frequently in the PRCR-response-group than in the SDPD-group (for all SNV types), in

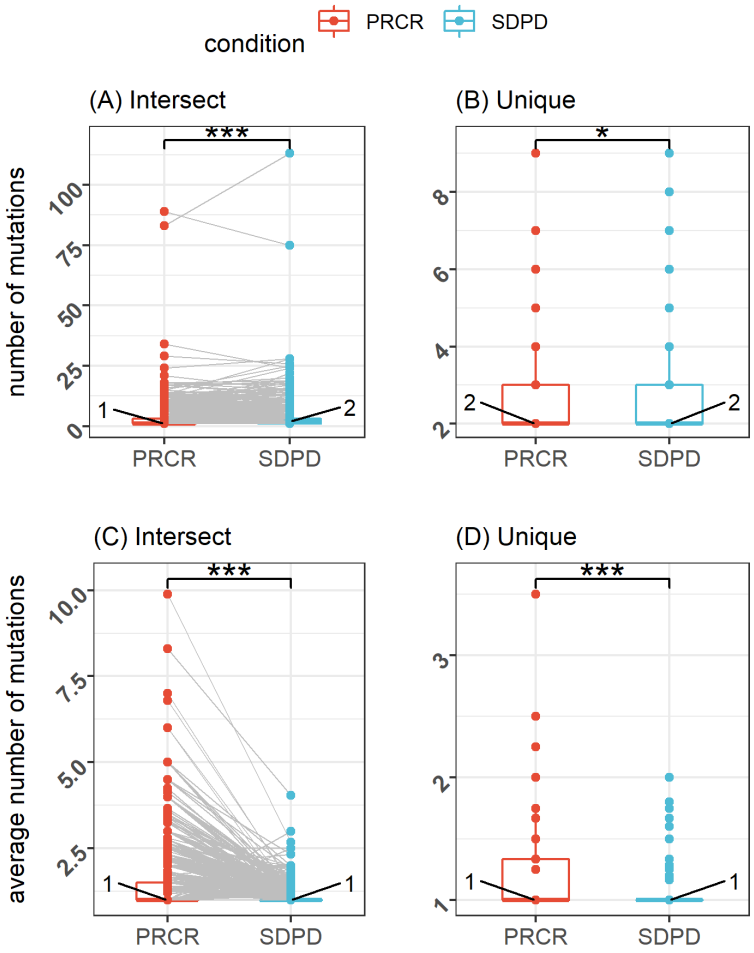

Figure 5: Comparison of two response groups using the non-synonymous mutations of all the mutated genes. **(A)** Comparison for mutations of response-intersecting genes (n=4065). Alternative hypothesis tested for PRCR < SDPD (p=1.973e-11). **(B)** Comparison for mutations of response-unique genes (n=1564: PRCR unique=458, SDPD unique=1106). Alternative hypothesis tested for PRCR > SDPD (p=0.015). **(C)** Comparison for average mutations per patient of response-intersecting genes. Alternative hypothesis tested for PRCR > SDPD (p<2.2e-16). **(D)** Comparison for average mutations of response-unique genes. Alternative hypothesis tested for PRCR > SDPD (p<2.2e-16). The average mutations per gene is calculated only for patients where the gene had mutated (thus not complete response group). Comparisons in A and C were computed with paired two-sample tests, and those in B and D with the non- paired two-sample test (both Wilcoxon). Red indicates genes from patients who responded to treatment. Blue indicates genes from patients who did not respond. * p < 0.05, ** p < 0.01, *** p < 0.001.

line with the fact that the patients in the PRCR group have on average more mutations than SDPD group patients (suppl. Table 2, 4 and 6) (Schumacher and Schreiber, 2015, Riaz et al., 2017). To show this more clearly, we compared all mutated genes (unique and intersect) in two response groups (figure 5).

The results showed that the total number of mutations and the average number of mutations of a gene were significantly different between response groups. The total number of mutations was significantly less for the response-intersecting genes in the PRCR group compared to the SDPD group because of the group size (figure 5a). Contrastingly, in the case of the response-unique mutations, the total number of mutations were significantly higher for the PRCR group, even though the group was smaller (figure 5b).

To account for this difference in sample size, we tested the average mutations as well. Both the response-intersect and unique genes were significantly higher in the PRCR group in this case (figure 5c, 5d). These results suggest that the mutational load (especially the number of non-synonymous mutations) is a good indicator of the immunotherapy outcome, confirming the findings of Riaz et. al. 2017. Please note that, we showed in the previous neoantigen section that there is a very strong correlation between the mutational load and the number of predicted neoantigen. Therefore, the higher mutational load generates more T cell targets in PRCR patients and stimulates anti-tumour T cell responses, which in turn contributes to the success of the immunotherapies.

In terms of chromosomes, most non-synonymous mutations were found for chromosome 1, followed by 19 and 2 (suppl. Table 3 and 4). When corrected for the size of the chromosomes (as Chromosomes 1 and 2 are the largest ones), it became clear that chromosome 19 has the most mutations per Mb (suppl. Table 3 and 4). Chromosome 19 was previously associated with lung cancer (Wang, et. al. 2015), but to our knowledge it is not yet reported that chromosome 19 is enriched in mutations in melanoma patients. Next, we analysed the type of variants and found that missense variants occurred most in all patients, in agreement with Kang, et. al (2020) and Zhang, et. al (2021). As expected, the missense variant occurred more often in the PRCR-group (suppl. Table 5 and 6).

Finally, there were characteristics that were shared by all patients in the PRCR or SDPD group: all PRCR patients at least had mutations (1) with G>A nucleotide change, (2) on chromosome 1, 2 and 12, and (3) by missense variants; all SDPD had missense variant, with most patients (n=49) having mutations on chromosome 1 and 19, followed by patients (n=47) with mutations on chromosome 2 and 11, and another majority (n=51) all having G>A, C>T, A>G nucleotide changes.

Characterizing genes unique for positive response: PRCR unique

The GO results of our top mutated genes (table 1), including the top of the response-unique genes in the previous section (table 2), required more details for response differentiation. Interestingly, the GO results revealed that mutations of immunity associated genes occur as well. Mapping these genes might aid us to predict therapy outcome e.g., the mutations of HLA-DQB1 were SDPD-related in Table 2. Thus, instead of focussing only on the top mutated genes, we featured the complete set of genes that were found to be PRCR-response unique (n=458). Five different ontology queries were performed: molecular functions, biological processes, cellular components, protein classes, and even pathways.

First, by assessing the molecular functions (figure 6a), we found that most PRCR-unique genes were related to binding (41.8%), catalytic activity (26.1%) and molecular function regulation (17.3%). In terms of cellular component (figure 6b), intracellular (36.6%) and cellular

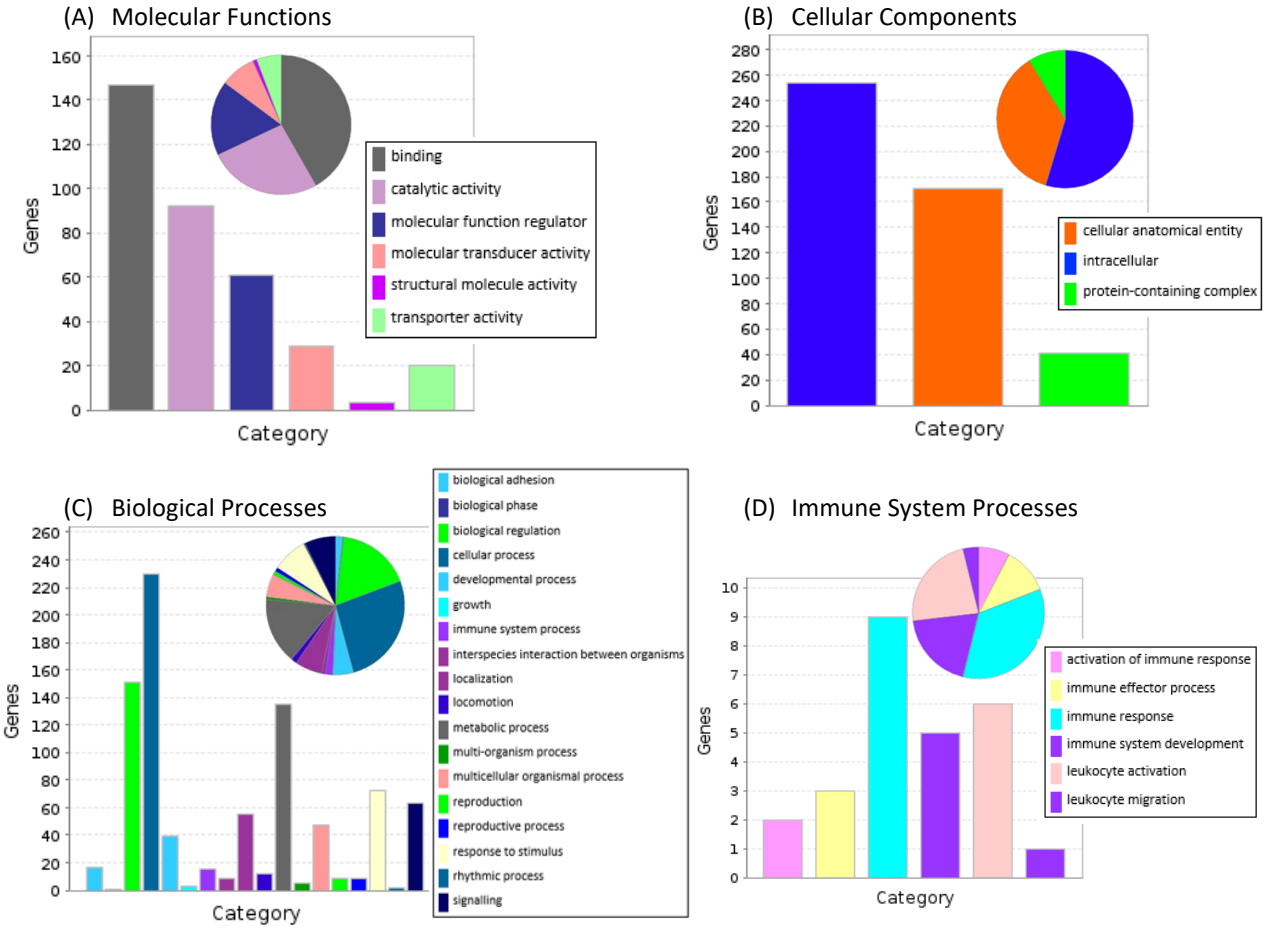

Figure 6: Gene ontology analyses of the PRCR-unique genes. **(A)** Hits for molecular function (n=352). **(B)** Hits for cellular component (n=465). **(C)** Hits for biological process (n=870). **(D)** Hits for immune system processes (n=26). Colours indicate identified categories shown in the legenda's, bar chart, and pie chart classification.

anatomical entity (54.6%) were the largest hits. For biological processes (figure 6c), the largest hits were for biological regulation (17.4%) and metabolic process (15.5%). Immune system processes were only a small percentage (n=26, 1.7%). Within the latter (figure 6d), immune response (34.6%), leukocyte activation (23.1%), and immune system development (19.2%) were abundant. Suppl. table 7 and 8 show the PRCR-unique genes related to immunity processes and immunity protein classes, respectively.

When we divide PRCR-unique genes into protein classes (figure 7a), the largest contributor was the metabolite interconversion enzyme (17.9%), followed by transmembrane signal receptor (12.3%), gene-specific transcriptional regulator (11.9%), protein modifying enzyme (11.9%), and transporter proteins (10.5%). Immunity related proteins (figure 7b) were only a small fraction (n=7, 2.5%), with the immunoglobulin receptor superfamily (4 out of 7) as the dominant class. The most heterogeneous results however were generated by the pathway analysis (suppl. figure 2) where the most relevant pathways were the integrin signalling pathway (5.6 %), T cell activation (2.8 %) and B cell activation (1.4 %).

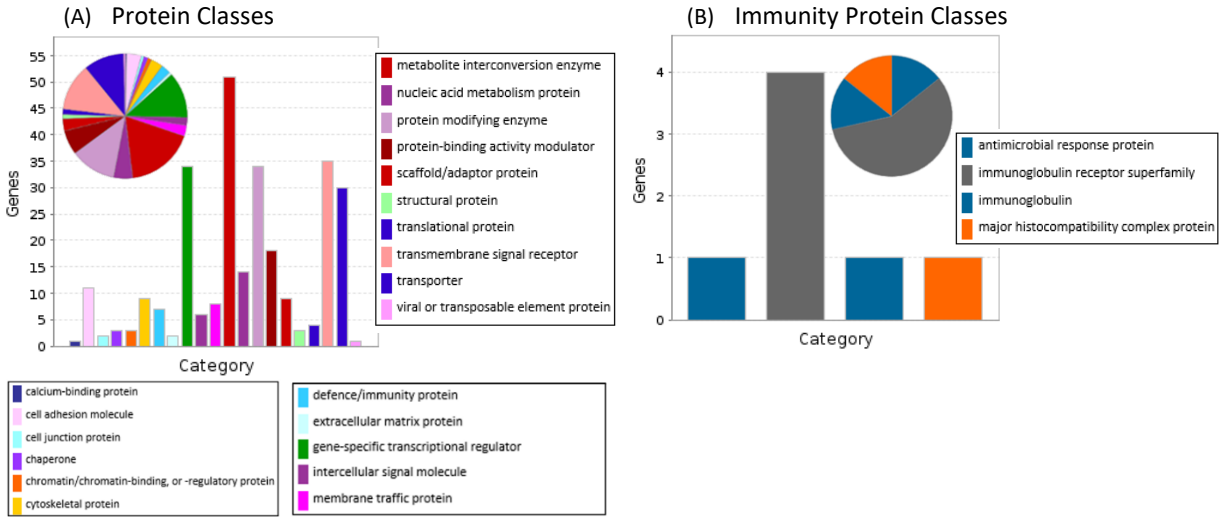

Figure 7: Gene ontology analyses of the PRCR-unique genes. **(A)** Hits for protein class (n=285). **(B)** Hits for the defence/immunity protein class (n=7). Colours indicate identified categories shown in the legenda's, bar chart, and pie chart classification.

Lastly, we analysed whether these PRCR-genes could separate PRCR from SDPD patients based on the underlying tumoral gene expression. Suppl. figure 3 shows a heatmap of these mutated genes that were PRCR-unique and also measured in the RNA sequencing dataset. As expected, the patients do not cluster according to their response groups (see the top bars in

the heat map). Moreover, there is also a not clear pattern emerging from this heat map. If we repeat the same by using only the top 50 (highest median expressed) PRCR-unique genes (suppl. figure 4), a separate cluster of four genes that were relatively high in expression in *all patients* emerged (thus not only in PRCR group): PGK1, HNRNPC, CSDE1 and RHOA.

All four genes have previously been identified to have associations with melanoma i.e., namely (1) CSDE1 was found to be a critical modulator of melanoma metastasis while it was overexpressed in melanoma tumours and promoted invasion and metastasis (Wurth et al., 2016), (2) HNRNPC exhibited overexpression in melanoma cells (Mulnix et al, 2014), (3) RHOA overexpression was associated with thinner tumours, higher grade of tumour-infiltrating lymphocytes and lack of disease recurrence: a suppressive role in skin melanoma (Kaczorowski et al.,2019), (4) PGK1 expression was highest and upregulated in metastatic cells compared with melanocytes (Janik et al., 2018).

Additionally, these genes have previously been identified with cancer types besides melanoma (e.g., Hu et al., 2017; Liu et al., 2020; Wu et al., 2018; Ottolini et al., 2020), establishing that an oncogenic role has thus been linked to the (high) expression of these genes. Our results show that mutations in these genes were PRCR unique, supporting their role as potential targets to promote an anti-tumour immune response.

Characterizing genes unique for negative response: SDPD unique

For the completeness, we extended our analysis from the previous section. We show the results for the same five queries however now for the SDPD-unique genes.

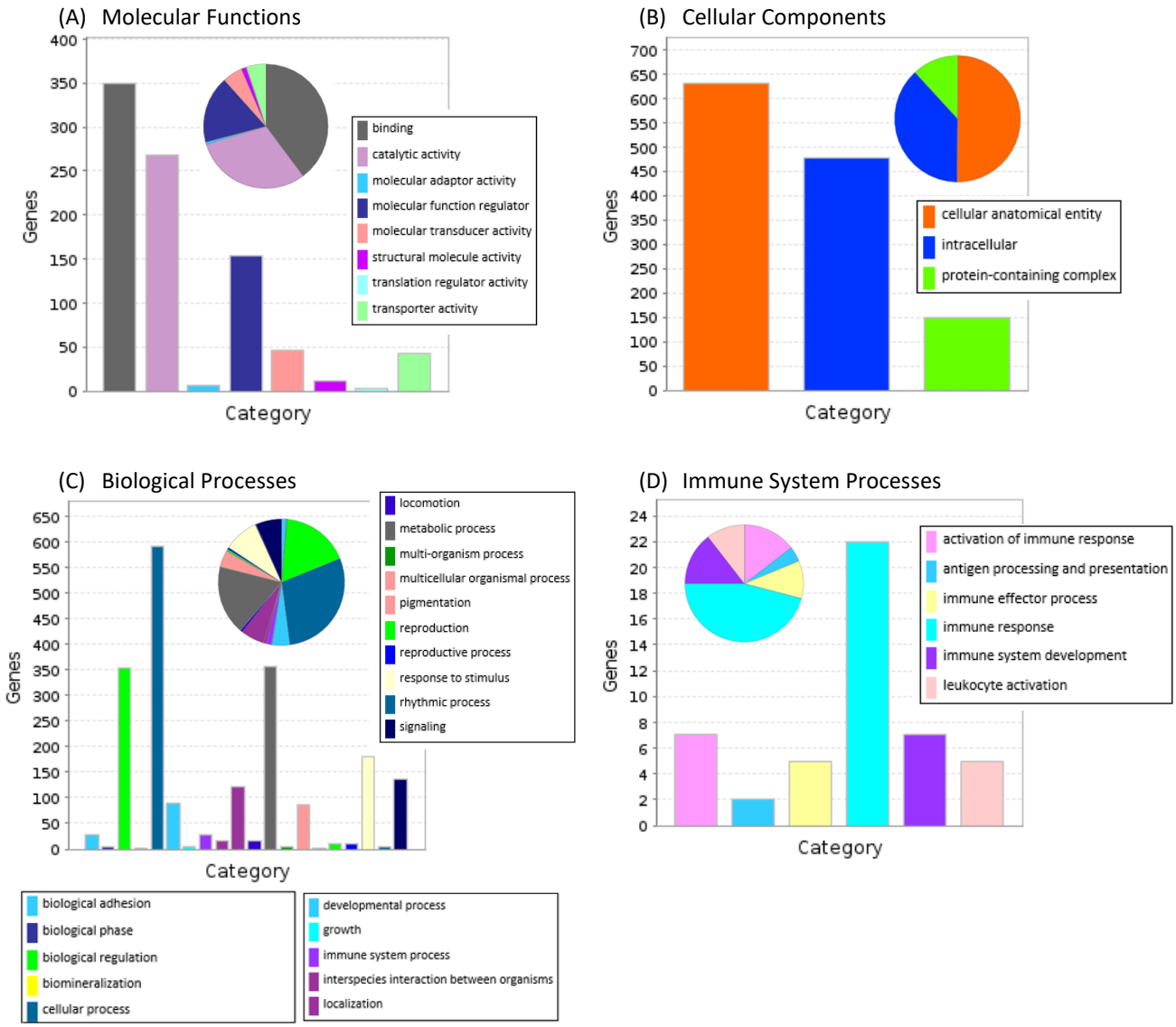

Figure 8: Gene ontology analyses of the SDPD-unique genes. **(A)** Hits for molecular function (n=880). **(B)** Hits for cellular component (n=1260). **(C)** Hits for biological process (n=2043).**(D)** Hits for immune system processes (n=48). Colours indicate identified categories shown in the legenda's, bar chart, and pie chart classification.

For biological processes (figure 8), protein classes (figure 9), and pathways (Suppl. figure 5) mainly similar categories to PRCR-unique genes were found. Interestingly, the immunity proteins for the SDPD-unique genes (n=13) were classified to only two classes: immunoglobulin receptor superfamily (76.9%) and major histocompatibility complex protein

(23.1%). Suppl. table 9 and 10 show the SDPD-unique genes in the immunity processes and SDPD immunity protein classes, respectively.

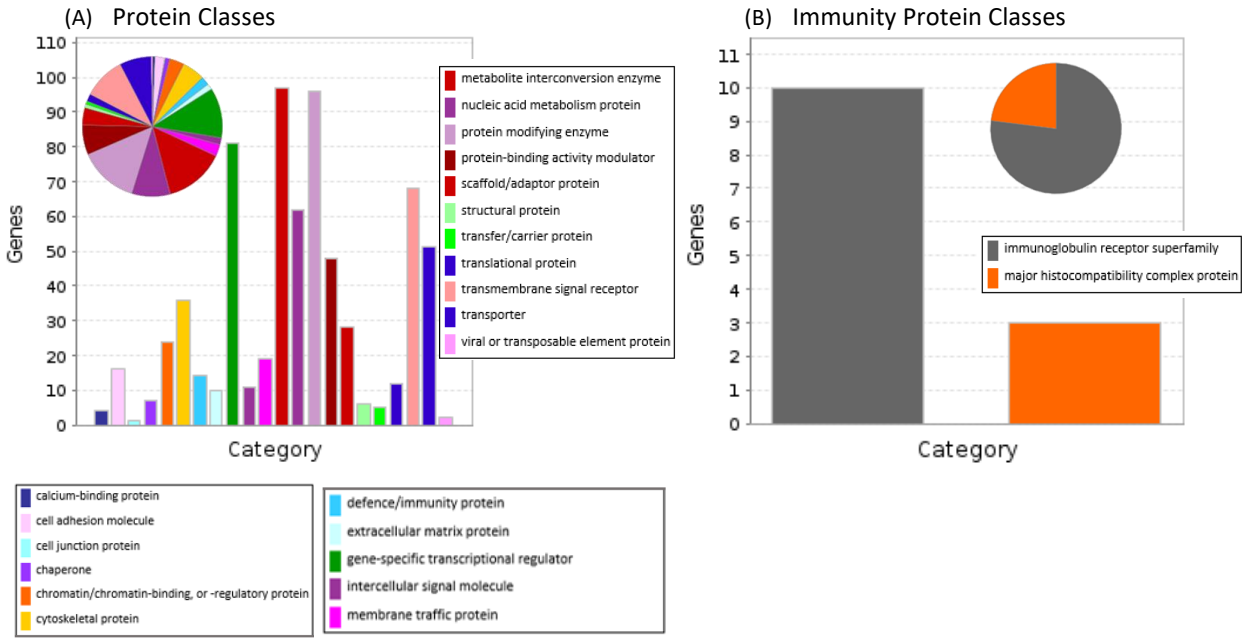

Figure 9: Gene ontology analyses of the PRCR-unique genes. **(A)** Hits found for protein class (n=698). **(B)** Hits found for the defence/immunity protein class (n=13). Colours indicate identified categories shown in the legenda's, bar chart, and pie chart classification.

Although this heat map of the top 50 highly expressed SDPD-unique genes did also not show a clear pattern, it distanced a cluster with three highly expressed genes for *all patients* (suppl. figure 6). It contained two immune-system-related, and a ribosomal protein: HLA-A, HLA-B, and RPL4, respectively. Another important gene was TYRP1 which showed greatest variation in terms of gene expression and divided the patient hierarchies into two.

Moreover, also for these genes a link with melanoma has been reported i.e., namely (1) RPL4 is from a series of ribosomal proteins that are overexpressed in the melanoma exosomes (Mathivanan, S. and Simpson, 2009), (2) HLA-B (antigens) expression by metastatic melanoma cell lines and melanocytes were variable, while HLA-A (antigens) were consistently expressed in both cell types (Marincola et al., 1994), (3) TYRP1 expression in melanoma skin metastases was found to correlate with both distant metastasis-free survival, overall survival and with Breslow thickness (Journe et al., 2011). Except for TYRP1, the other three genes were reported for non-melanoma cancer types as well (Kim et al., 2021; Menon et al., 2002).

In short, our findings agree with these studies in the sense that RPL4 showed high expression stability, down-regulation of HLA-A can possibly benefit long-term survival (see next section), and that TYRP1 indeed might emerge as a marker for metastases of (thin) melanomas considering it separated our patients in two groups. Thus, again oncologic roles, including for melanoma, have been found for our top expressed response-uniquely mutated genes (SDPD in this case).

Tumour expression landscape

To examine the gene expression landscape, we computed the heatmap for the complete RNA-sequencing dataset and investigated the top expressed genes (top 50) (figure 10). In total 6 mutated genes were present in this top selection. Three of these were SDPD-unique and included HLA-A, HLA-B and RPL4. The three other genes were response-intersecting genes and included HSP90AA1, PABPC1 and FN1. No PRCR-unique genes were present in this top gene criteria. In addition, HLA-A and HLA-B were the only genes identified with somatic mutations that clustered together. Interestingly, from the classical HLA I loci (HLA-A,-B,-C),

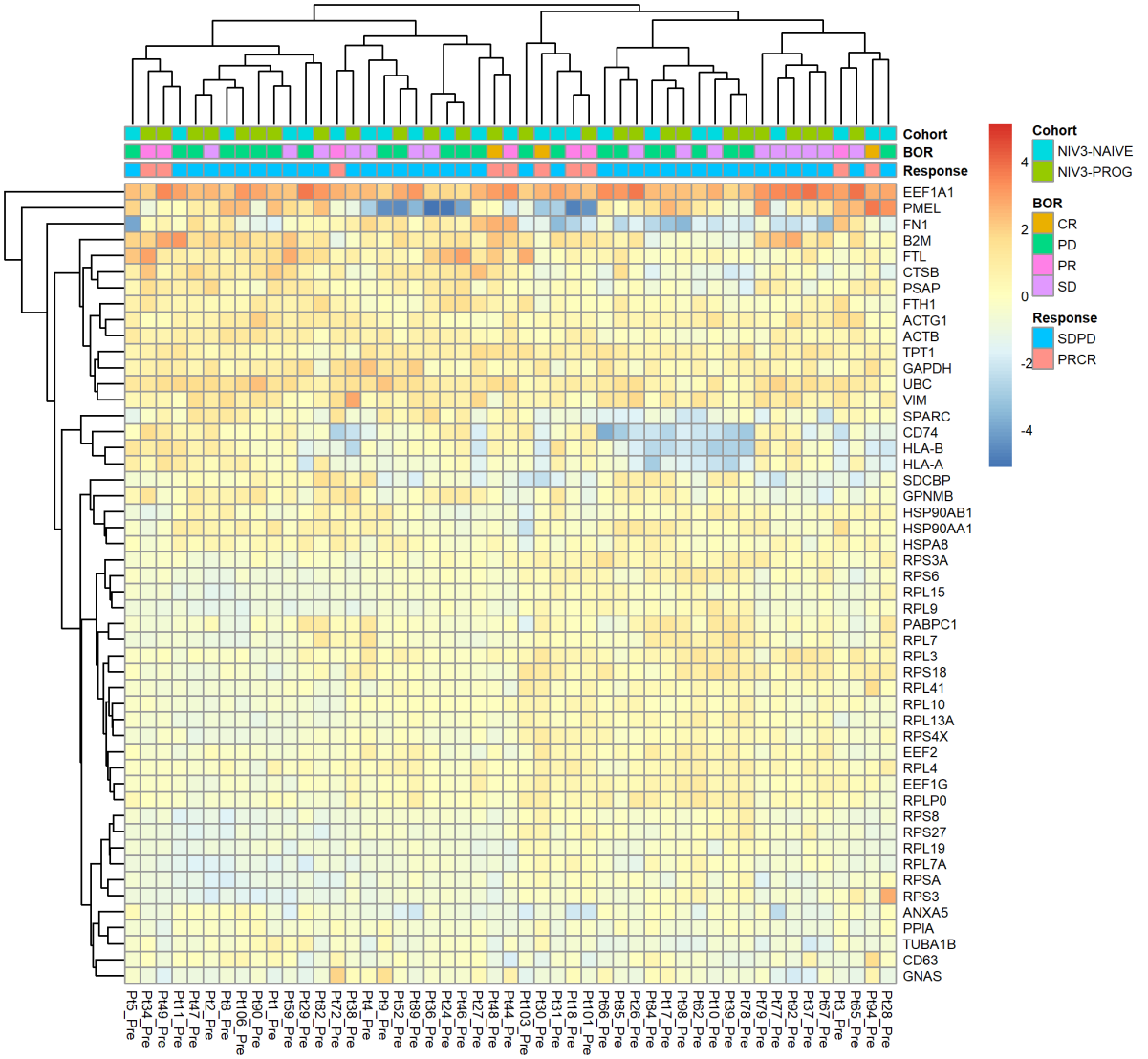

Figure 10: Clustered heatmap of the top 50 highest median expressed genes in the entire RNA-sequencing dataset (n=18194). Values were centred and scaled in the column direction. Both axes show the hierarchical clustering. Cohort, best overall response (BOR) and response group (PRCR or SDPD) are indicated in the top axis for each patient. Red to blue colour scale indicates the gene expression values.

only HLA-C was not found among these top expressed genes. At the same time, three genes were clearly separated: eEF1A1 (eukaryotic elongation factor 1A1), PMEL (Premelanosome Protein), and FN1 (Fibronectin 1). Gene eEF1A1 was highly expressed in *all patients* and had the highest median expression, while PMEL and FN1 showed the greatest variation in up- and down-regulation.

All three have been associated with melanoma. Overexpression of eEF1A1 occurs in melanomas and tumours of the pancreas, breast, lung, prostate, and colon, and therefore supports importance of eEF1A1 in tumorigenesis (Johnsson et al., 2000; Grant et al., 1992; Zhang et al., 1997;Xie et al., 2002; Mohler et al., 2002; de Wit et al., 2002) because of its possibly anti-apoptotic properties in the context of p53-family signalling (Blanch et al., 2013). In the case of PMEL, expression has been found to be significantly higher in both skin cutaneous melanoma (SKCM) and SKCM-metastasis when compared with other cancers (Zhang et al., 2021). More specifically, in SKCM, high PMEL expression associated with poor overall survival, and in both SKCM and SKCM-metastasis patients, PMEL expression even negatively correlated with the infiltration cells of cytotoxic (CD8) T cells, macrophages, and neutrophils. Furthermore, for FN1, small downregulation of FN1 suppressed migration, invasion, adhesion, proliferation capabilities and induced apoptosis of melanoma cells (Li et al., 2019).

Next, to understand how top expressed genes (from figure 10) differ between immunotherapy outcome, we divided the RNA sequencing dataset into two and analysed the top 50 expressed genes per outcome. We check which genes overlap and which do not. As a result, the groups differed by 6 genes. In the case of the PRCR group (Suppl. figure 7) the different genes included COL3A1, HLA-DRA, TMSB4X, RPSA, A2M, LDHA, whilst in the case of the SDPD group (Suppl. figure 8) the different genes were SDCBP, HLA-A, CD63, ANXA5, RPL7A and GNAS. Strikingly, all 12 genes have been associated with melanoma features (Su et al., 2020; Makowiecka et al., 2019; van Tuyn et al., 2017; Simon et al., 1996; Brand et al., 2016; Das et al., 2016; Lupia et al., 2014; Jang & Lee, 2003; Arroyo-Berdugo et al., 2014; Larribère & Utikal., 2020; Marincola et al., 1994; Chen et al., 2019). In the rest of this paper, we will call the set of COL3A1, HLA-DRA, TMSB4X, RPSA, A2M, LDHA genes as the “response-expression-

signature (RES)" and the set of SDCBP, HLA-A, CD63, ANXA5, RPL7A and GNAS genes as "non-response-signature (NRES)".

Finally, three HLAs were important in the top 50 differentially expressed genes from these two response groups: HLA-A, -DRA, and -B. These three showed different behaviours when we compared them. First, the expression of HLA-A did not rank among the top 50 expressed genes for the PRCR group. Support for this behaviour comes from Menon et al. (2002), who reported that down-regulation of HLA-A was their only prognostic factor correlated with a lower tumour stage and longer disease-free survival in (colorectal) cancer patients, and in our case, seemingly important to invoke an anti-melanoma immune response. The second antigen, HLA-DRA, ranked among the top genes of the PRCR group and at the same time was missing in the top of the SDPD, which suggests that presentation of peptide antigens directly to helper (CD4) T cells was more important for the responders to immunotherapy. Finally, because both the PRCR and SDPD group included the class II HLA-B in their top gene sets, the role of antigenic presentation to CD8 T cells and formation of ligands for receptors on NK cells was ambiguous, in line with Marincola et al. (1994) who reported varying expression of HLA-B by melanoma cell lines (cancer) and melanocytes (non-cancer).

Tumour antigenic landscape: HLA and CD antigens

To investigate the complete HLA transcriptional landscape we filtered the RNAseq dataset solely for HLA expressions (figure 11). Interestingly, the classical HLA class I genes still did not cluster together: HLA-C separated from both HLA-A and HLA-B, based on its lower expression. Instead, the cluster exhibiting the highest expression consisted of HLA-A, -B, and -E (class I HLAs) together with HLA-DRA (class II).

There is evidence that HLA-E favours both tumour escape and tumour immune surveillance (Monaco et al., 2011). To find out if this is the case for our patients, we separated the HLA heatmaps per response group. This way we enable HLA clustering per response, so that HLA patterns can differ between the PRCR group (suppl. figure 9) and SDPD group (suppl. figure 10). Yet, both response groups did not show different HLA-E clustering. In both cases HLA-E remained highly expressed and still clustered with HLA-A,-B,-DRA, similar to the combined heatmap of Figure 11, and thus arguably shows dual favourality of HLA-E for immune escape and immune response. The separated HLA heatmaps also showed unchanging HLA-C grouping. Even after separation, it remained relatively lower expressed and separated from

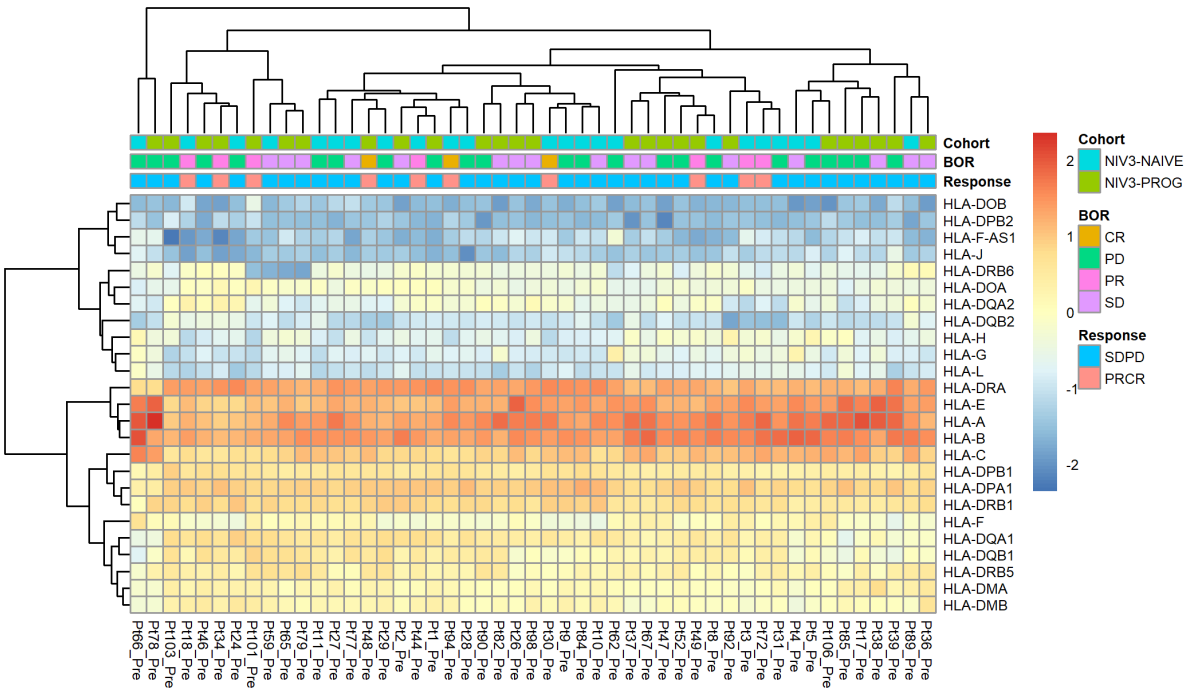

Figure 11: Clustered heatmap of all HLA genes (n=25) in the RNA-sequencing dataset. Values were centred and scaled in the column direction. Both axes show the hierarchical clustering. Cohort, best overall response (BOR) and response group (PRCR or SDPD) are indicated in the top axis for each patient. Red to blue colour scale indicates the gene expression values.

the other highly polymorphic HLA genes (HLA-A,-B, -DRA) where only HLA-E is considered oligomorphic (Parham, 2014).

As expected, heatmaps based on alternative combinations of genes did not improve clustering of response groups. This was true for heatmaps based on mutated HLA genes in the RNA-sequencing dataset (n=8; suppl. figure 11), heatmaps based on human CD antigen genes (n=279; suppl. figure 12), and mutated human CD antigen genes in the RNA-sequencing dataset (n=126; suppl. figure 13), where we also analysed the top 50 genes. These maps did however reveal highly expressed CD antigens (e.g., CD74, CD59, ITGB1, CD63 and CD44; figure 11 and suppl. figure 12) and mutated genes exhibiting high expression (e.g., CD44; suppl. figure 13). Indicating that aside from (mutated) HLA's that also (mutated) CD antigenic genes achieved high expression.

We next analysed the amount of mutations found for HLA, human CD antigen, and PD-1 related genes (suppl. Table 13, 14 and 15, respectively). All HLA mutations occurred on chromosome 6 whereas the mutations of CD antigen genes occurred on a variety of chromosomes. For HLA-genes the total mutations were highest for class II HLA genes (HLA-DR and DQ). In the case of CD antigens, the CD163 and CD163L, which are potential inflammation biomarkers and therapeutic targets (Etzerodt and Moestrup, 2013), mutated the most (high CD163 expression in macrophages is a characteristic of tissues responding to inflammation). Interestingly, PD-L1 (CD274) was not found to have mutated. Even other PD-1 related genes (PD-L2, PD-1, CD96 and CTLA4) mutated in maximum 2 patients, which could imply that these genes are more robust to mutations.

Finally, to understand how HLA relates with other antigens found on the cell surface of leukocytes, we analysed the top 50 genes in a heatmap of HLAs combined with CD antigens (n=294; figure 12). Like before, we focus again on the two clusters with classical class I HLA genes. While the cluster with HLA-C did not include CD antigens, the highest expressed cluster (HLA-A,-B,-E,-DRA) associated with CD74. We separated this heatmap to enable different clustering patterns for the PRCR group (suppl. figure 14) and SDPD group (suppl. figure 15) again. Notably, the results remained the same: HLA-C did not group with antigens and CD74 is still grouped with the high expressed HLA genes. Note that this latter behaviour can also be

seen in figure 10 of the previous section, where we evaluated top 50 genes in the entire RNA-sequencing dataset, and CD74 clustered with HLA-A and HLA-B already. Strikingly, evidence from literature investigating CD74 as a potential therapeutic target in the treatment of melanoma patients supports this response duality (Imaoka et al., 2019; Ekmekcioglu et al., 2016; Ogata et al., 2020). Thus, as for HLE-E in the previous paragraph, response separation showed similar CD74 clustering in both response groups, and therefore also imply dual favouriting for immune escape and immune response linked to this leukocyte antigen.

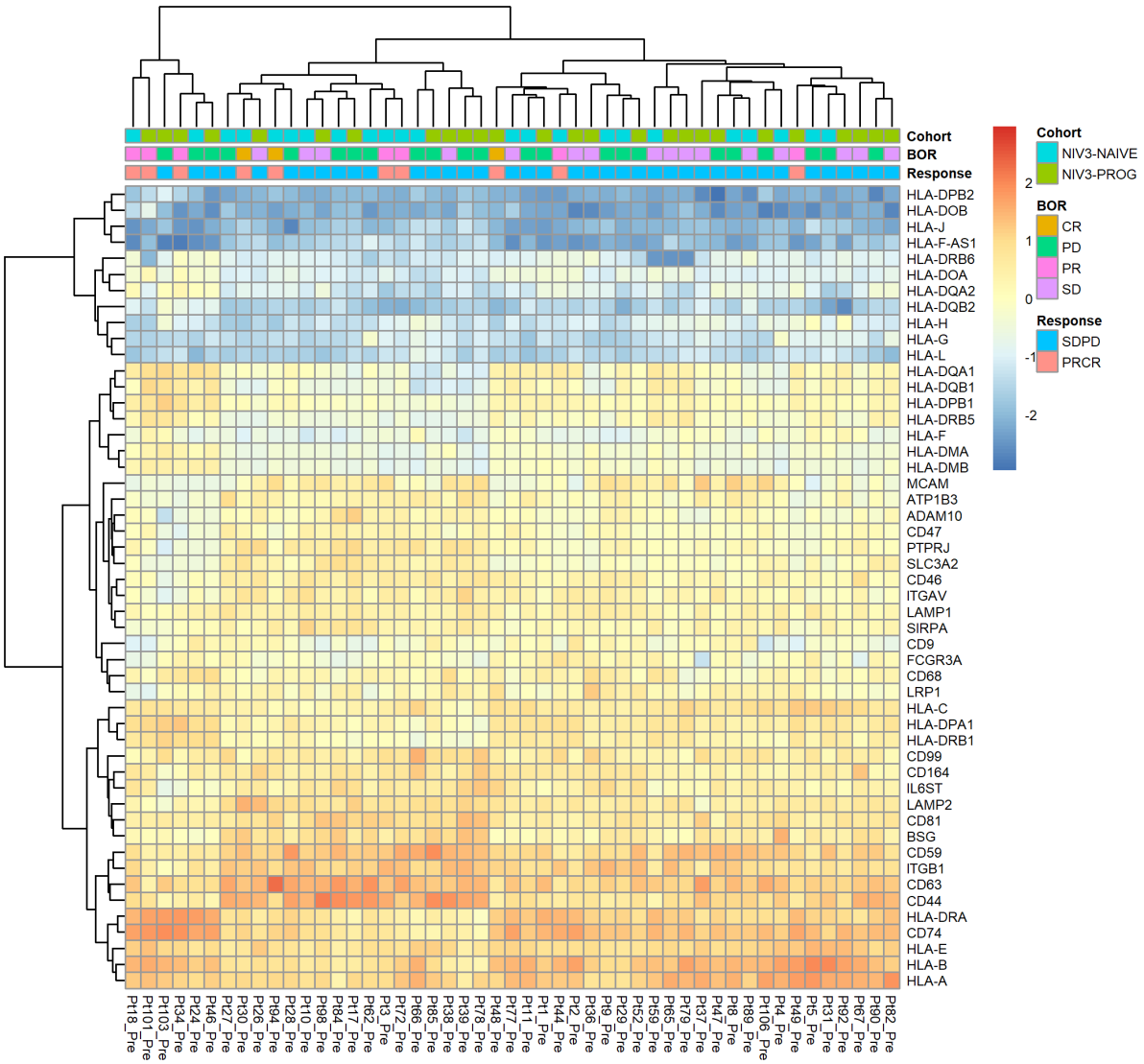

Figure 12: Clustered heatmap of the top 50 highest median expressed genes for the RNA-sequencing dataset only containing HLA (n=25) and human CD antigen genes (n=279). Values were centred and scaled in the column direction. Both axes show the hierarchical clustering. Cohort, best overall response (BOR) and response group (PRCR or SDPD) are indicated in the top axis for each patient. Red to blue colour scale indicates the gene expression values.

Linking DEGs and mutational expression with therapy outcome

It is clear that a single factor is not enough to classify the patients into one group or the other. Instead of focussing on genes individually, we tested for response difference by comparing the expression of genes in groups. To do so, we calculate the median expression for a gene,

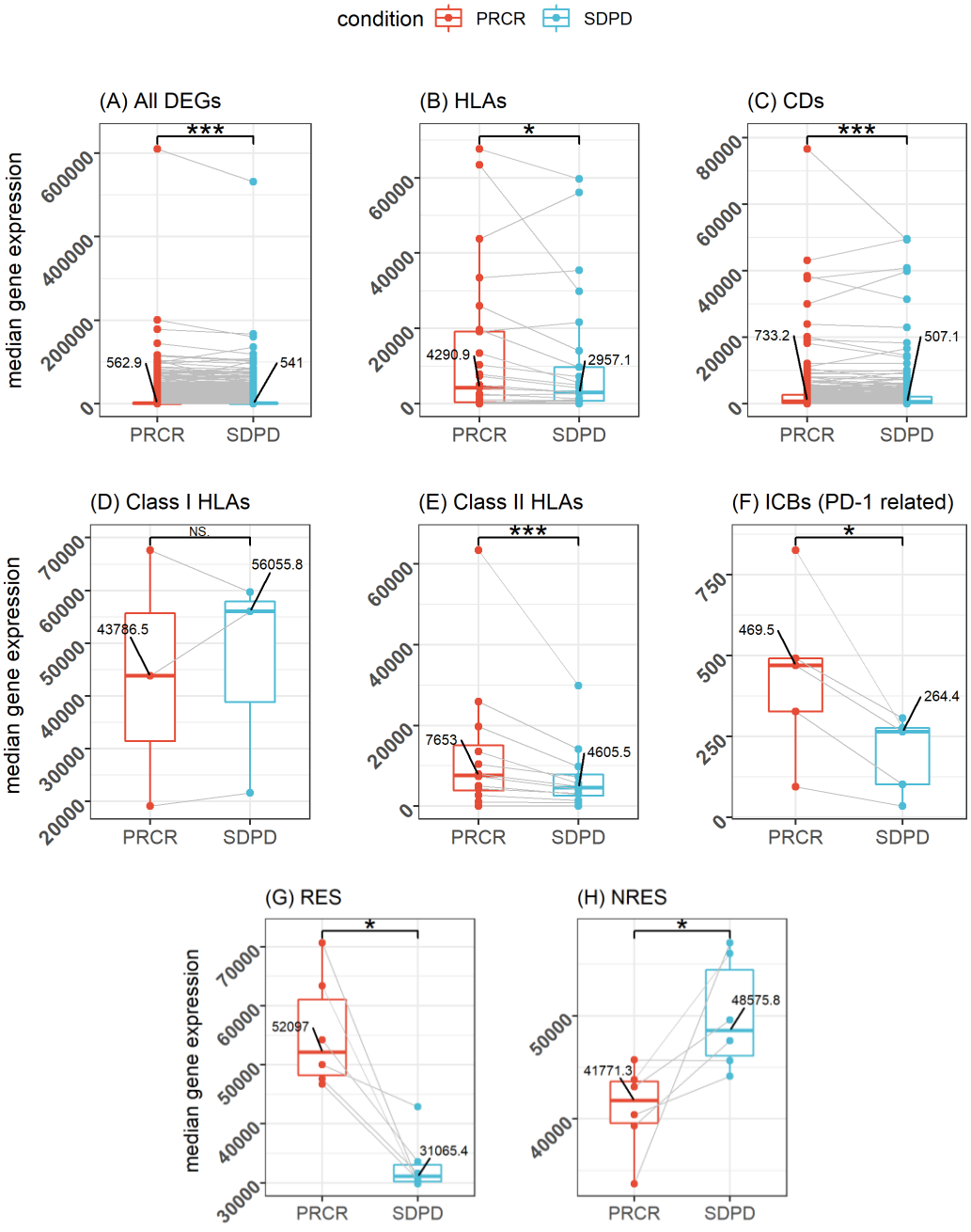

Figure 13: Comparison of two response groups using the median gene expressions. **(A)** Comparison for expression of all genes (n=18194). Alternative hypothesis tested for PRCR > SDPD (p<2.2e-16). **B)** Comparison for expression of all HLA genes (n=25). Alternative hypothesis tested for PRCR > SDPD (p=0.033). **C)** Comparison for expression of all human CD antigen genes (n=279). Alternative hypothesis tested for PRCR > SDPD (p=7.35e-16). **(D)** Comparison for expression of HLA class I genes (n=3: HLA-A, HLA-B and HLA-C; Parham, 2014). Alternative hypothesis tested for both directions (not significant). **(E)** Comparison for expression of HLA class II genes (n=12:

All HLA-D genes from figure 11 except HLA-DQB2, HLA-DQA2, HLA-DPB2; Parham, 2014). Alternative hypothesis tested for PRCR > SDPD (p=2.44e-4). **(F)** Comparison for expression of PD-1 related (co-expressed) genes (n=5: CD96, CTLA4, PD-L1 ,PDCD1 (PD-1), PD-L2). Alternative hypothesis tested for PRCR > SDPD (p=0.032). **(G)** Comparison for RES genes (COL3A1, HLA-DRA, TMSB4X, RPSA, A2M, LDHA). Alternative hypothesis tested for PRCR > SDPD (p=0.016). **(H)** Comparison for NRES genes (SDCBP, HLA-A, CD63, ANXA5, RPL7A, GNAS). Alternative hypothesis tested for PRCR < SDPD (p=0.032). Red indicates genes from patients who responded to treatment. Blue indicates genes from patients who did not respond. All comparisons performed were paired two-sample tests (Wilcoxon). NS: p>0.05, * p < 0.05, ** p < 0.01, and *** p < 0.001.

from all patients, per response, and then compare the expression of these genes in two groups. Afterwards, statistical significance is calculated for various sets of genes by means of two-sample tests (figure 13).

From all tests, the only group of genes that did not prove to result in response differentiation, was the expressional pattern of the class I HLA-genes. This suggests that for differentiating between response at the gene level, antigen presentation to CD8 T cells and formation of NK-ligands for receptors was not significant (figure 13d), which in turn confirms our results from previous section that presentation of peptide antigens directly to CD4 T cells was more important for the responders to immunotherapy (figure 13e). Other groups of genes were all significant for distinguishing an eventual immune response; the DEGs, HLAs, CD antigens, class II HLAs, ICBs (PD-1 related), and RES genes (see tumour mutational landscape 3 sections earlier). Moreover, all these genes were significantly higher in PRCR group than SDPD, except for NRES genes. Here, SDPD expression was greater than PRCR instead (figure 13h). Overall, expressional values thus have mattered for segregating a responsive outcome on the genotypical level.

Additionally, we tested the expression values of mutated genes. Earlier we showed results that validated the average number of mutations per patient per gene as a good predicter for the outcome of therapy (figure 5). Still, it is clearly only one of the factors shaping the outcome as there are several patients with high mutational loads not responding to the immunotherapy as well as patients with low mutational load responding very well. Therefore, we hypothesized that a combination of the gene expression with the amount of mutations might be an even better predictor. To this end, we linked mutated genes with their expression values (figure 14). Response-intersecting, PRCR-unique, and SDPD-unique genes were all significantly different for therapy outcome at genotypical level, with the intersecting genes

having the highest p-value (p<0.001, figure 14a-c). The same was true for immunity related mutations identified by the GO characterizations earlier (figure 14d-f, see suppl. table 9-12 for genes per category). Furthermore, for every test shown, the gene expression of the PRCR group was relatively greater than for the SDPD group, implying that mutated genes (likely T cell targets) generally have been higher expressed in responders.

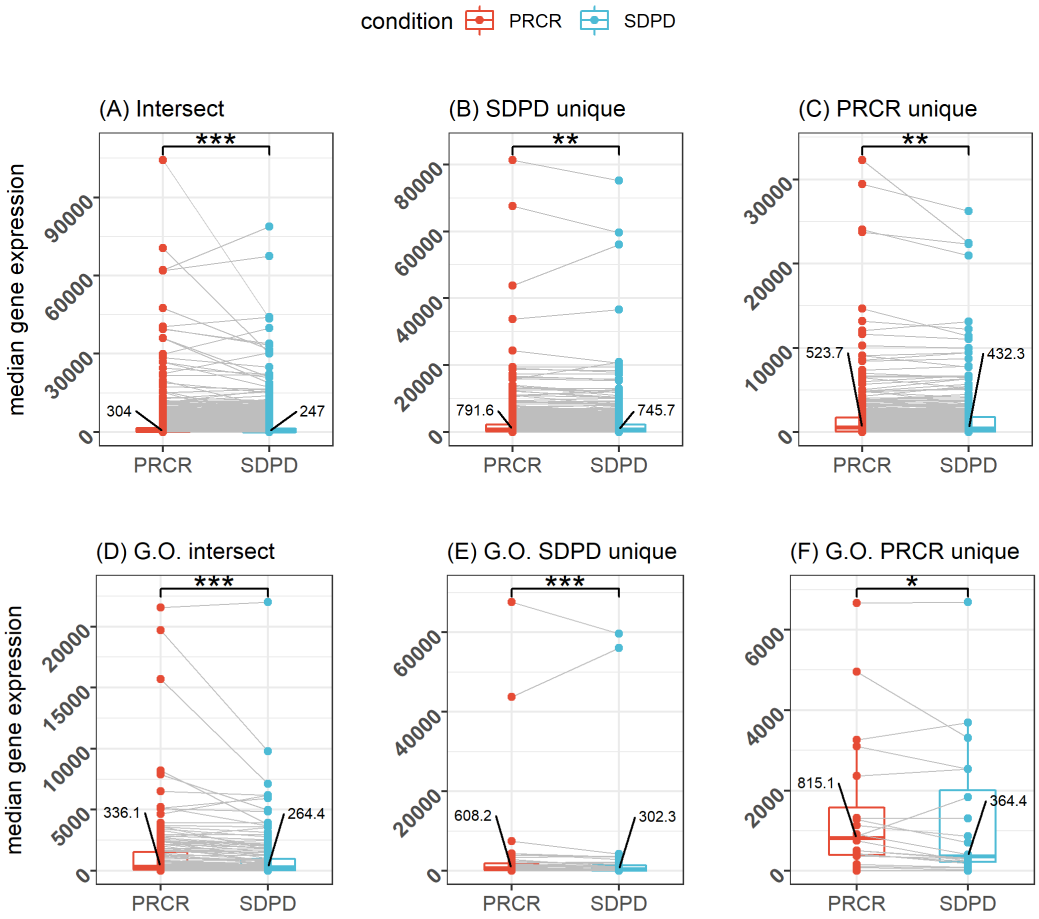

Figure 14: Comparison of two response groups using the gene expressions of the mutated genes. **(A)** Comparison for expression of response-intersecting genes (n=3231). Alternative hypothesis tested for PRCR > SDPD (p<2.2e-16). **(B)** Comparison for expression of SDPD-response-unique genes (SDPD unique=943). Alternative hypothesis tested for PRCR > SDPD (p=0.002). **(C)** Comparison for expression of PRCR-response-unique genes (PRCR unique=334). Alternative hypothesis tested for PRCR > SDPD (p=0.001). **(D)** Comparison for expression of response-intersecting genes related to immunity in GO search (n=147). Alternative hypothesis tested for PRCR > SDPD (p=4.974e-15). **(E)** Comparison for expression of SDPD-response-unique genes related to immunity in GO search (n=39). Alternative hypothesis tested for PRCR > SDPD (non-p=1.511e-4). **(F)** Comparison for expression of PRCR-response-unique genes related to immunity in GO search (n=20). Alternative hypothesis tested for PRCR > SDPD (p=0.013). See suppl. table 9, 10, 11 and 12 for a list of the G.O. related immunity genes used in the tests. All comparisons performed were paired two-sample tests (Wilcoxon). Red indicates genes from patients who responded to treatment. Blue indicates genes from patients who did not respond. * $p < 0.05$, ** $p < 0.01$, and *** $p < 0.001$.

Surprisingly, when we do not compare the same set of genes between each response, but all PRCR unique genes against all SDPD unique genes instead, the expression of response unique genes in SDPD group tests significantly higher than PRCR (Suppl. figure 16). Suggesting that even though there are more T cell targets in the PRCR group, these targets are probably presented in lower copy numbers on the cell surface than in the SDPD group. However, this is likely a bias because there are less PRCR unique genes (943 SDPD unique versus 334 PRCR unique genes).

Linking DEGS and mutational expression at the patient level

To confirm if the underlying tumour mutational expression pattern matter for discriminating response at the patient level (responsive phenotype), we calculated the average gene expression per patient, and then compare the two response groups. We tested the same set of genes from the previous section to assess whether the genes could produce significant results for response differentiation (figure 15). Note that in de previous sections we focussed

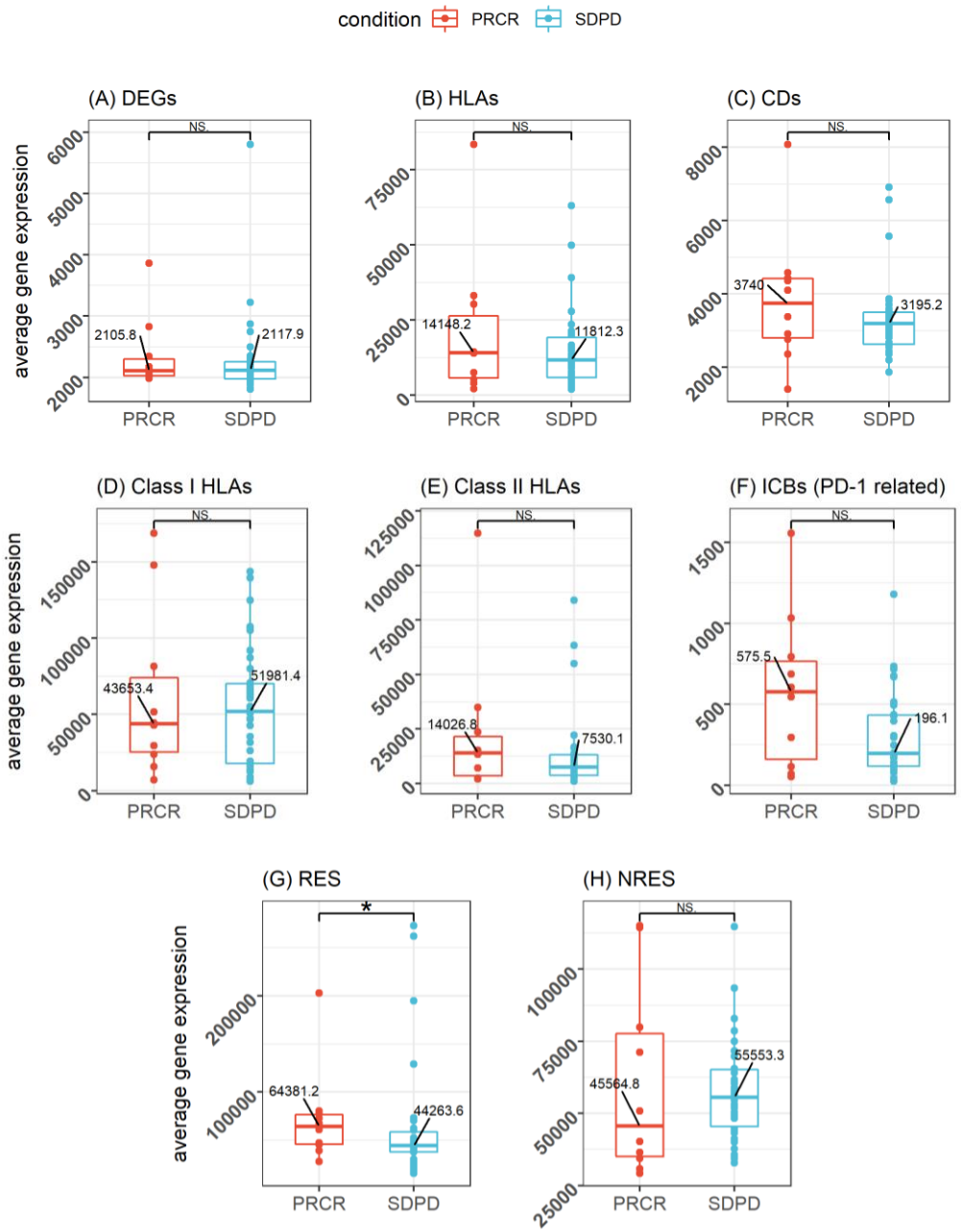

Figure 15: Comparison of two response groups using the average gene expression per patient (n=44). **(A)** Comparison for average expression of all genes (n=18197) per patient. Alternative hypothesis tested for both directions (not significant). **(B)** Comparison for average expression of all HLA genes (n=25) per patient. Alternative hypothesis tested for both directions (not significant). **(C)** Comparison for average expression of human CD

antigen genes (n=279) per patient. Alternative hypothesis tested for both directions (not significant). **(D)** Comparison for average expression of HLA class I genes (n=3: HLA-A, HLA-B and HLA-C; Parham, 2014) per patient. Alternative hypothesis tested for both directions (not significant). **(E)** Comparison for average expression of HLA class II genes (n=12: All HLA-D genes from figure 11 except HLA-DQB2, HLA-DQA2, HLA-DPB2; Parham, 2014) per patient. Alternative hypothesis tested for both directions (not significant). **(F)** Comparison for average expression of PD-1 related (co-expressed) genes (n=5: CD96, CTLA4, PD-L1 ,PDCD1 (PD-1), PD-L2). Alternative hypothesis tested for both directions (not significant). **(G)** Comparison for RES genes (COL3A1, HLA-DRA, TMSB4X, RPSA, A2M, LDHA). Alternative hypothesis tested for PRCR > SDPD (p=0.048). **(H)** Comparison for NRES genes (SDCBP, HLA-A, CD63, ANXA5, RPL7A, GNAS). Alternative hypothesis tested for PRCR < SDPD (not significant). All comparisons performed were non-paired two sample tests (Wilcoxon). Red indicates genes from patients who responded to treatment. Blue indicates genes from patients who did not respond. NS: p>0.05 and * p < 0.05.

median and not the mean expression values because the former described top expressed genes better. From this point on we switch to mean, because outlier values within an individual do not affect calculations for other patients anymore (as much).

Strikingly, the only set of genes that proved to be useful for response prediction were the RES genes: COL3A1, HLA-DRA, TMSB4X, RPSA, A2M, LDHA (figure 15g). The transcriptome, HLAs, CD antigens, both HLA classes, and PD-1 related (ICBs) genes all proved not to be sufficient on the patient level. We next extended this analysis to the mutated genes (figure 16). The results show that response-intersecting, SDPD-unique, PRCR-unique, as well as their immunity genes were equally not adequate enough to describe a difference in responsive versus non-responsive patients

To assess if personalized vaccines for melanoma-cancer immunotherapy would improve our findings we computed the personalized average mutational expression of a patient. That is, the expression of a patient is now averaged only over genes that actually mutate in the individual itself, and not throughout the complete data set. Note that the neoantigens being generated in each patient were correlated to the tumoral mutation load by a ratio of nearly 1:1 (in the first section). Therefore, by calculating the average expression of mutated genes per patient, and then comparing two groups, what we now test is the average expression of the neoantigens being generated in each patient (figure 17). The results show that not the response-intersecting genes (figure 17a), but the response- unique genes (figure 17b) are

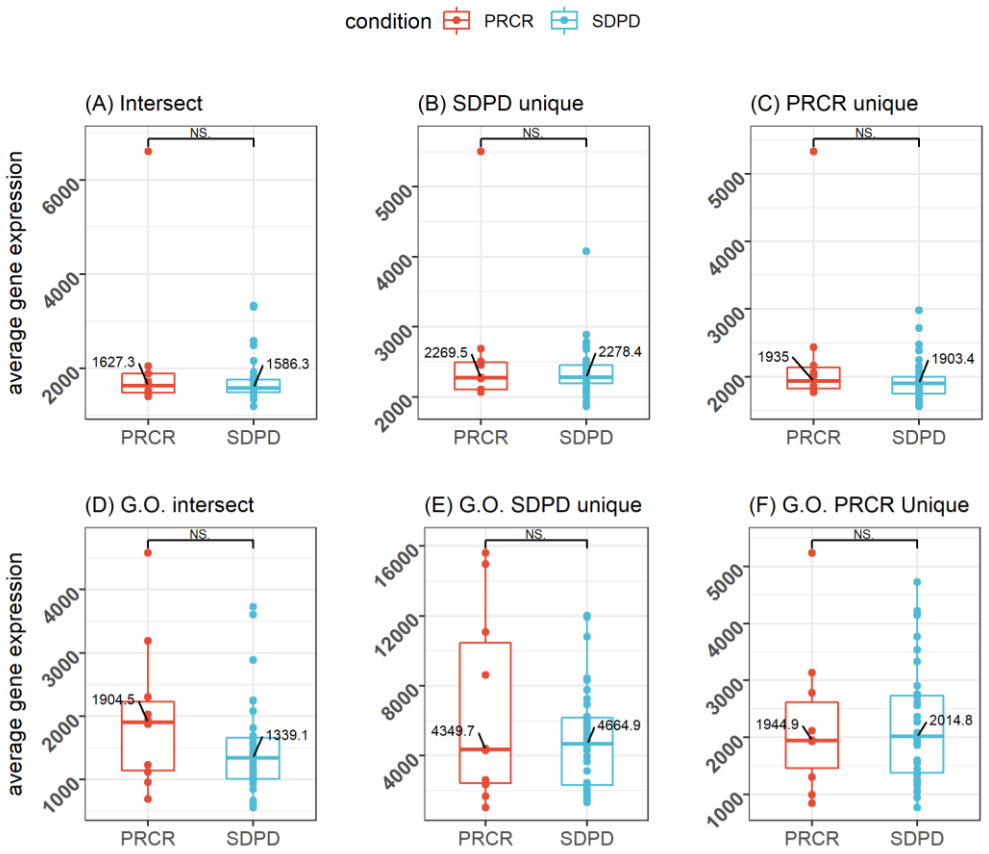

Figure 16: Comparison of two response groups using the average mutational gene expression per patient (n=44). **(A)** Comparison for average expression of all response-intersecting genes (n=4065) per patient. Alternative hypothesis tested for both directions (p=0.376). **(B)** Comparison for average expression of all SDPD-response-unique genes (n=1106) per patient. Alternative hypothesis tested for both directions (p=0.484). **(C)** Comparison for average expression of all PRCR-response-unique genes (n=147) per patient. Alternative hypothesis tested for both directions (p=0.184). **(D)** Comparison for average expression of response-intersecting genes related to immunity in GO search (n=147) per patient. Alternative hypothesis tested for both directions (p=0.184). **(E)** Comparison for average expression of SDPD-response-unique genes related to immunity in GO search (n=39). Alternative hypothesis tested for both directions (p=0.355). **(F)** Comparison for average expression of SDPD-response-unique genes related to immunity in GO search (n=20). Alternative hypothesis tested for both directions (p=0.44). See suppl. table 9, 10, 11 and 12 for a list of the G.O. related immunity genes used in the tests. All comparisons performed were non-paired two-sample test (Wilcoxon). Red indicates genes from patients who responded to treatment. Blue indicates genes from patients who did not respond. NS: p>0.05.

important for differentiation response at the (personalized) patient level. Importantly, our results here point out that within the mutational landscape of a patient, only a selection of the mutational expressions are insightful for predicting response, here characterized as the individual's exome excluding our response-intersecting genes. In short, our findings expose that only a part of the underlying gene expression from non-synonymous mutations (exomic landscape) of a patient should appeal to personalized vaccines as suggested by ahin and Türeci, 2018.

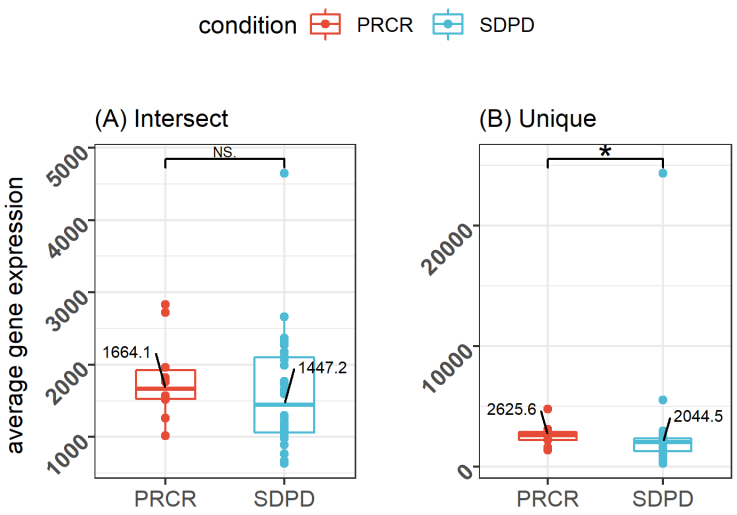

Figure 17: Comparison of two response groups using the average gene expression of mutated genes within one patient. **(A)** Comparison for average expression of personal response-intersecting genes per patient (n=44). Alternative hypothesis tested for both directions (not significant). **(B)** Comparison for average expression of personal response-unique per patient (n=42). Alternative hypothesis tested for PRCR > SDPD (p=0.016). Both comparisons performed were non-paired two-sample test (Wilcoxon). Red indicates genes from patients who responded to treatment. Blue indicates genes from patients who did not respond. NS: $p>0.05$ and * $p < 0.05$.

Discussion

Here we present our computational analysis with a focus on identifying biomarkers to stratify the outcome to immunotherapy in melanoma patients. Throughout literature there is numerous support for TMB to be a good measure for tumour immunogenicity assessment, and subsequently response differentiation in ICB. Our findings confirm this to be the case for responders in this study as well. Specifically, after we analysed the exomic profile of the non-synonymous mutations we show that the genes of patients with a response to the therapy have on average more mutations (SNVs) than patients without a response (figure 5). For these patients with a responsive outcome we can argue in favour of a higher mutational load that generates more T cell targets and consequently stimulates anti-tumour T cell responses, which in turn contributes to the success of the immunotherapies. Non-responding patients however also achieved high TMB and neo-antigenic lead, comparable with high levels in responders. For this reason, we set out to search for other biomarkers than the TMB.

By characterizing the genes that mutate only in one response group (figure 4, suppl. figure 1), we confirm that the underlying gene expression of mutations contains high expressed genes (suppl. figure 3, 4 and 6), which throughout literature also find support for being melanoma related. Still, even though characterization of the response-unique genes reveal mutations which are exclusive to a response group, both groups mainly related to similar processes according to five different GO queries (figure 6-9, suppl. figure 2 and 5).

What matters most for a response to control cancer, the number of T cell targets (i.e., mutations) or how well these targets are expressed? On the genotypic level, both show importance. First, for the expressions, genes were significantly different between response, except for the class I HLAs (figure 13d). Despite that the class I HLA genes did not significantly differ between response; all other sets of genes did, including the class II HLA genes (figure 13e). This implies that antigenic peptide presentation directly to CD4 T cells, and not CD8, was more important for invoking an immune response. Second, for the mutations, all mutation categories tested significantly different (figure 14). The mutations of response-intersecting, response-unique, and the immune-related-GO mutations all were important at the gene level.

Since only class I HLA genes did not differentiate response, we propose that this is the result of immune evasion mechanisms. The reason is as follows. During the assessment of the tumour antigenic landscape we noticed signs supporting both immune response evasion versus immune response evocation (figure 10): we separated the heatmap of HLA (and later with CD antigens) by the two response groups and found that HLA-E, HLA-C and CD74 exhbit similar cluster behaviour in both (figure 11 and 12, respectfully), even when taken apart from each other (suppl. figure 9, 10, 14 and 15). Interestingly, melanoma literature associated with these genes impose a duality for response. We here describe these scenarios for HLA-E with HLA-C, and afterwards for CD74.

A common feature of immune escape in virus-infected cells and tumours is insensitivity of natural killer (NK) cells to selective loss of expression of a particular class I locus (Parham, 2014). In short, NK cells assess the quantity of HLA-A,-B, and -C in a potential target cell by the amount of HLA-E at the cell's surface and uses this a measure of 'health'. For healthy target cells expressing normal levels of HLA-E, an inhibitory signal prevents the NK cell from attacking, and if the NK cell finds an unhealthy cell with deficient expression of HLA-E, the NK-cell's cytotoxic machinery is mobilized and kills the unhealthy cell (infection and malignancy frequently reduce the cell-surface expression of MHC molecules). In addition, the expression of HLA-C is at one-tenth level of HLA-A and HLA-B. Thus, a selective loss (depletion) of HLA-C would reduce the total amount of HLA class I only slightly (9% according to Parham, 2014).

We cannot confirm HLA-C reduction upon melanoma progression for our analysis because our measurements are from one time point only. However, the lower expression of HLA-C, compared to other highly polymorphic HLAs, is suggestive (figure 11). According to literature, as an immune evasion phenotype, a selective loss of HLA-A,-B, and -C alleles is suggested to alleviate competition for β2m, allowing ligand donation from relieved class I allele(s) in amounts sufficient to stabilize HLA-E, enhance HLA-E's surface expression, engage the inhibitory NKG2A receptor, and further promote immune escape. Eventually, contributing to protection of tumour cells from lysis by NK cells (Monaco et al., 2011).

However, some state a problem with this view of the inhibitory mechanism (Tremante et al., 2014). What is more, there are opposing studies where high HLA-E seems to correlate with

good, and not poor, prognosis in melanoma (John et al., 2008, Mandruzato et al., 2006). These show that at the same time HLA-E is apparently a very efficient mechanism in some tumours, with a positive role for immune response and survival (Monaco et al., 2011). Our analysis can agree with both scenarios; immunotherapy patients had high HLA-E levels but no anti-tumour response, and immunotherapy patients had high HLA-E levels, and yet still produced an immune response. Hence, studies where HLA-E is seemingly widely expressed or upregulated in human tumours or malignant tissues, are difficult to match with opposing reports, describing low surface expression or down-regulation of HLA-E in melanoma (Derré et al., 2006; Marín et al., 2003; Palmisano et al., 2005, Monaco et al., 2011; Tremante et al., 2014).

This dual sided role of HLA-E has also implications for the two statements from earlier: (1) that NK cells are insensitive to selective loss of expression of a particular class I locus (HLA-C) (2) and that NK cells kill target cells with deficient expression of HLA-E. According to the findings from Tremante et al. (2014), compared to melanocytes, HLA-E is relatively up-regulated in melanoma, both in tissues and on the cell surface. The study shows that melanocytes express very low (if any) levels of surface HLA-E whilst remain harmless from NK cell lysis. More, though lytic enhancements were only evident in 30% in melanoma cultures, and no effect was found in melanocyte cultures (0%), this so-called elective melanoma killing does not appear to correlate with HLA-E surface level (in the cases that had lytic effect). Suggesting that NK lysis works via an HLA-E-independent mechanism (Palmisano et al., 2005, Monaco et al., 2011; Tremante et al., 2014). Further research should be done for more clarification between these duplicities in results.

We tried to address this issue by looking at the HLA in combination with CD antigens to include a broader range of leukocyte antigens (figure 12). However, CD74 in the separated heatmaps of the response groups also imply a dual favourality for immune escape and immune response (in both cases it clustered the same, only with HLA-DRA). To illustrate, a significant correlation has been shown between the expression levels of PD-L1 and CD74 in melanoma tissue samples (Imaoka et al., 2019). The expression of PD-L1 on tumour cells can contribute to cancer immune evasion by interacting with PD-1 on immune cells (Wu et al., 2015). Moreover, PD-L1 is mediated by MIF-CD74 interactions which directly regulate its expression, implying that activation of the MIF-CD74 interaction plays a (critical) role in melanoma cells, and helps

(tumour cells) escape from antitumorigenic immune responses by causing immune evasion (Imaoka et al., 2019).

Blocking this MIF-CD74 signalling is therefore supported by (1) Figueiredo et al. (2018) where MIF–CD74 interference on macrophage and dendritic cells, decreases expression of immunosuppressive factors from macrophages, and increases the capacity of dendritic cells to activate cytotoxic T cells. Note that dendritic and macrophage cells both express CD74, the main MIF receptor (Su et al., 2017). Blocking is also noted by (2) de Azevedo et al. (2020) where MIF-CD74 signal inhibition combined with ipilimumab, enhanced T-cell infiltration (increased CD8 TIL), and eventually reduces PD-L1 expression in resistant melanoma cells.

However, also with these anti-tumour-invoking findings there is a dispute. One is that although (innate and adaptive) immunity is mobilized after MIF-CD74 (axis) inhibition, other pathways that can possibly contribute to restore the immunogenicity of the tumour cannot be ruled out. Even more opposing are inflammatory marker tests that report prognostic value for high CD74 (as a useful tumour cell protein marker). Namely, (1) in melanoma tumour cells from stage III melanoma patients, higher CD74 percentage or intensity of protein expression associated with longer survival (Ekmekcioglu et al., 2016), (2) in stage IV melanoma patients, only high expression (above median) of CD74 expression associated with good survival and better prognosis prediction, when compared with low (below median) expression (Ogata et al., 2020). For these oppositions, further research is also necessary.

So what matters for an immune response? Eventually, two approaches generated a result that was significant for response stratification on both the genotypical as well as patient level. The first is the set of six genes (RES) which included COL3A1, HLA-DRA, TMSB4X, RPSA, A2M, LDHA (figure 15g). All have been reported about in other melanoma-related studies (Su et al., 2020; van Tuyn et al., 2017, Makowiecka et al., 2019; Zhou et al., 2014; Simon et al., 1996; Brand et al., 2016). The second is the unique mutations in a patient (figure 17b). As a static set of genes, like above, the somatic mutations do not differentiate response at gene and patient level simultaneously. However, by only selecting the average expression of response-unique mutations that actually occur in a patient, the response division tests significant. Thus,

response prediction based on mutations, should be done without the response-intersecting part that we identified.

Additional improvements can be made by performing our response-unique-revealing data transformation on other and larger cancer-datasets. Likewise, gene-network and single cell sequencing analysis might provide more understanding of the underlying gene expression dynamics, related to response-unique mutated genes. A limiting factor in this study is the sample size i.e.., the total amount of patients (figure 1). Fortunately, despite the limited size, we find nearly consistent results as large-scale studies with over 100's of patient. For example, compared to TCGA studies by Kang et. al (2020) and Zhang et. al (2021) whom looked at 467 and 472 melanoma patients, respectively, we find nearly the same top frequently mutated melanoma genes (8 out of their top 10, with the other 2 ranked lower here) and the same top type of variant (missense) (table 1, suppl. table 1-4). More, we extend these findings by assessing the chromosomes and splitting the results for therapy outcome (suppl. table 3). Satisfying is that we identify highly expressed genes likely related to melanoma and sometimes even broader oncological relevance (see references in sections of PRCR- and SDPD-unique characterizations and heatmaps).

Ultimately, because the neo-antigens and tumour mutations were nearly linearly related (figure 2a), we extrapolate the results from the expressions to the neo-antigens, and propose that the average expression of the neo-antigens being generated by the patient's unique part of mutations, is a significant TMB extension to describe our patients' immune response. In support of personalized inoculations (Sahin and Türeci, 2018). We also suggest that further research is needed to elaborate on the combined eff ect of the RES genes COL3A1, HLA-DRA, TMSB4X, RPSA, A2M, LDHA.

Conclusion

To summarize, the data presented here demonstrate that the TMB is a good marker for immunotherapeutic efficacy. Non-responding patients to immunotherapy sometimes show similar levels of neoantigens and tumour mutational load, whereas responding patients likewise sometimes exhibit low mutational load, complicating interpretation of the marker. We quantitated the neo-antigens, the SNVs, tumour gene expressions, and tried to understand if a single factor can explain this problem. Instead, a set of six genes, and the response-unique part of a patient's mutations, help to distinguish response prediction. Our results are shown for responding, non-responding, Nivolumab-naïve, and Nivolumab-progressed patients. Hence, our findings also relate to more resistance to immune checkpoint blockade. Finally, aside from the average expression of neo-antigens (possible T cell targets), we demonstrate that a part of the underlying tumour expression pattern facilitates an outcome of the immunotherapies, and subsequently, should be considered to predict the response to immunotherapy.

References

Ajona, Daniel, et al. "A combined PD-1/C5a blockade synergistically protects against lung cancer growth and metastasis." Cancer discovery 7.7 (2017): 694-703.

Anagnostou, Valsamo, et al. "Integrative tumor and immune cell multi-omic analyses predict response to immune checkpoint blockade in melanoma." Cell Reports Medicine 1.8 (2020): 100139.

Arroyo-Berdugo, Yoana, et al. "Involvement of ANXA5 and ILKAP in susceptibility to malignant melanoma." Plos one 9.4 (2014): e95522.

Brand, Almut, et al. "LDHA-associated lactic acid production blunts tumor immunosurveillance by T and NK cells." Cell metabolism 24.5 (2016): 657-671.

Blanch, Alvaro, et al. "Eukaryotic translation elongation factor 1-alpha 1 inhibits p53 and p73 dependent apoptosis and chemotherapy sensitivity." PLoS One 8.6 (2013): e66436.

Blum, Amy, Peggy Wang, and Jean C. Zenklusen. "SnapShot: TCGA-analyzed tumors." Cell 173.2 (2018): 530-530.

Chan, Timothy A., et al. "Development of tumor mutation burden as an immunotherapy biomarker: utility for the oncology clinic." Annals of Oncology 30.1 (2019): 44-56.

Chen, Daniel S., and Ira Mellman. "Oncology meets immunology: the cancer-immunity cycle." immunity 39.1 (2013): 1-10.

Chen, Pei-Ling, et al. "Analysis of immune signatures in longitudinal tumor samples yields insight into biomarkers of response and mechanisms of resistance to immune checkpoint blockade." Cancer discovery 6.8 (2016): 827-837.

Chen, Yang-Yi, et al. "Expressions of HLA class II genes in cutaneous melanoma were associated with clinical outcome: bioinformatics approaches and systematic analysis of public microarray and RNA-Seq Datasets." Diagnostics 9.2 (2019): 59.

Cristescu, Razvan, et al. "Pan-tumor genomic biomarkers for PD-1 checkpoint blockade–based immunotherapy." Science 362.6411 (2018).

Das, Swadesh K., et al. "Knockout of MDA-9/Syntenin (SDCBP) expression in the microenvironment dampens tumor-supporting inflammation and inhibits melanoma metastasis." Oncotarget 7.30 (2016): 46848.

de Azevedo, Ricardo A., et al. "MIF inhibition as a strategy for overcoming resistance to immune checkpoint blockade therapy in melanoma." Oncoimmunology 9.1 (2020): 1846915.

de Wit, Nicole JW, et al. "Differentially expressed genes identified in human melanoma cell lines with different metastatic behaviour using high density oligonucleotide arrays." Melanoma research 12.1 (2002): 57-69.

Derré, Laurent, et al. "Expression and release of HLA-E by melanoma cells and melanocytes: potential impact on the response of cytotoxic effector cells." The Journal of Immunology 177.5 (2006): 3100-3107.

Eggermont, Alexander MM, Marka Crittenden, and Jennifer Wargo. "Combination immunotherapy development in melanoma." American Society of Clinical Oncology Educational Book 38 (2018): 197-207.

Ekmekcioglu, Suhendan, et al. "Inflammatory marker testing identifies CD74 expression in melanoma tumor cells, and its expression associates with favorable survival for stage III melanoma." Clinical Cancer Research 22.12 (2016): 3016-3024.

Etzerodt, Anders, and Søren K. Moestrup. "CD163 and inflammation: biological, diagnostic, and therapeutic aspects." Antioxidants & redox signaling 18.17 (2013): 2352-2363.

Figueiredo, Carlos R., et al. "Blockade of MIF–CD74 signalling on macrophages and dendritic cells restores the antitumour immune response against metastatic melanoma." Frontiers in immunology 9 (2018): 1132.

Forschner, Andrea, et al. "Tumor mutation burden and circulating tumor DNA in combined CTLA-4 and PD-1 antibody therapy in metastatic melanoma–results of a prospective biomarker study." Journal for immunotherapy of cancer 7.1 (2019): 1-15.

Grant, Anne G., et al. "Differential screening of a human pancreatic adenocarcinoma λgt11 expression library has identified increased transcription of elongation factor ef-1α in tumour cells." International journal of cancer 50.5 (1992): 740-745.

Hamid, O., et al. "Five-year survival outcomes for patients with advanced melanoma treated with pembrolizumab in KEYNOTE-001." Annals of Oncology 30.4 (2019): 582-588.

Heydt, Carina, et al. "Analysis of tumor mutational burden: correlation of five large gene panels with whole exome sequencing." Scientific Reports 10.1 (2020): 1-10.

Hu, Hongli, et al. "Acetylation of PGK1 promotes liver cancer cell proliferation and tumorigenesis." Hepatology 65.2 (2017): 515-528.

Hugo, Willy, et al. "Genomic and transcriptomic features of response to anti-PD-1 therapy in metastatic melanoma." Cell 165.1 (2016): 35-44.

Iengar, Prathima. "An analysis of substitution, deletion and insertion mutations in cancer genes." Nucleic acids research 40.14 (2012): 6401-6413.

Imaoka, Masako, et al. "Macrophage migration inhibitory factor-CD 74 interaction regulates the expression of programmed cell death ligand 1 in melanoma cells." Cancer science 110.7 (2019): 2273-2283.

Jang, Hwa-In, and Hansoo Lee. "A decrease in the expression of CD63 tetraspanin protein elevates invasive potential of human melanoma cells." Experimental & molecular medicine 35.4 (2003): 317-323.

Janik, Marcelina E., et al. "RT-qPCR analysis of human melanoma progression-related genes–A novel workflow for selection and validation of candidate reference genes." The international journal of biochemistry & cell biology 101 (2018): 12-18.

Jardim, Denis L., et al. "The challenges of tumor mutational burden as an immunotherapy biomarker." Cancer cell (2020).

John, Thomas, et al. "Predicting clinical outcome through molecular profiling in stage III melanoma." Clinical Cancer Research 14.16 (2008): 5173-5180.

Johnsson, A., et al. "Identification of genes differentially expressed in association with acquired cisplatin resistance." British journal of cancer 83.8 (2000): 1047-1054.

Journe, Fabrice, et al. "TYRP1 mRNA expression in melanoma metastases correlates with clinical outcome." British journal of cancer 105.11 (2011): 1726-1732.

Kaczorowski, Maciej, et al. "Low RhoA expression is associated with adverse outcome in melanoma patients: a clinicopathological analysis." American journal of translational research 11.7 (2019): 4524.

Kandoth, Cyriac, et al. "Mutational landscape and significance across 12 major cancer types." Nature 502.7471 (2013): 333-339.

Kang, Kai, et al. "Significance of tumor mutation burden in immune infiltration and prognosis in cutaneous melanoma." Frontiers in oncology 10 (2020).

Kim, Saetbyul, et al. "Metastasis prognostic factors and cancer stem cell-related transcription factors associated with metastasis induction in canine metastatic mammary gland tumors." Journal of Veterinary Science 22.5 (2021).

Larkin, James, et al. "Five-year survival with combined nivolumab and ipilimumab in advanced melanoma." New England Journal of Medicine 381.16 (2019): 1535-1546.

Larribère, Lionel, and Jochen Utikal. "Update on GNA alterations in cancer: Implications for uveal melanoma treatment." Cancers 12.6 (2020): 1524.

Linares, Miguel A., Alan Zakaria, and Parminder Nizran. "Skin cancer." Primary care 42.4 (2015): 645-659.

Litchfield, Kevin, et al. "Meta-analysis of tumor-and T cell-intrinsic mechanisms of sensitization to checkpoint inhibition." Cell 184.3 (2021): 596-614.

Li, Bifei, et al. "Fibronectin 1 promotes melanoma proliferation and metastasis by inhibiting apoptosis and regulating EMT." OncoTargets and therapy 12 (2019): 3207.

Liu, Hui, et al. "Cold shock domain containing E1 (CSDE1) protein is overexpressed and can be targeted to inhibit invasiveness in pancreatic cancer cells." Proteomics 20.10 (2020): 1900331.

Lupia, Antonella, et al. "CD63 tetraspanin is a negative driver of epithelial-to-mesenchymal transition in human melanoma cells." Journal of Investigative Dermatology 134.12 (2014): 2947-2956.

Makowiecka, Aleksandra, et al. "Thymosin β4 regulates focal adhesion formation in human melanoma cells and affects their migration and invasion." Frontiers in cell and developmental biology 7 (2019): 304.

Mariathasan, Sanjeev, et al. "TGFβ attenuates tumour response to PD-L1 blockade by contributing to exclusion of T cells." Nature 554.7693 (2018): 544-548.

Marín, Rosario, et al. "Analysis of HLA-E expression in human tumors." Immunogenetics 54.11 (2003): 767-775.

Marincola, Francesco M., et al. "Loss of HLA haplotype and B locus down-regulation in melanoma cell lines." The journal of Immunology 153.3 (1994): 1225-1237.

Marzagalli, Monica, Nancy D. Ebelt, and Edwin R. Manuel. "Unraveling the crosstalk between melanoma and immune cells in the tumor microenvironment." Seminars in cancer biology. Vol. 59. Academic Press, 2019.

Mathivanan, Suresh, and Richard J. Simpson. "ExoCarta: A compendium of exosomal proteins and RNA." Proteomics 9.21 (2009): 4997-5000.

McGranahan, Nicholas, et al. "Clonal status of actionable driver events and the timing of mutational processes in cancer evolution." Science translational medicine 7.283 (2015): 283ra54-283ra54.

Menon, Anand G., et al. "Down-regulation of HLA-A expression correlates with a better prognosis in colorectal cancer patients." Laboratory investigation 82.12 (2002): 1725-1733.

Mohler, James L., et al. "Identification of differentially expressed genes associated with androgen-independent growth of prostate cancer." The Prostate 51.4 (2002): 247-255.

Monaco, Elisa Lo, et al. "Human leukocyte antigen E contributes to protect tumor cells from lysis by natural killer cells." Neoplasia 13.9 (2011): 822-IN14.

Morrison, Carl, et al. "Predicting response to checkpoint inhibitors in melanoma beyond PD-L1 and mutational burden." Journal for immunotherapy of cancer 6.1 (2018): 1-12.

Mulnix, Richard E., et al. "hnRNP C1/C2 and Pur-beta proteins mediate induction of senescence by oligonucleotides homologous to the telomere overhang." OncoTargets and therapy 7 (2014): 23.

Ogata, Dai, et al. "The expression of cd74-regulated inflammatory markers in stage iv melanoma: Risk of cns metastasis and patient survival." Cancers 12.12 (2020): 3754.

Ottolini, Barbara, et al. "Multiple mutations at exon 2 of RHOA detected in plasma from patients with peripheral T-cell lymphoma." Blood advances 4.11 (2020): 2392-2403.

Palmisano, Giulio Lelio, et al. "HLA-E surface expression is independent of the availability of HLA class I signal sequence-derived peptides in human tumor cell lines." Human immunology 66.1 (2005): 1-12.

Parham, Peter. The immune system. Garland Science, 2014.

Razzak, Mina. "Anti-PD-1 approaches—important steps forward in metastatic melanoma." Nature reviews Clinical oncology 10.7 (2013): 365-365.

Riaz, Nadeem, et al. "Tumor and microenvironment evolution during immunotherapy with nivolumab." Cell 171.4 (2017): 934-949.

Rizvi, Naiyer A., et al. "Mutational landscape determines sensitivity to PD-1 blockade in non–small cell lung cancer." Science 348.6230 (2015): 124-128.

Sade-Feldman, Moshe, et al. "Defining T cell states associated with response to checkpoint immunotherapy in melanoma." Cell 175.4 (2018): 998-1013.

Sahin, Ugur, and Özlem Türeci. "Personalized vaccines for cancer immunotherapy." Science 359.6382 (2018): 1355-1360.

Schreuer, Max, et al. "Combination of dabrafenib plus trametinib for BRAF and MEK inhibitor pretreated patients with advanced BRAFV600-mutant melanoma: an open-label, single arm, dual-centre, phase 2 clinical trial." The Lancet Oncology 18.4 (2017): 464-472.

Schumacher, Ton N., Can Kesmir, and Marit M. van Buuren. "Biomarkers in cancer immunotherapy." Cancer cell 27.1 (2015): 12-14.

Schumacher, Ton N., and Robert D. Schreiber. "Neoantigens in cancer immunotherapy." Science 348.6230 (2015): 69-74.

Sha, Dan, et al. "Tumor mutational burden as a predictive biomarker in solid tumors." Cancer discovery 10.12 (2020): 1808-1825.

Simon, Hans-Georg, et al. "Identification of differentially expressed messenger RNAs in human melanocytes and melanoma cells." Cancer research 56.13 (1996): 3112-3117.

Su, Huiting, et al. "The biological function and significance of CD74 in immune diseases." Inflammation Research 66.3 (2017): 209-216.

Su, Wenxing, et al. "Bioinformatic analysis reveals hub genes and pathways that promote melanoma metastasis." BMC cancer 20.1 (2020): 1-10.

Subramanian, Aravind, et al. "GSEA-P: a desktop application for Gene Set Enrichment Analysis." Bioinformatics 23.23 (2007): 3251-3253.

Tremante, Elisa, et al. "A melanoma immune response signature including Human Leukocyte Antigen-E." Pigment cell & melanoma research 27.1 (2014): 103-112.

Tumeh, Paul C., et al. "PD-1 blockade induces responses by inhibiting adaptive immune resistance." Nature 515.7528 (2014): 568-571.

Van Allen, Eliezer M., et al. "Genomic correlates of response to CTLA-4 blockade in metastatic melanoma." Science 350.6257 (2015): 207-211.

Van Tuyn, John, et al. "Oncogene-expressing senescent melanocytes up-regulate MHC class II, a candidate melanoma suppressor function." Journal of Investigative Dermatology 137.10 (2017): 2197-2207.

Wang, F., et al. "Safety, efficacy and tumor mutational burden as a biomarker of overall survival benefit in chemo-refractory gastric cancer treated with toripalimab, a PD-1 antibody in phase Ib/II clinical trial NCT02915432." Annals of Oncology 30.9 (2019): 1479-1486.

Wang, Liwei, et al. "Gene expression and immune infiltration in melanoma patients with different mutation burden." BMC cancer 21.1 (2021): 1-12.

Weiss, Sarah A., Jedd D. Wolchok, and Mario Sznol. "Immunotherapy of melanoma: facts and hopes." Clinical Cancer Research 25.17 (2019): 5191-5201.

Wu, Pin, et al. "PD-L1 and survival in solid tumors: a meta-analysis." PloS one 10.6 (2015): e0131403.

Wu, Yusheng, et al. "Function of HNRNPC in breast cancer cells by controlling the dsRNA-induced interferon response." The EMBO journal 37.23 (2018): e99017.

Wurth, Laurence, et al. "UNR/CSDE1 drives a post-transcriptional program to promote melanoma invasion and metastasis." Cancer cell 30.5 (2016): 694-707.

Xie, Dong, et al. "Discovery of over-expressed genes and genetic alterations in breast cancer cells using a combination of suppression subtractive hybridization, multiplex FISH and comparative genomic hybridization." International journal of oncology 21.3 (2002): 499-507.

Zhang, Chuan, et al. "Identification of tumor mutation burden-related hub genes and the underlying mechanism in melanoma." Journal of Cancer 12.8 (2021): 2440.

Zhang, Shuguang, et al. "PMEL as a Prognostic Biomarker and Negatively Associated With Immune Infiltration in Skin Cutaneous Melanoma (SKCM)." Journal of Immunotherapy 44.6 (2021): 214-223.

Zhang, Lin, et al. "Gene expression profiles in normal and cancer cells." Science 276.5316 (1997): 1268-1272.

Zhou, Jianda, et al. "miR-199a-5p regulates the expression of metastasis-associated genes in B16F10 melanoma cells." International journal of clinical and experimental pathology 7.10 (2014): 7182.

Supplementary materials: Appendix

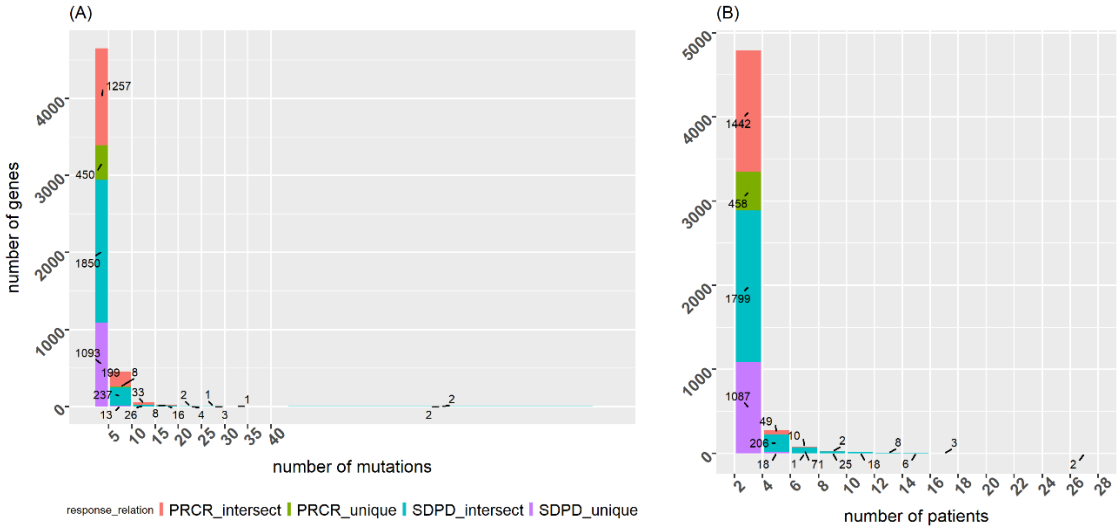

Suppl. Figure 1: Mutation histograms with the distribution counts shown for the response itself (instead of only the indication whether a gene is involved in multiple responses e.g., figure 3). Results are shown for 5629 genes. Genes have mutated in at least 2 patients. Purple indicates that a response-unique-gene is related to the SDPD therapy outcome (SDPD-unique). Green indicates that a response-unique gene is related to the PRCR therapy outcome (PRCR-unique). Blue indicates that a gene is related to both therapy outcomes but measured in SDPD patients only (SDPD-intersect). Red indicates that a gene is related to both therapy outcomes but measured in PRCR patients only (PRCR-intersect).

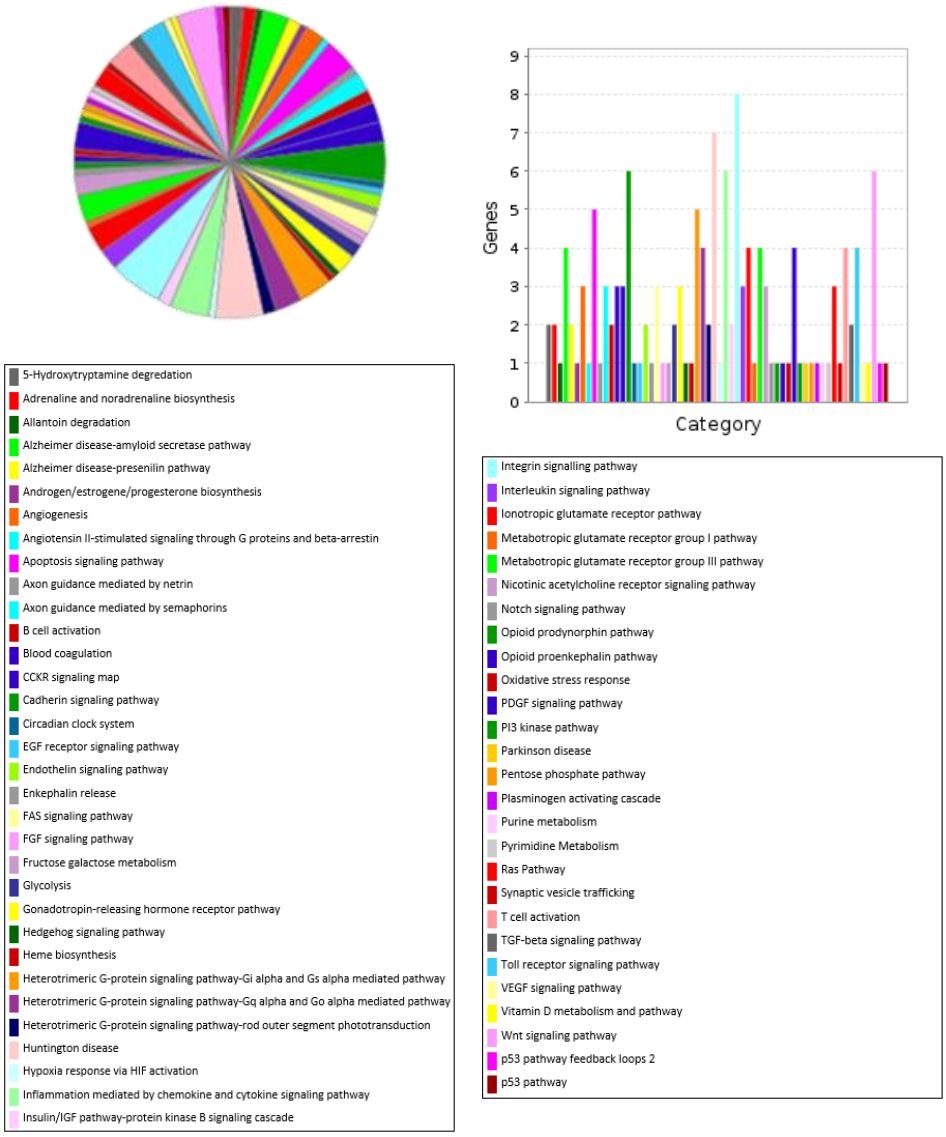

Suppl. Figure 2: Gene ontology analysis of the PRCR unique genes for pathways. Functional classification is viewed by bar chart and pie chart. Colours indicate identified categories. Molecular function analysis had a total of 144 pathway hits.

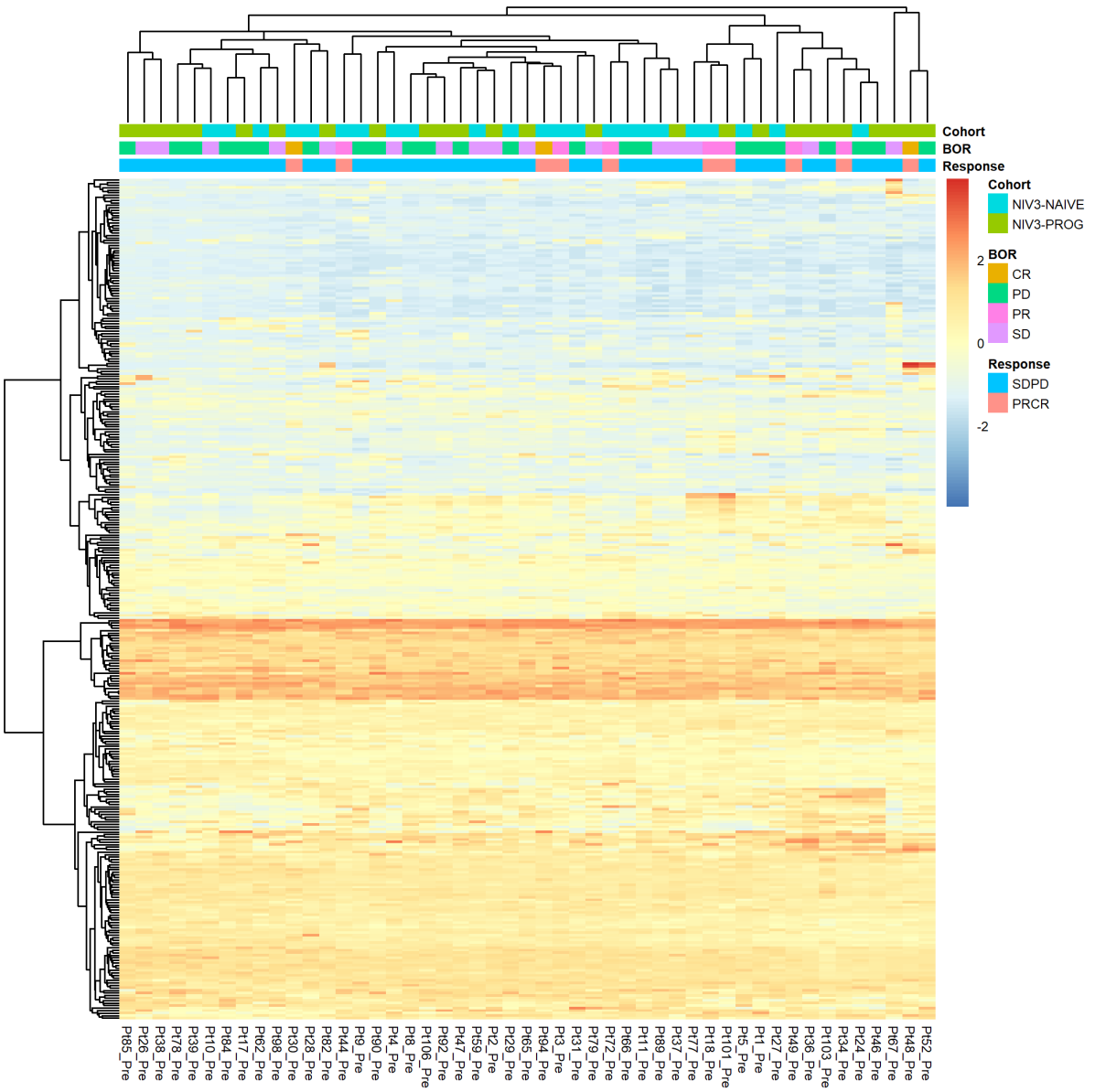

Suppl. Figure 3: Clustered heatmap of all PRCR unique mutated genes. A total of 334 of the 458 PRCR-unique genes were also present in the RNA-sequencing data set. Both axes show hierarchical clustering. The colours inside the matrix show the gene expression of which values were centred and scaled in the column direction.

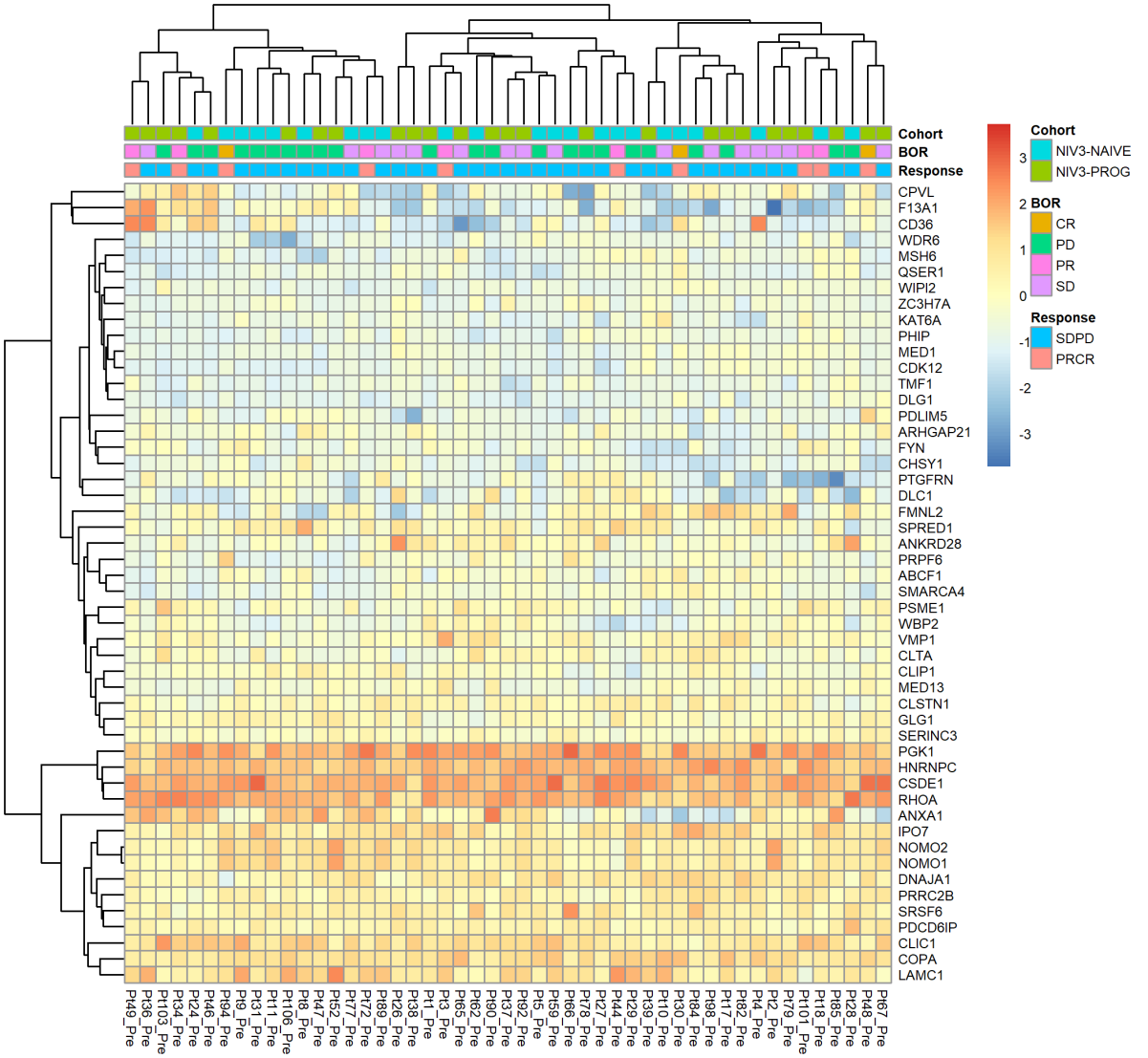

Suppl. Figure 4: Clustered heatmap of the top 50 highest median expressed PRCR unique genes that were present in the RNA-sequencing dataset. Values were centred and scaled in the column direction. Both axes show the hierarchical clustering. Cohort, best overall response (BOR) and response group (PRCR or SDPD) are indicated in the top axis for each patient. Red to blue colour scale indicates the gene expression values.

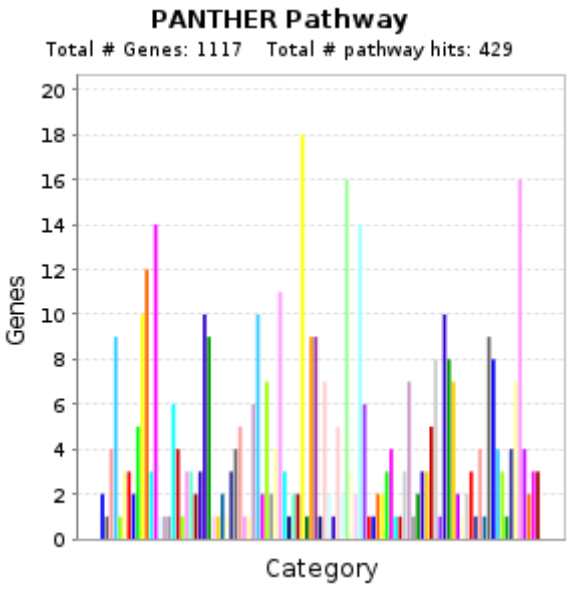

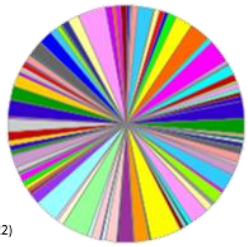

- 2-arachidonoylglycerol biosynthesis (P05726)
- 5-Hydroxytryptamine degredation (P04372)
- 5HT1 type receptor mediated signaling pathway (P04373)
- 5HT2 type receptor mediated signaling pathway (P04374)
- 5HT3 type receptor mediated signaling pathway (P04375)
- 5HT4 type receptor mediated signaling pathway (P04376)
- Adrenaline and noradrenaline biosynthesis (P00001)
- Alpha adrenergic receptor signaling pathway (P00002)
- Alzheimer disease-amyloid secretase pathway (P00003)
- Alzheimer disease-presenilin pathway (P00004)
- Angiogenesis (P00005)
- Angiotensin II-stimulated signaling through G proteins and beta-arrestin (P05911)
- Apoptosis signaling pathway (P00006)
- Asparagine and aspartate biosynthesis (P02730)
- Axon guidance mediated by Slit/Robo (P00008)
- Axon guidance mediated by netrin (P00009)
- Axon guidance mediated by semaphorins (P00007)
- B cell activation (P00010)
- BMP/activin signaling pathway-drosophila (P06211)
- Beta1 adrenergic receptor signaling pathway (P04377)
- Beta2 adrenergic receptor signaling pathway (P04378)
- Beta3 adrenergic receptor signaling pathway (P04379)
- Blood coagulation (P00011)
- CCKR signaling map (P06959)
- Cadherin signaling pathway (P00012)
- Carnitine metabolism (P02733)
- Cell cycle (P00013)
- Circadian clock system (P00015)
- Coenzyme A linked carnitine metabolism (P02732)
- Cortocotropin releasing factor receptor signaling pathway (P04380)
- Cytoskeletal regulation by Rho GTPase (P00016)
- DNA replication (P00017)
- DPP signaling pathway (P06213)
- DPP-SCW signaling pathway (P06212)
- Dopamine receptor mediated signaling pathway (P05912)
- EGF receptor signaling pathway (P00018)
- Endogenous cannabinoid signaling (P05730)
- Endothelin signaling pathway (P00019)
- Enkephalin release (P05913)
- FAS signaling pathway (P00020)
- FGF signaling pathway (P00021)
- GABA-B receptor II signaling (P05731)
- Gamma-aminobutyric acid synthesis (P04384)
- General transcription by RNA polymerase I (P00022)
- General transcription regulation (P00023)
- Gonadotropin-releasing hormone receptor pathway (P06664)
- Hedgehog signaling pathway (P00025)
- Heterotrimeric G-protein signaling pathway-Gi alpha and Gs alpha mediated pathway (P00026)
- Heterotrimeric G-protein signaling pathway-Gq alpha and Go alpha mediated pathway (P00027)
- Heterotrimeric G-protein signaling pathway-rod outer segment phototransduction (P00028)
- Histamine H1 receptor mediated signaling pathway (P04385)
- Histamine H2 receptor mediated signaling pathway (P04386)
- Histidine biosynthesis (P02747)
- Huntington disease (P00029)
- Hypoxia response via HIF activation (P00030)
- Inflammation mediated by chemokine and cytokine signaling pathway (P00031)
- Insulin/IGF pathway-mitogen activated protein kinase kinase/MAP kinase cascade (P00032)
- Insulin/IGF pathway-protein kinase B signaling cascade (P00033)
- Integrin signalling pathway (P00034)
- Interleukin signaling pathway (P00036)
- Ionotropic glutamate receptor pathway (P00037)
- JAK/STAT signaling pathway (P00038)
- Metabotropic glutamate receptor group I pathway (P00041)
- Metabotropic glutamate receptor group II pathway (P00040)
- Metabotropic glutamate receptor group III pathway (P00039)
- Muscarinic acetylcholine receptor 1 and 3 signaling pathway (P00042)
- Muscarinic acetylcholine receptor 2 and 4 signaling pathway (P00043)
- Nicotine degradation (P05914)
- Nicotine pharmacodynamics pathway (P06587)
- Nicotinic acetylcholine receptor signaling pathway (P00044)
- Notch signaling pathway (P00045)
- Opioid prodynorphin pathway (P05916)
- Opioid proenkephalin pathway (P05915)
- Opioid proopiomelanocortin pathway (P05917)
- Oxidative stress response (P00046)
- Oxytocin receptor mediated signaling pathway (P04391)
- P53 pathway feedback loops 1 (P04392)
- PDGF signaling pathway (P00047)
- PI3 kinase pathway (P00048)
- Parkinson disease (P00049)
- Plasminogen activating cascade (P00050)
- Proline biosynthesis (P02768)
- Pyrimidine Metabolism (P02771)
- Ras Pathway (P04393)
- SCW signaling pathway (P06216)
- T cell activation (P00053)
- TCA cycle (P00051)
- TGF-beta signaling pathway (P00052)
- Thyrotropin-releasing hormone receptor signaling pathway (P04394)
- Toll receptor signaling pathway (P00054)
- Transcription regulation by bZIP transcription factor (P00055)
- Tyrosine biosynthesis (P02784)
- Ubiquitin proteasome pathway (P00060)
- VEGF signaling pathway (P00056)
- Wnt signaling pathway (P00057)
- p38 MAPK pathway (P05918)
- p53 pathway by glucose deprivation (P04397)
- p53 pathway feedback loops 2 (P04398)
- p53 pathway (P00059)

Suppl. Figure 5: Gene ontology analysis of the SDPD unique genes for pathways. Functional classification is viewed by bar chart and pie chart. Colours indicate identified categories. Molecular function analysis had a total of 429 pathway hits.

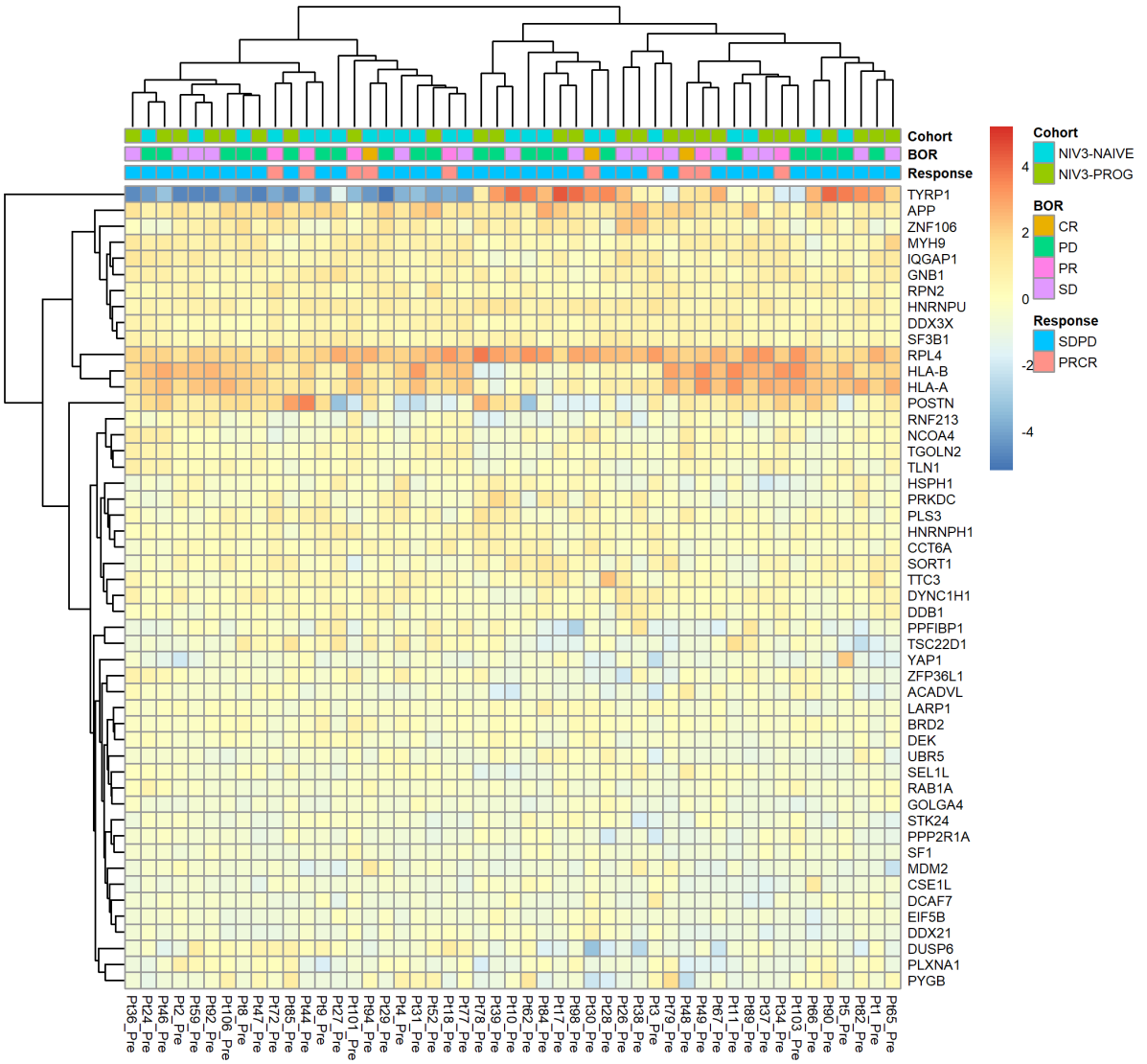

Suppl. Figure 6: Clustered heatmap of the top 50 highest median expressed SDPD unique genes that were present in the RNA-sequencing dataset. Values were centred and scaled in the column direction. Both axes show the hierarchical clustering. Cohort, best overall response (BOR) and response group (PRCR or SDPD) are indicated in the top axis for each patient. Red to blue colour scale indicates the gene expression values.

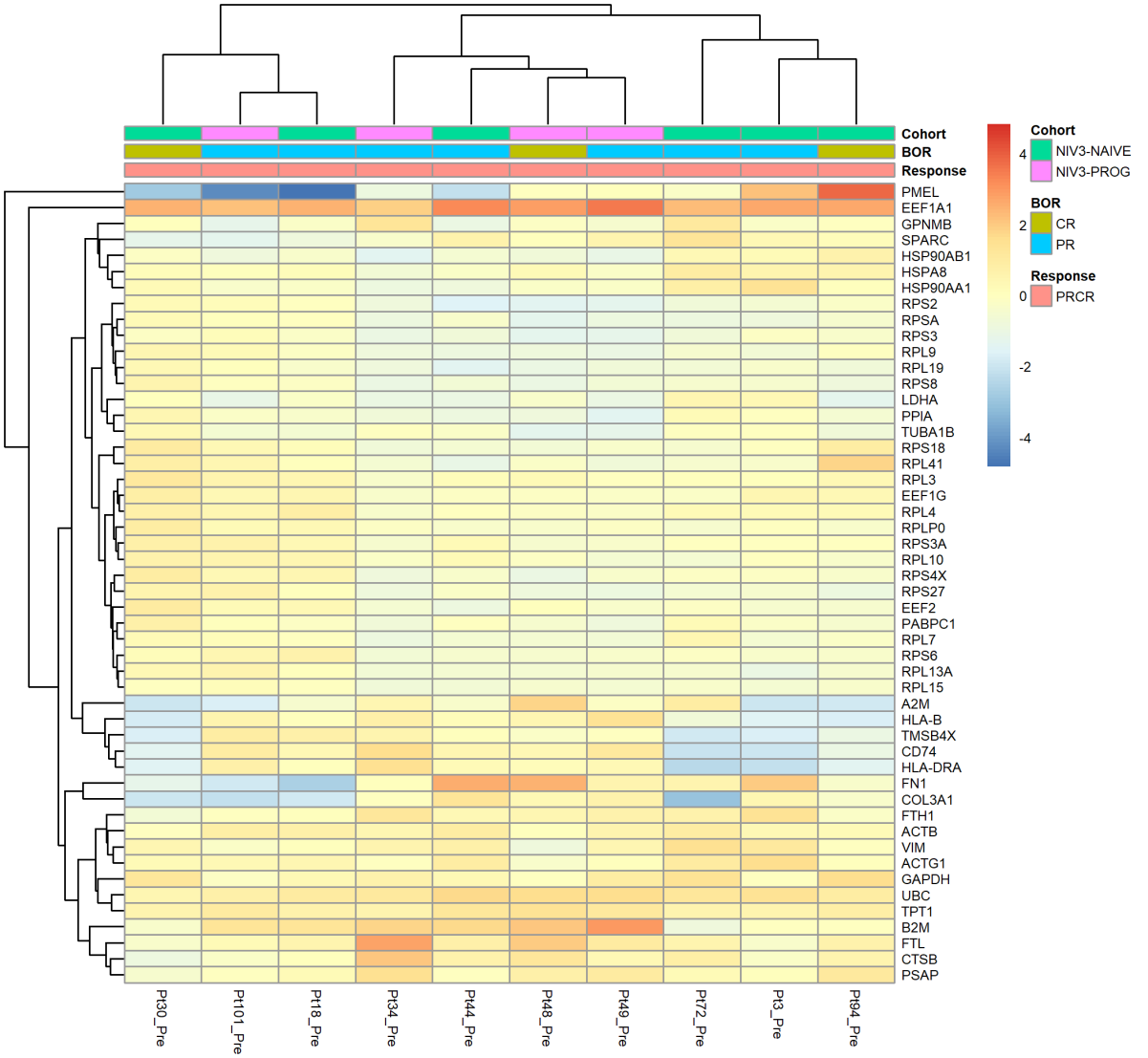

Suppl. Figure 7: Clustered heatmap of the top 50 highest median expressed genes in the PRCR group. Values were centred and scaled in the column direction. Both axes show the hierarchical clustering. Cohort, best overall response (BOR) and response group (PRCR) are indicated in the top axis for each patient. Red to blue colour scale indicates the gene expression values.

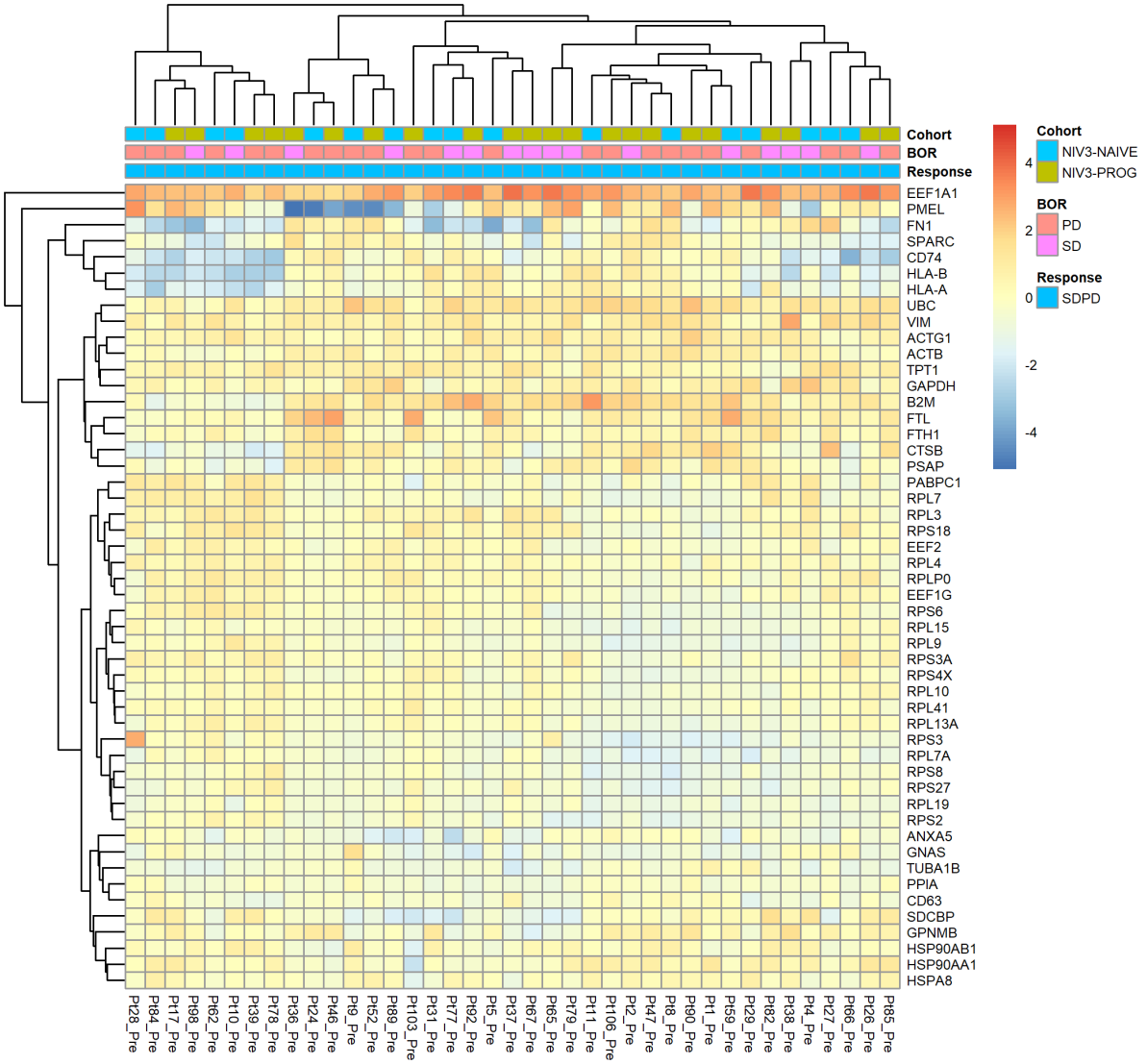

Suppl. Figure 8: Clustered heatmap of the top 50 highest median expressed genes in the SDPD group. Values were centred and scaled in the column direction. Both axes show the hierarchical clustering. Cohort, best overall response (BOR) and response group (SDPD) are indicated in the top axis for each patient. Red to blue colour scale indicates the gene expression values.

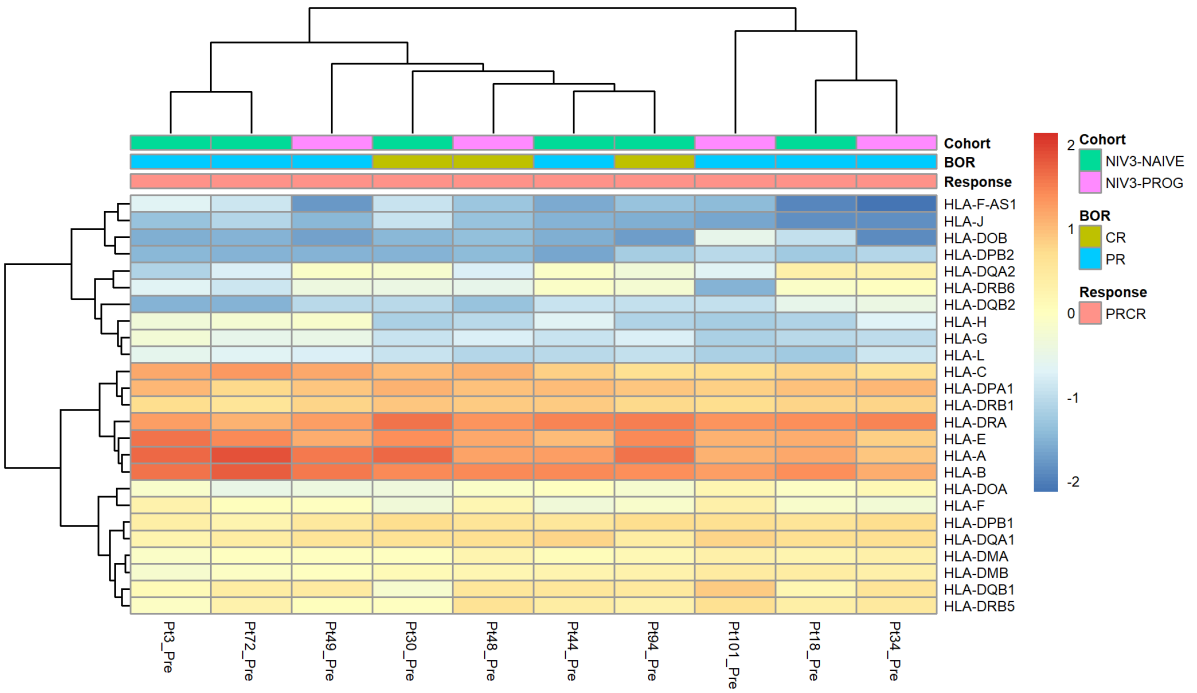

Suppl. Figure 9: Clustered heatmap of the HLA-genes (n=25)in the PRCR group. Values were centred and scaled in the column direction. Both axes show the hierarchical clustering. Cohort, best overall response (BOR) and response group (SDPD) are indicated in the top axis for each patient. Red to blue colour scale indicates the gene expression values.

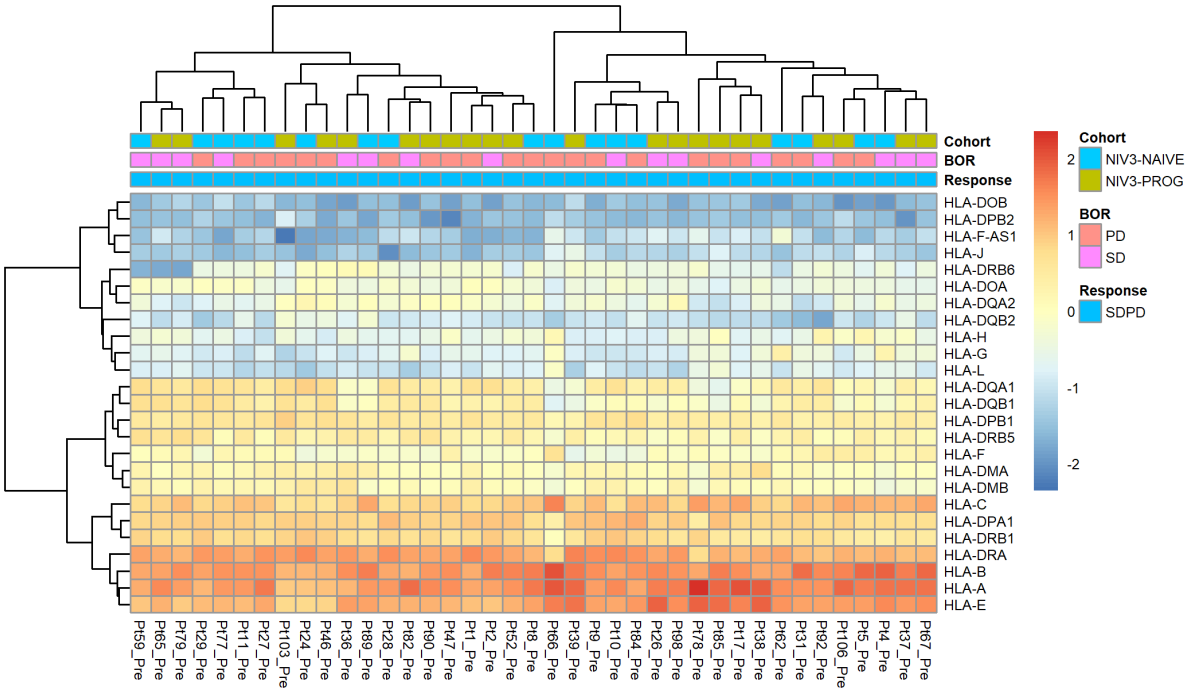

Suppl. Figure 10: Clustered heatmap of the HLA-genes (n=25)in the SDPD group. Values were centred and scaled in the column direction. Both axes show the hierarchical clustering. Cohort, best overall response (BOR) and response group (SDPD) are indicated in the top axis for each patient. Red to blue colour scale indicates the gene expression values.

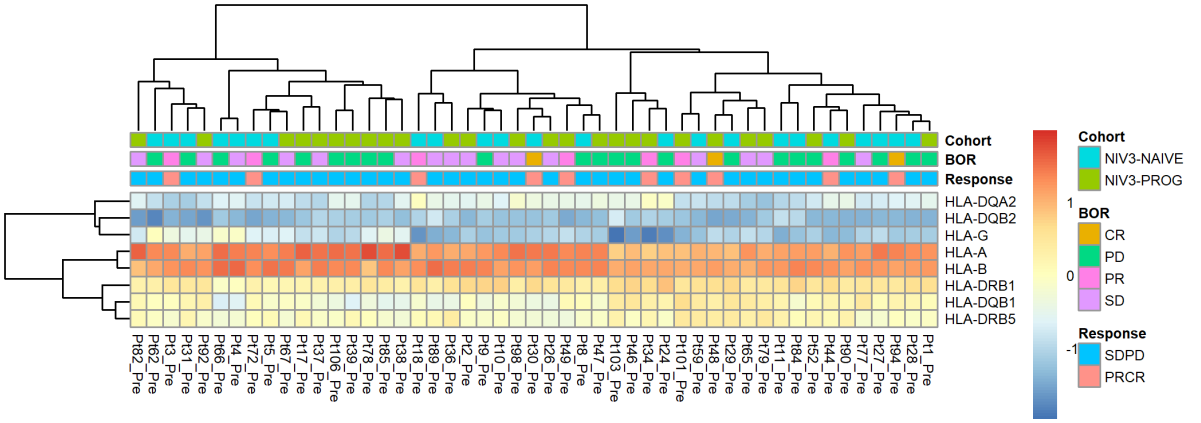

Suppl. Figure 11: Clustered heatmap of HLA genes in the RNA-sequencing dataset with non-synonymous mutations in at least 2 patients (n=8). Values were centred and scaled in the column direction. Cohort, best overall response (BOR) and response group (PRCR or SDPD) are indicated in the top axis for each patient. Both axes show the hierarchical clustering. Red to blue colour scale indicates the gene expression values.

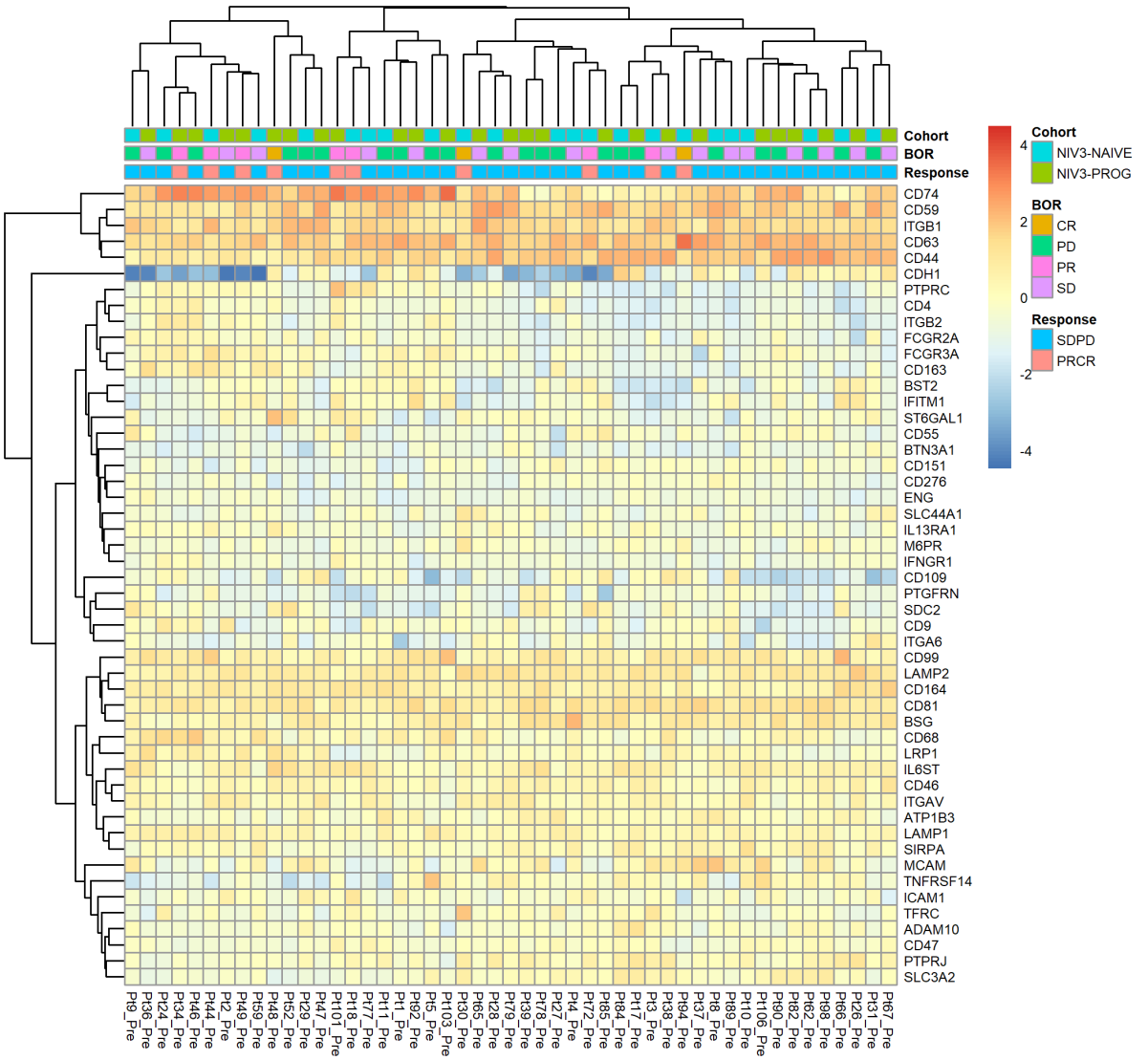

Suppl. Figure 12: Clustered heatmap of the top 50 highest median expressed human CD antigen genes in the RNA-sequencing dataset (n=279). Values were centred and scaled in the column direction. Both axes show the hierarchical clustering. Cohort, best overall response (BOR) and response group (PRCR or SDPD) are indicated in the top axis for each patient. Red to blue colour scale indicates the gene expression values.

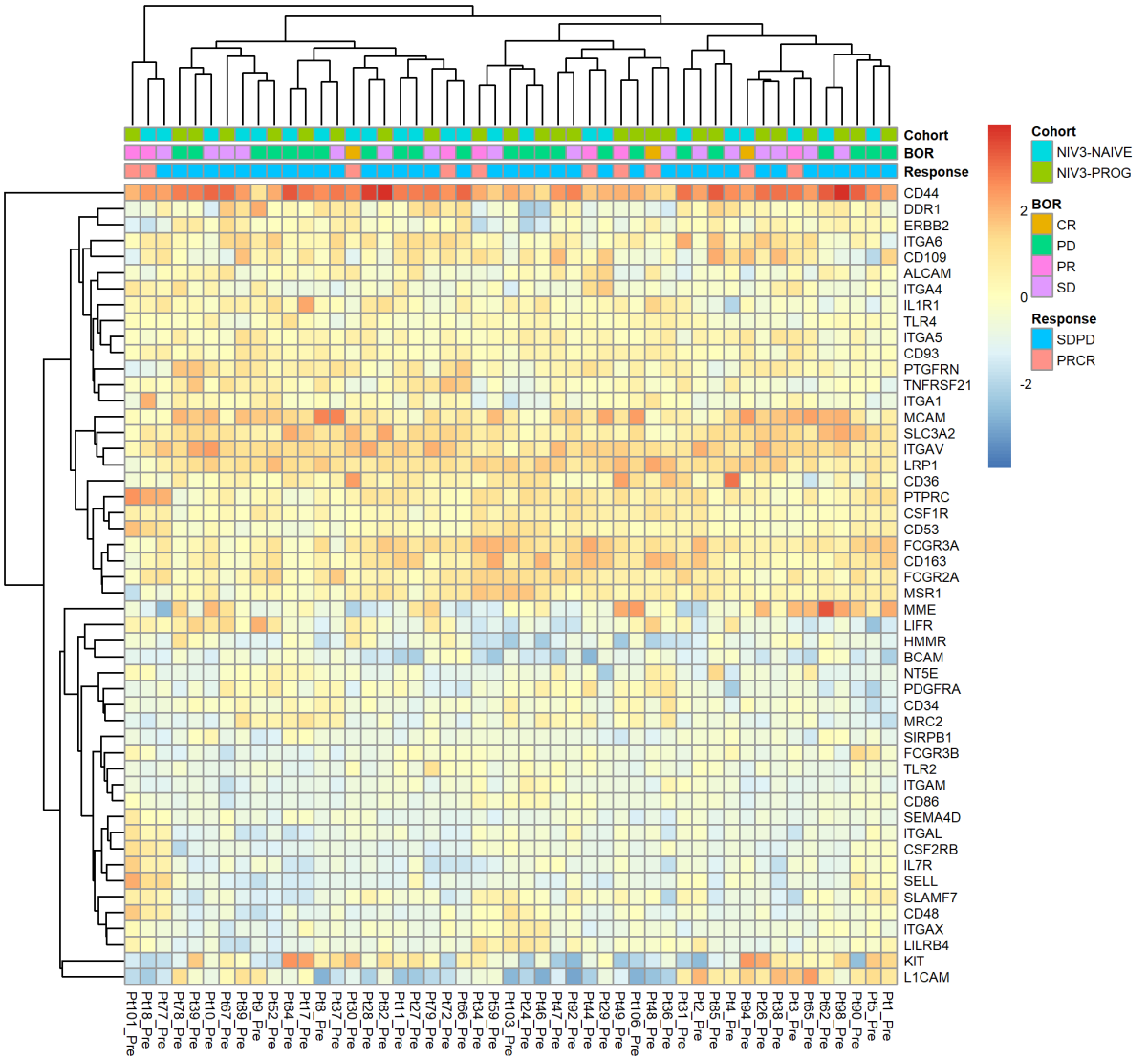

Suppl. Figure 13: Clustered heatmap of human CD antigen genes in the RNA-sequencing dataset with non-synonymous mutations in at least 2 patients (n=126). The top 50 highest median expressed genes are shown. Values were centred and scaled in the column direction. Cohort, best overall response (BOR) and response group (PRCR or SDPD) are indicated in the top axis for each patient. Both axes show the hierarchical clustering. Red to blue colour scale indicates the gene expression values.

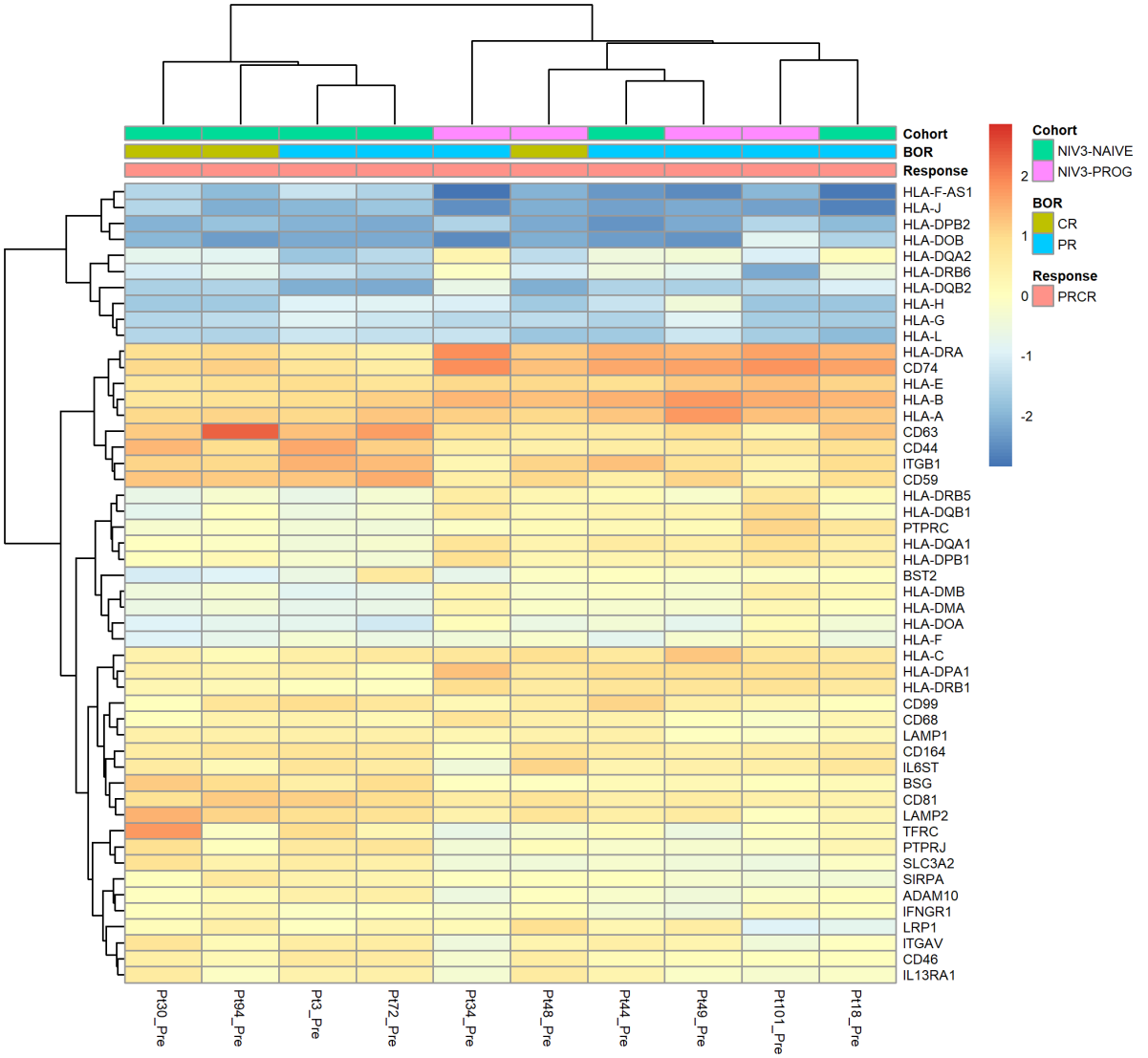

Suppl. Figure 14: Clustered heatmap of the top 50 highest median expressed genes in the PRCR group for the RNA-sequencing dataset only containing HLA (n=25) and human CD antigen genes (n=279). Values were centred and scaled in the column direction. Both axes show the hierarchical clustering. Cohort, best overall response (BOR) and response group (PRCR) are indicated in the top axis for each patient. Red to blue colour scale indicates the gene expression values.

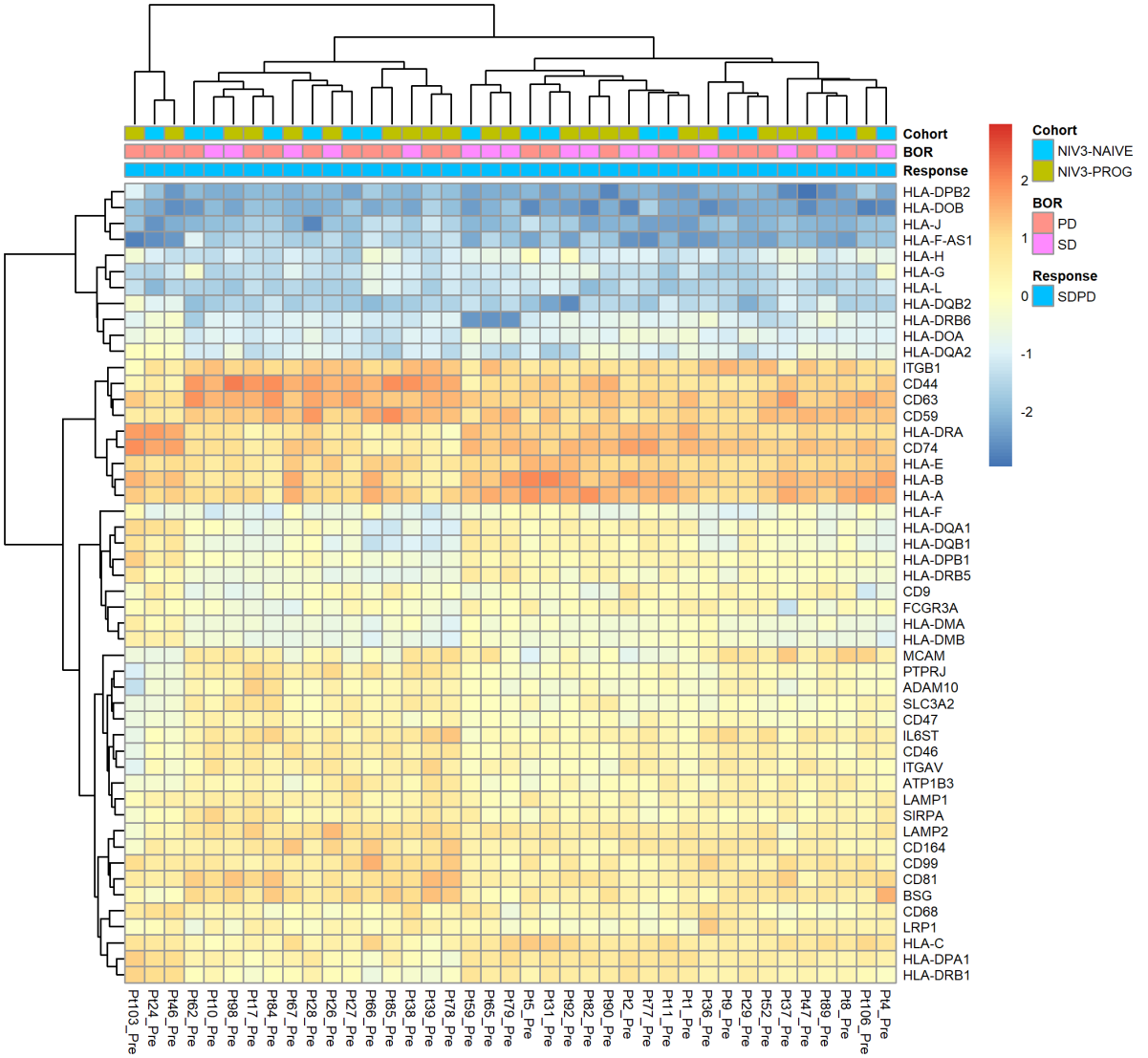

Suppl. Figure 15: Clustered heatmap of the top 50 highest median expressed genes in the SDPD group for the RNA-sequencing dataset only containing HLA (n=25) and human CD antigen genes (n=279). Values were centred and scaled in the column direction. Both axes show the hierarchical clustering. Cohort, best overall response (BOR) and response group (SDPD) are indicated in the top axis for each patient. Red to blue colour scale indicates the gene expression values.

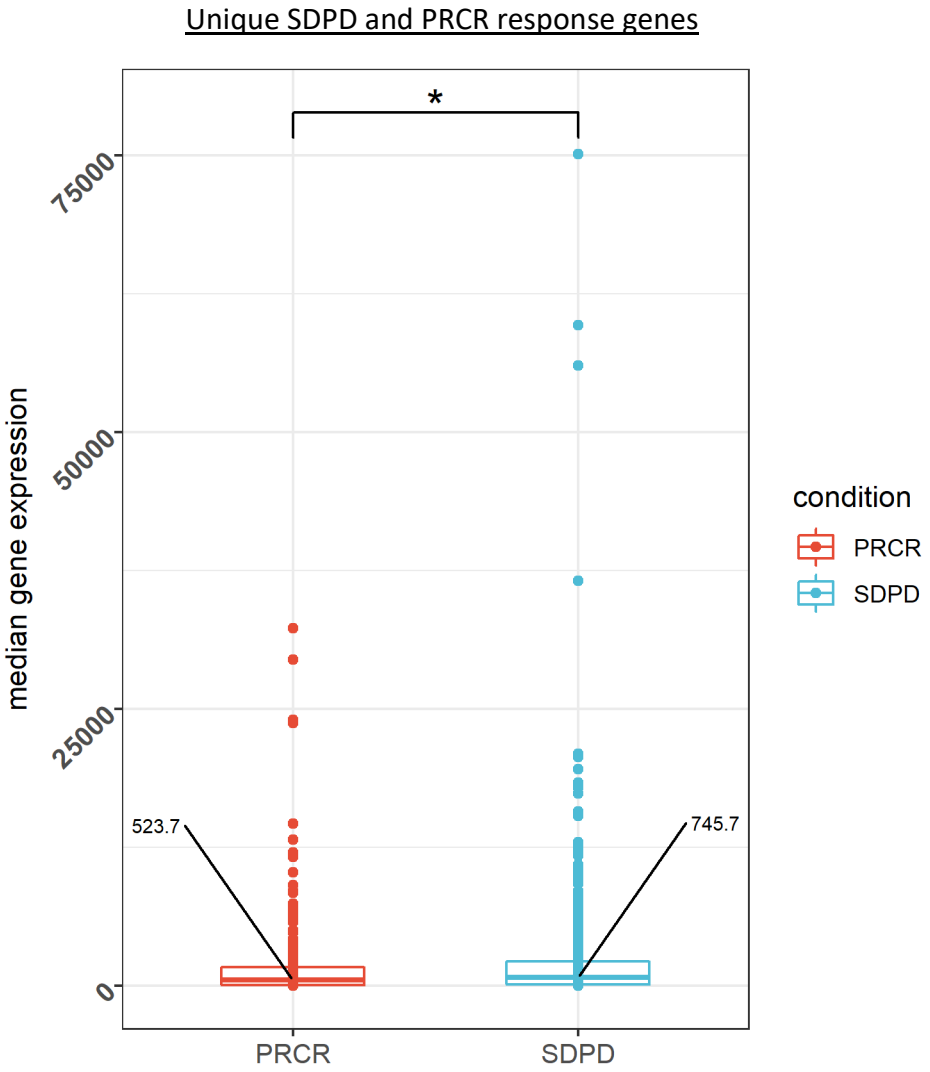

Suppl. Figure 16: Comparison of two response groups using the expression of all the response-unique genes (n=1277: PRCR unique=334; SDPD unique=943). Alternative hypothesis tested for PRCR > SDPD (non-paired two-sample test, p=0.014).

Suppl. Table 1: mutations characterized by SNV nucleotide change.

SNV type	Total mutations	Total Patients	Average mutations
G>A	12266	66	185.85
C>T	12313	65	189.43
A>G	615	65	9.46
G>T	527	63	8.37
G>C	322	60	5.37
C>G	308	58	5.31
T>C	466	57	8.18
A>T	438	56	7.82
C>A	414	56	7.39
T>G	292	55	5.31
T>A	360	53	6.79
A>C	268	53	5.06

Suppl. Table 2: Mutations characterized by SNV nucleotide change and further divided per response. The average mutations is calculated only for where it had mutated (thus not complete response group).

Response	SNV type	Total mutations	Total Patients	Average mutations
PRCR	C>T	6069	14	433.50
PRCR	G>A	5407	15	360.47
SDPD	G>A	6859	51	134.49
SDPD	C>T	6244	51	122.43
PRCR	A>T	184	12	15.33
PRCR	A>G	174	14	12.43
PRCR	G>T	160	14	11.43
PRCR	T>A	145	13	11.15
PRCR	T>C	148	14	10.57
PRCR	C>A	120	12	10.00
PRCR	G>C	122	14	8.71
SDPD	A>G	441	51	8.65
PRCR	T>G	105	13	8.08
PRCR	C>G	105	14	7.50
SDPD	G>T	367	49	7.49
SDPD	T>C	318	43	7.40
PRCR	A>C	81	11	7.36
SDPD	C>A	294	44	6.68
SDPD	A>T	254	44	5.77
SDPD	T>A	215	40	5.38
SDPD	C>G	203	44	4.61
SDPD	A>C	187	42	4.45
SDPD	T>G	187	42	4.45
SDPD	G>C	200	46	4.35

Suppl. Table 3: Mutations per chromosome and divided per response. The average mutations is calculated only for where it had mutated (thus not complete response group).

Response	Chromosome	Per million base pairs	Total mutations	Total patients	Average mutations in patients	Average mutations in chromosomes
PRCR	1	248,956,422	1285	15	85.67	5,16E-06
PRCR	2	242,193,529	1034	15	68.93	4,27E-06
PRCR	19	58,617,616	964	14	68.86	1,64E-05
PRCR	5	181,538,259	709	11	64.45	3,91E-06
PRCR	3	198,295,559	813	14	58.07	4,1E-06
PRCR	6	170,805,979	751	14	53.64	4,4E-06
PRCR	11	135,086,622	697	13	53.62	5,16E-06
PRCR	7	159,345,973	701	14	50.07	4,4E-06
PRCR	12	133,275,309	735	15	49.00	5,51E-06
PRCR	17	83,257,441	545	14	38.93	6,55E-06
PRCR	4	190,214,555	538	14	38.43	2,83E-06
PRCR	8	145,138,636	488	13	37.54	3,36E-06
PRCR	10	133,797,422	497	14	35.50	3,71E-06
PRCR	9	138,394,717	447	13	34.38	3,23E-06
SDPD	1	248,956,422	1670	49	34.08	6,71E-06
PRCR	16	90,338,345	430	13	33.08	4,76E-06
PRCR	X	156,040,895	372	13	28.62	2,38E-06
PRCR	15	101,991,189	349	13	26.85	3,42E-06
PRCR	20	64,444,167	340	13	26.15	5,28E-06
SDPD	2	242,193,529	1202	47	25.57	4,96E-06
PRCR	14	107,043,718	292	12	24.33	2,73E-06
SDPD	19	58,617,616	1143	49	23.33	1,95E-05
PRCR	18	80,373,285	255	12	21.25	3,17E-06
SDPD	12	133,275,309	929	44	21.11	6,97E-06
SDPD	3	198,295,559	934	45	20.76	4,71E-06
PRCR	13	114,364,328	228	12	19.00	1,99E-06
SDPD	7	159,345,973	851	45	18.91	5,34E-06
SDPD	17	83,257,441	865	46	18.80	1,04E-05
SDPD	11	135,086,622	882	47	18.77	6,53E-06
SDPD	6	170,805,979	839	45	18.64	4,91E-06
SDPD	5	181,538,259	715	42	17.02	3,94E-06
PRCR	22	50,818,468	219	13	16.85	4,31E-06
SDPD	4	190,214,555	666	42	15.86	3,5E-06
SDPD	10	133,797,422	557	43	12.95	4,16E-06
SDPD	X	156,040,895	592	46	12.87	3,79E-06
SDPD	16	90,338,345	511	40	12.78	5,66E-06
SDPD	8	145,138,636	570	46	12.39	3,93E-06
SDPD	9	138,394,717	544	45	12.09	3,93E-06
SDPD	15	101,991,189	468	40	11.70	4,59E-06
SDPD	14	107,043,718	465	40	11.63	4,34E-06
PRCR	21	46,709,983	127	11	11.55	2,72E-06
SDPD	20	64,444,167	360	36	10.00	5,59E-06
SDPD	22	50,818,468	293	39	7.51	5,77E-06
SDPD	18	80,373,285	282	38	7.42	3,51E-06
SDPD	13	114,364,328	261	42	6.21	2,28E-06
SDPD	21	46,709,983	166	34	4.88	3,55E-06
PRCR	Y	57,227,415	4	2	2.00	6,99E-08
SDPD	Y	57,227,415	4	3	1.33	6,99E-08

Suppl. Table 4: Mutations characterized by variant classification and further divided per response. The average mutations is calculated only for where it had mutated (thus not complete response group).

Response	Variant classification	Total mutations	Total patients	Average Mutations
PRCR	missense variant	11546	15	769.73
SDPD	missense variant	13909	53	262.43
PRCR	stop gained	683	14	48.79
PRCR	missense variant & splice region variant	274	13	21.08
SDPD	stop gained	865	48	18.02
SDPD	missense variant & splice region variant	415	42	9.88
PRCR	protein protein contact	100	11	9.09
PRCR	splice acceptor variant & intron variant	110	13	8.46
PRCR	start lost	24	4	6.00
SDPD	splice acceptor variant & intron variant	198	36	5.50
SDPD	splice donor variant & intron variant	190	36	5.28
PRCR	splice donor variant & intron variant	63	12	5.25
SDPD	protein protein contact	137	33	4.15
PRCR	stop gained & splice region variant	18	6	3.00
SDPD	stop gained & splice region variant	32	20	1.60
SDPD	start lost	18	14	1.29
SDPD	start lost & splice region variant	1	1	1.00
SDPD	splice acceptor variant& splice donor variant & intron variant	3	3	1.00
PRCR	stop lost	2	2	1.00
SDPD	Stop lost	1	1	1.00

Suppl. Table 5: Overview of mutated genes unique to the PRCR-response whilst related to immune system processes.

Activation of immune response	Immune effector process	Immune response	Immune system development	Leukocyte activation	Leukocyte migration
FYN	OAS3	CCR2	ANXA1	ANXA1	ANXA1
MNDA	ANXA1	ANXA1	CD3D	CD3D	
	TLR8	TRIM62	IL36B	IL36B	
		FYN	TNFSF8	TIGIT	
		IL36B	KIT	TNFSF8	
		TLR8		KIT	
		PTX3			
		MNDA			
		PDCD1			

Suppl. Table 6: Overview of mutated genes unique to the PRCR-response whilst related to defence/immunity proteins.

Antimicrobial response protein	Immunoglobulin receptor superfamily	Immunoglobulin	Major histocompatibility complex protein	B cell activation	T cell activation
DEFB125	PTGFRN	OPCML	HLA-DQA2	PIK3CB	PIK3CB
	LILRA2			JUN	JUN
	KIR3DL2				HLA-DQA2
	FCRL4				CD3D

Suppl. Table 7: Overview of mutated genes unique to the SDPD-response whilst related to immune system processes.

Activation of immune response	Antigen processing and presentation	Immune effector process	Immune system development	Leukocyte activation	Immune response	
TEC	HLA-A	HLA-A	SRC	FES	TEC	ITK
SH2B2	HLA-B	FES	CSF1R	IL27RA	HLA-A	ACKR2
SLK		HLA-B	ITK	ITK	FES	CD86
ITK		SYK	SYK	CD86	TRIM51	SYK
SYK		CRP	CEBPE	SYK	FRK	SPN
SLC39A10			ALAS2		SRMS	SLC39A10
CRP			UBASH3B		SRC	IL1F10
					SH2B2	ANG
					SLK	CCR9
					TRIM64C	PARP9
					HLA-B	CRP

Suppl. Table 8: Overview of mutated genes unique to the SDPD-response whilst related to defence/immunity proteins.

Major histocompatibility complex protein	B cell activation	T cell activation	Immunoglobulin receptor superfamily	
HLA-A	FRK	NFKB2	CD96	SLAMF1
HLA-B	NFKB2	ZAP70	FCAMR	HAVCR2
HLA-DQB1	SYK	CD86	FCRL6	PIGR
	SOS1	SOS1	CD300A	SLAMF7
			CD86	CD300LG

Suppl. Table 9: Overview of HLA-genes with non-synonymous mutations in at least 2 patients.

Response overlap	Gene	Chromosome of SNVs	Total mutations	Total patients
Intersect	HLA-DRB5	6	10	6
SDPD unique	HLA-DQB1	6	9	5
Intersect	HLA-DRB1	6	8	5
Intersect	HLA-DQB2	6	5	4
SDPD unique	HLA-A	6	4	3
SDPD unique	HLA-B	6	3	2
PRCR unique	HLA-DQA2	6	2	2
Intersect	HLA-G	6	2	2

Suppl. Table 10: Overview of human CD antigen genes with non-synonymous mutations in at least 5 patients.

Response overlap	Gene	Chromosome	Total mutations	Total patients
Intersect	CD163	12	17	11
Intersect	CD163L1	12	13	8
Intersect	ITGA1	5	9	8
Intersect	SIRPB1	20	9	7
Intersect	FGFR2	10	8	7
Intersect	ACE	17	7	7
Intersect	TLR4	9	9	6
Intersect	CR2	1	8	6
Intersect	ALK	2	7	6
Intersect	CD33	19	6	6
Intersect	SELP	1	6	6
SDPD unique	ITGAX	16	6	5
Intersect	LILRB1	19	6	5
Intersect	IL7R	5	5	5
SDPD unique	RHAG	6	5	5
Intersect	LILRB4	19	5	5
Intersect	PTPRC	1	5	5
Intersect	CEACAM5	19	5	5
Intersect	ITGA2B	17	5	5

Suppl. Table 11: Overview of PD-1 related antigen genes with non-synonymous mutations.

Response overlap	Gene	Chromosome	Total mutations	Total patients
intersect	PDCD1LG2 (PD-L2)	9	2	2
PRCR_unique	PDCD1 (PD-1)	2	2	2
SDPD_unique	CD96 (Tactile)	3	2	2
intersect	CTLA4	2	2	2

Miniconda environment installations

Base

# platform: win-64
brotlipy=0.7.0=py39h2bbff1b_1003
ca-certificates=2021.1.19=haa95532_1
certifi=2020.12.5=py39haa95532_0
cffi=1.14.5=py39hcd4344a_0
chardet=4.0.0=py39haa95532_1003
conda=4.9.2=py39haa95532_0
conda-package-handling=1.7.2=py39h8cc25b3_1
console_shortcut=0.1.1=4
cryptography=3.4.7=py39h71e12ea_0
idna=2.10=pyhd3eb1b0_0
menuinst=1.4.16=py39h2bbff1b_0
openssl=1.1.1k=h2bbff1b_0
pip=21.0.1=py39haa95532_0
powershell_shortcut=0.0.1=3
pycosat=0.6.3=py39h2bbff1b_0
pycparser=2.20=py_2
pyopenssl=20.0.1=pyhd3eb1b0_1
pysocks=1.7.1=py39haa95532_0
python=3.9.1=h6244533_2
pywin32=228=py39he774522_0
requests=2.25.1=pyhd3eb1b0_0
ruamel_yaml=0.15.100=py39h2bbff1b_0
setuptools=52.0.0=py39haa95532_0
six=1.15.0=py39haa95532_0
sqlite=3.35.2=h2bbff1b_0
tqdm=4.59.0=pyhd3eb1b0_1
tzdata=2020f=h52ac0ba_0
urllib3=1.26.4=pyhd3eb1b0_0
vc=14.2=h21ff451_1
vs2015_runtime=14.27.29016=h5e58377_2
wheel=0.36.2=pyhd3eb1b0_0
win_inet_pton=1.1.0=py39haa95532_0
wincertstore=0.2=py39h2bbff1b_0
yaml=0.2.5=he774522_0

Virtual environment

platform: win-64
_r-mutex=1.0.0=anacondar_1
anyio=2.2.0=py39haa95532_0
argon2-cffi=20.1.0=py39h2bbff1b_1
async_generator=1.10=pyhd3eb1b0_0
attrs=20.3.0=pyhd3eb1b0_0
babel=2.9.0=pyhd3eb1b0_0
backcall=0.2.0=pyhd3eb1b0_0
bleach=3.3.0=pyhd3eb1b0_0
brotlipy=0.7.0=py39h2bbff1b_1003
ca-certificates=2021.1.19=haa95532_1

certifi=2020.12.5=py39haa95532_0
cffi=1.14.5=py39hcd4344a_0
chardet=4.0.0=py39haa95532_1003
colorama=0.4.4=pyhd3eb1b0_0
cryptography=3.4.7=py39h71e12ea_0
decorator=4.4.2=pyhd3eb1b0_0
defusedxml=0.7.1=pyhd3eb1b0_0
entrypoints=0.3=py39haa95532_0
idna=2.10=pyhd3eb1b0_0
importlib-metadata=3.7.3=py39haa95532_1
importlib_metadata=3.7.3=hd3eb1b0_1
ipykernel=5.3.4=py39h7b7c402_0
ipython=7.21.0=py39hd4e2768_0
ipython_genutils=0.2.0=pyhd3eb1b0_1
jedi=0.17.2=py39haa95532_1
jinja2=2.11.3=pyhd3eb1b0_0
json5=0.9.5=py_0
jsonschema=3.2.0=py_2
jupyter-packaging=0.7.12=pyhd3eb1b0_0
jupyter_client=6.1.7=py_0
jupyter_core=4.7.1=py39haa95532_0
jupyter_server=1.4.1=py39haa95532_0
jupyterlab=3.0.11=pyhd3eb1b0_0
jupyterlab_pygments=0.1.2=py_0
jupyterlab_server=2.3.0=pyhd3eb1b0_0
libsodium=1.0.18=h62dcd97_0
m2w64-bwidget=1.9.10=2
m2w64-bzip2=1.0.6=6
m2w64-expat=2.1.1=2
m2w64-fftw=3.3.4=6
m2w64-flac=1.3.1=3
m2w64-gcc-libgfortran=5.3.0=6
m2w64-gcc-libs=5.3.0=7
m2w64-gcc-libs-core=5.3.0=7
m2w64-gettext=0.19.7=2
m2w64-gmp=6.1.0=2
m2w64-gsl=2.1=2
m2w64-libiconv=1.14=6
m2w64-libjpeg-turbo=1.4.2=3
m2w64-libogg=1.3.2=3
m2w64-libpng=1.6.21=2
m2w64-libsndfile=1.0.26=2
m2w64-libsodium=1.0.10=2
m2w64-libtiff=4.0.6=2
m2w64-libvorbis=1.3.5=2
m2w64-libwinpthread-git=5.0.0.4634.697f757=2
m2w64-libxml2=2.9.3=4
m2w64-mpfr=3.1.4=4

m2w64-openblas=0.2.19=1
m2w64-pcre=8.38=2
m2w64-speex=1.2rc2=3
m2w64-speexdsp=1.2rc3=3
m2w64-tcl=8.6.5=3
m2w64-tk=8.6.5=3
m2w64-tktable=2.10=5
m2w64-wineditline=2.101=5
m2w64-xz=5.2.2=2
m2w64-zeromq=4.1.4=2
m2w64-zlib=1.2.8=10
markupsafe=1.1.1=py39h2bbff1b_0
mistune=0.8.4=py39h2bbff1b_1000
msys2-conda-epoch=20160418=1
nbclassic=0.2.6=pyhd3eb1b0_0
nbclient=0.5.3=pyhd3eb1b0_0
nbconvert=6.0.7=py39haa95532_0
nbformat=5.1.2=pyhd3eb1b0_1
nest-asyncio=1.5.1=pyhd3eb1b0_0
notebook=6.3.0=py39haa95532_0
openssl=1.1.1k=h2bbff1b_0
packaging=20.9=pyhd3eb1b0_0
pandoc=2.12=haa95532_0
pandocfilters=1.4.3=py39haa95532_1
parso=0.7.0=py_0
pickleshare=0.7.5=pyhd3eb1b0_1003
pip=21.0.1=py39haa95532_0
prometheus_client=0.9.0=pyhd3eb1b0_0
prompt-toolkit=3.0.17=pyh06a4308_0
pycparser=2.20=py_2
pygments=2.8.1=pyhd3eb1b0_0
pyopenssl=20.0.1=pyhd3eb1b0_1
pyparsing=2.4.7=pyhd3eb1b0_0
pyrsistent=0.17.3=py39h2bbff1b_0
pysocks=1.7.1=py39haa95532_0
python=3.9.2=h6244533_0
python-dateutil=2.8.1=pyhd3eb1b0_0
pytz=2021.1=pyhd3eb1b0_0
pywin32=228=py39he774522_0
pywinpty=0.5.7=py39haa95532_0
pyzmq=20.0.0=py39hd77b12b_1
r-base=3.6.1=hf18239d_1
r-base64enc=0.1_3=r36h6115d3f_4
r-crayon=1.3.4=r36h6115d3f_0
r-digest=0.6.18=r36h6115d3f_0
r-evaluate=0.13=r36h6115d3f_0
r-foreign=0.8_71=r36h6115d3f_0
r-htmltools=0.3.6=r36h6115d3f_0

r-irdisplay=0.7.0=r36h6115d3f_0
r-irkernel=0.8.15=r36_0
r-jsonlite=1.6=r36h6115d3f_0
r-pbdzmq=0.3_3=r36h6115d3f_0
r-rcpp=1.0.1=r36h6115d3f_0
r-repr=0.19.2=r36h6115d3f_0
r-uuid=0.1_2=r36h6115d3f_4
requests=2.25.1=pyhd3eb1b0_0
send2trash=1.5.0=pyhd3eb1b0_1
setuptools=52.0.0=py39haa95532_0
six=1.15.0=py39haa95532_0
sniffio=1.2.0=py39haa95532_1
sqlite=3.35.2=h2bbff1b_0
terminado=0.9.3=py39haa95532_0
testpath=0.4.4=pyhd3eb1b0_0
tornado=6.1=py39h2bbff1b_0
traitlets=5.0.5=pyhd3eb1b0_0
tzdata=2020f=h52ac0ba_0
urllib3=1.26.4=pyhd3eb1b0_0
vc=14.2=h21ff451_1
vs2015_runtime=14.27.29016=h5e58377_2
wcwidth=0.2.5=py_0
webencodings=0.5.1=py39haa95532_1
wheel=0.36.2=pyhd3eb1b0_0
win_inet_pton=1.1.0=py39haa95532_0
wincertstore=0.2=py39h2bbff1b_0
winpty=0.4.3=4
zeromq=4.3.3=ha925a31_3
zipp=3.4.1=pyhd3eb1b0_0

R package versions

Session info

```
R version 3.6.1 (2019-07-05)
Platform: x86_64-w64-mingw32/x64 (64-bit)
Running under: Windows 10 x64 (build 19042)

Matrix products: default

locale:
[1] LC_COLLATE=English_Netherlands.1252  LC_CTYPE=English_Netherlands.1252
[3] LC_MONETARY=English_Netherlands.1252 LC_NUMERIC=C
[5] LC_TIME=English_Netherlands.1252

attached base packages:
 [1] parallel  stats4    grid      stats     graphics  grDevices utils
 [8] datasets  methods   base

other attached packages:
 [1] umap_0.2.7.0
 [2] Rtsne_0.15
 [3] Hmisc_4.5-0
 [4] Formula_1.2-4
 [5] lattice_0.20-41
 [6] coin_1.4-1
 [7] survival_3.2-10
 [8] rstatix_0.7.0
 [9] ggpubr_0.4.0
[10] gridExtra_2.3
[11] ggrepel_0.9.1
[12] stringr_1.4.0
[13] tidyr_1.1.3
[14] pheatmap_1.0.12
[15] forcats_0.5.1
[16] dplyr_1.0.5
[17] plyr_1.8.6
[18] IHW_1.14.0
[19] genefilter_1.68.0
[20] org.Hs.eg.db_3.10.0
[21] annotate_1.64.0
[22] XML_3.99-0.3
[23] TxDb.Hsapiens.UCSC.hg19.knownGene_3.2.2
[24] GenomicFeatures_1.38.2
[25] AnnotationDbi_1.48.0
[26] DESeq2_1.26.0
[27] SummarizedExperiment_1.16.1
[28] DelayedArray_0.12.3
[29] BiocParallel_1.20.1
[30] matrixStats_0.58.0
[31] Biobase_2.46.0
[32] GenomicRanges_1.38.0
[33] GenomeInfoDb_1.22.1
[34] IRanges_2.20.2
[35] S4Vectors_0.24.4
[36] BiocGenerics_0.32.0
[37] sqldf_0.4-11
[38] RSQLite_2.2.4
[39] gsubfn_0.7
[40] proto_1.0.0
```

```
[41] ggplot2_3.3.3
[42] nrstats_0.1.0

loaded via a namespace (and not attached):
  [1] utf8_1.2.1                reticulate_1.18           rms_6.2-0
  [4] R.utils_2.10.1            tidyselect_1.1.0          htmlwidgets_1.5.3
  [7] 78unsell_0.5.0             codetools_0.2-18          chron_2.3-56
 [10] pbdZMQ_0.3-3              withr_2.4.1               colorspace_2.0-0
 [13] knitr_1.31                uuid_0.1-2                rstudioapi_0.13
 [16] ROCR_1.0-11               ggsignif_0.6.1            labeling_0.4.2
 [19] slam_0.1-48               repr_0.19.2          GenomeInfoDbData_1.2.2
 [22] lpsymphony_1.14.0         bit64_4.0.5               farver_2.1.0
 [25] vctrs_0.3.6               generics_0.1.0            TH.data_1.0-10
 [28] xfun_0.22                 BiocFileCache_1.10.2      R6_2.5.0
 [31] locfit_1.5-9.4            bitops_1.0-6              cachem_1.0.4
 [34] reshape_0.8.8             assertthat_0.2.1          scales_1.1.1
 [37] multcomp_1.4-16           nnet_7.3-15               gtable_0.3.0
 [40] conquer_1.0.2             sandwich_3.0-0            rlang_0.4.10
 [43] MatrixModels_0.5-0        cmprsk_2.2-10             splines_3.6.1
 [46] rtracklayer_1.46.0        broom_0.7.6               checkmate_2.0.0
 [49] abind_1.4-5               backports_1.2.1           tools_3.6.1
 [52] tcltk_3.6.1               ellipsis_0.3.1            RcolorBrewer_1.1-2
 [55] Rcpp_1.0.3                base64enc_0.1-3           progress_1.2.2
 [58] zlibbioc_1.32.0           purrr_0.3.4               Rcurl_1.98-1.3
 [61] prettyunits_1.1.1         rpart_4.1-15              openssl_1.4.3
 [64] cowplot_1.1.1             zoo_1.8-9                 haven_2.3.1
 [67] cluster_2.1.1             magrittr_2.0.1            data.table_1.14.0
 [70] Rspectra_0.16-0           openxlsx_4.2.3            SparseM_1.81
 [73] mvtnorm_1.1-1             hms_1.0.0                 evaluate_0.13
 [76] xtable_1.8-4              rio_0.5.26                jpeg_0.1-8.1
 [79] readxl_1.3.1              compiler_3.6.1            biomaRt_2.42.1
 [82] tibble_3.1.0              crayon_1.4.1              R.oo_1.24.0
 [85] htmltools_0.3.6           geneplotter_1.64.0        libcoin_1.0-8
 [88] DBI_1.1.1                 dbplyr_2.1.1              MASS_7.3-53.1
 [91] rappdirs_0.3.3            Matrix_1.3-2              car_3.0-10
 [94] cli_2.4.0                 R.methodsS3_1.8.1         pkgconfig_2.0.3
 [97] GenomicAlignments_1.22.1 foreign_0.8-71             Irdisplay_0.7.0
[100] Xvector_0.26.0            digest_0.6.18             Biostrings_2.54.0
[103] cellranger_1.1.0          htmlTable_2.1.0           curl_4.3
[106] Rsamtools_2.2.3           quantreg_5.85             modeltools_0.2-23
[109] lifecycle_1.0.0           nlme_3.1-152              jsonlite_1.6
[112] carData_3.0-4             askpass_1.1               fansi_0.4.2
[115] pillar_1.6.0              ggsci_2.9                 Ggally_2.1.1
[118] fastmap_1.1.0             httr_1.4.2                glue_1.4.2
[121] zip_2.1.1                 fdrtool_1.2.16            png_0.1-7
[124] bit_4.0.4                 stringi_1.5.3             blob_1.2.1
[127] polspline_1.1.19          latticeExtra_0.6-29       memoise_2.0.0
[130] Irkernel_0.8.15
```

Installed packages

Package	Version
abind	1.4-5
annotate	1.64.0
AnnotationDbi	1.48.0
askpass	1.1
assertthat	0.2.1
backports	1.2.1
base64enc	0.1-3
BH	1.75.0-0
Biobase	2.46.0
BiocFileCache	1.10.2
BiocGenerics	0.32.0
BiocManager	1.30.12
BiocParallel	1.20.1
BiocVersion	3.10.1
biomaRt	2.42.1
Biostrings	2.54.0
bit	4.0.4
bit64	4.0.5
bitops	1.0-6
blob	1.2.1
brew	1.0-6
brio	1.1.1
broom	0.7.6
broom.helpers	1.2.1
bslib	0.2.4
cachem	1.0.4
callr	3.6.0
car	3.0-10
carData	3.0-4
caTools	1.18.2
cellranger	1.1.0
checkmate	2.0.0
chemometrics	1.4.2
chron	2.3-56
circlize	0.4.12
classInt	0.4-3
cli	2.4.0
clipr	0.7.1
clisymbols	1.2.0
clue	0.3-58
cmprsk	2.2-10
coda	0.19-4
coin	1.4-1
colorspace	2.0-0
commonmark	1.7
ComplexHeatmap	2.2.0
conquer	1.0.2
corpcor	1.6.9
corrplot	0.84
covr	3.5.1
cowplot	1.1.1
cpp11	0.2.6
crayon	1.4.1
credentials	1.3.0
crosstalk	1.1.1
curl	4.3
cyclocomp	1.1.0
data.table	1.14.0
DBI	1.1.1

dbplyr	2.1.1
DelayedArray	0.12.3
dendextend	1.14.0
DEoptimR	1.0-8
desc	1.3.0
DESeq2	1.26.0
devtools	2.3.2
diffobj	0.3.4
digest	0.6.18
doParallel	1.0.16
doSNOW	1.0.19
downlit	0.2.1
dplyr	1.0.5
DT	0.17
dtplyr	1.1.0
e1071	1.7-6
egg	0.4.5
ellipsis	0.3.1
emmeans	1.5.5-1
estimability	1.3
evaluate	0.13
extrafont	0.17
extrafontdb	1.0
fansi	0.4.2
farver	2.1.0
fastmap	1.1.0
fdrtool	1.2.16
FNN	1.1.3
foghorn	1.3.2
fontBitstreamVera	0.1.1
fontLiberation	0.1.0
fontquiver	0.2.1
forcats	0.5.1
foreach	1.5.1
formatR	1.8
Formula	1.2-4
freetypeharfbuzz	0.2.6
fs	1.5.0
futile.logger	1.4.3
futile.options	1.0.1
gargle	1.0.0
gdtools	0.2.3
genefilter	1.68.0
geneplotter	1.64.0
generics	0.1.0
GenomeInfoDb	1.22.1
GenomeInfoDbData	1.2.2
GenomicAlignments	1.22.1
GenomicFeatures	1.38.2
GenomicRanges	1.38.0
geosphere	1.5-10
gert	1.2.0
GetoptLong	1.0.5
GGally	2.1.1
ggforce	0.3.3
ggplot2	3.3.3
ggplot2movies	0.0.1
ggpubr	0.4.0
ggrepel	0.9.1
ggsci	2.9
ggsignif	0.6.1

```
          gh      1.2.0
    gitcreds      0.1.1
GlobalOptions     0.1.2
        glue      1.4.2
       gmailr     1.0.0
  googledrive     1.0.1
googlesheets4     0.3.0
       gplots     3.1.1
    gridBase      0.4-7
   gridExtra        2.3
      gsubfn        0.7
      gtable      0.3.0
      gtools      3.8.2
       haven      2.3.1
      hexbin     1.28.2
       highr        0.8
       Hmisc      4.5-0
         hms      1.0.0
   htmlTable      2.1.0
   htmltools      0.3.6
  htmlwidgets     1.5.3
      httpuv      1.5.5
        httr      1.4.2
    hunspell      3.0.1
         ids      1.0.1
      igraph      1.2.6
         IHW     1.14.0
         ini      0.3.1
      inline     0.3.17
  intergraph      2.0-2
     IRanges     2.20.2
   IRdisplay      0.7.0
    IRkernel     0.8.15
     isoband      0.2.4
   iterators     1.0.13
        jpeg    0.1-8.1
   jquerylib      0.1.3
    jsonlite        1.6
     kernlab     0.9-29
       knitr       1.31
          ks     1.12.0
    labeling      0.4.2
    labelled      2.8.0
    lambda.r      1.2.4
        lars        1.2
       later    1.1.0.1
 latticeExtra     0.6-29
    lazyeval      0.2.2
     libcoin      1.0-8
   lifecycle      1.0.0
       lintr      2.0.1
        lme4     1.1-26
      locfit    1.5-9.4
         loo      2.4.1
  lpsymphony     1.14.0
   lubridate     1.7.10
         M3C      1.8.0
    magrittr      2.0.1
     mapproj      1.2.7
        maps      3.3.0
    maptools      1.1-1
```

```
    markdown        1.1
  matrixcalc      1.0-3
MatrixModels      0.5-0
 matrixStats     0.58.0
      mclust      5.4.7
     memoise      2.0.0
        mice     3.13.0
        mime       0.10
       minqa      1.2.4
       misc3d     0.9-0
     mockery      0.4.2
      modelr      0.1.8
  modeltools     0.2-23
    multcomp     1.4-16
   multicool     0.1-11
     munsell      0.5.0
     mvtnorm      1.1-1
     network     1.16.1
      nloptr    1.2.2.2
         NMF     0.23.0
     nrstats      0.1.0
    numDeriv 2016.8-1.1
     openssl      1.4.3
    openxlsx      4.2.3
org.Hs.eg.db     3.10.0
   parsedate      1.2.0
      pbdZMQ      0.3-3
    pbkrtest      0.5.1
       pcaPP     1.9-73
    pheatmap     1.0.12
      pillar      1.6.0
       pingr      2.0.1
    pkgbuild      1.2.0
   pkgconfig      2.0.3
     pkgdown      1.6.1
   pkgKitten      0.2.1
     pkgload      1.2.0
    pkgmaker     0.32.2
       plogr      0.2.0
      plot3D        1.3
      plotly      4.9.3
         pls      2.7-3
        plyr      1.8.6
         png      0.1-7
   polspline     1.1.19
    polyclip     1.10-0
     polynom      1.4-0
      praise      1.0.0
 prettyunits      1.1.1
    processx      3.5.0
     profvis      0.3.7
    progress      1.2.2
    promises    1.2.0.1
       proto      1.0.0
       proxy     0.4-25
          ps      1.6.0
       purrr      0.3.4
    quantreg       5.85
R.methodsS3      1.8.1
        R.oo     1.24.0
     R.utils     2.10.1
```

```
          R6      2.5.0
        ragg      1.1.2
    rappdirs      0.3.3
  rbenchmark      1.0.0
   rcmdcheck      1.3.3
RColorBrewer      1.1-2
        Rcpp      1.0.3
RcppArmadillo 0.10.2.2.0
   RcppEigen  0.3.3.9.1
RcppParallel      5.0.3
       RCurl   1.98-1.3
       readr      1.4.0
      readxl      1.3.1
    registry      0.5-1
     rematch      1.0.1
    rematch2      2.1.2
     remotes      2.2.0
        repr     0.19.2
      reprex      2.0.0
     reshape      0.8.8
    reshape2      1.4.4
  reticulate       1.18
         rex      1.2.0
       rgeos      0.5-5
         RH2      0.2.4
     Rhtslib     1.18.1
        rhub      1.1.1
         rio     0.5.26
       rJava     0.9-13
       RJDBC      0.2-8
       rjson     0.2.20
       rlang     0.4.10
         rle      0.9.2
   rmarkdown        2.7
         rms      6.2-0
        rmsb      0.0.2
      RMySQL    0.10.21
    rngtools        1.5
  robustbase     0.93-7
        ROCR     1.0-11
    roxygen2      7.1.1
 RPostgreSQL      0.6-2
   rprojroot      2.0.2
   Rsamtools      2.2.3
    RSpectra     0.16-0
     RSQLite      2.2.4
       rstan     2.21.2
  rstantools      2.1.1
     rstatix      0.7.0
  rstudioapi       0.13
 rtracklayer     1.46.0
        Rtsne       0.15
     Rttf2pt1      1.3.8
    rversions      2.0.2
        rvest      1.0.0
   S4Vectors     0.24.4
    sandwich      3.0-0
        sass      0.3.1
 scagnostics    0.2-4.1
      scales      1.1.1
     selectr      0.4-2
```

sessioninfo	1.1.1
sf	0.9-8
shape	1.4.5
shiny	1.6.0
sigclust	1.1.0
slam	0.1-48
sna	2.6
snow	0.4-3
som	0.3-5.1
sourcetools	0.1.7
sp	1.4-5
SparseM	1.81
spelling	2.2
sqldf	0.4-11
StanHeaders	2.21.0-7
statmod	1.4.35
statnet.common	4.4.1
stringi	1.5.3
stringr	1.4.0
SummarizedExperiment	1.16.1
svglite	2.0.0
svUnit	1.0.3
sys	3.4
systemfonts	1.0.1
testthat	3.0.2
textshaping	0.3.3
TH.data	1.0-10
tibble	3.1.0
tidyr	1.1.3
tidyselect	1.1.0
tidyverse	1.3.1
tinytest	1.2.4
tinytex	0.30
translations	3.6.1
tweenr	1.0.2
TxDb.Hsapiens.UCSC.hg19.knownGene	3.2.2
umap	0.2.7.0
units	0.7-1
usethis	2.0.1
utf8	1.2.1
uuid	0.1-2
V8	3.4.0
vctrs	0.3.6
vdiffr	0.3.3
viridis	0.5.1
viridisLite	0.3.0
waldo	0.2.5
whisker	0.4
whoami	1.3.0
withr	2.4.1
xfun	0.22
XML	3.99-0.3
xml2	1.3.2
xmlparsedata	1.0.5
xopen	1.0.0
xtable	1.8-4
XVector	0.26.0
yaml	2.2.1
zip	2.1.1
zlibbioc	1.32.0
zoo	1.8-9